Expression studies and functional analysis of the genes *IDL1*, *IDL2* and *IDL3* in *Arabidopsis thaliana*

Nora Martinussen Tandstad

Thesis for the Degree of Master of Science

University of Oslo

Faculty of Mathematics and Natural Sciences

Department of Molecular Biosciences

Programme for Molecular Genetics

2005

ACKNOWLEDGEMENTS

The work presented in this thesis was carried out at the Department of Molecular Biosciences, University of Oslo, in the period between April 2004 and August 2005. Supervision has been provided by Professor Reidunn B. Aalen (formal supervisor) and PhD-students Bitte Stenvik and Melinka A. Butenko.

First I would like to thank Professor Reidunn B. Aalen for excellent and enthusiastic supervision provided during this project, and for assisting me throughout the writing process.

Bitte Stenvik and Melinka A. Butenko deserve special thanks for fantastic supervision, for being encouraging and inspiring, and for assisting me throughout the writing process. I am very grateful for all the help you have given me.

I wish to thank Solveig Hauge Engebretsen and Roy Fallet for making solutions and media, and Ragnhild Nestestog at the Norwegian Arabidopsis Research Center (NARC) for her assistance in genotyping.

I would also like to thank everyone at "genetikken" for creating a nice working environment.

Oslo, November 2005

Nora Martinussen Tandstad

ABSTRACT

Small peptides can act as signaling molecules that coordinate development, growth and differentiation. In interaction with a receptor the ligand can trigger downstream pathways which induce cellular responses or regulation of gene expression. Recently, a novel group of putative ligands in plants, the IDA-LIKE (IDL) proteins, were identified based on their similarities to IDA, a putative ligand involved in floral organ abscission (Butenko et al., 2003). In this thesis three of the five *AtIDL* genes, *AtIDL1*, *AtIDL2* and *AtIDL3*, have been studied.

Histochemical GUS-staining analyses of promoter-GUS constructs for *IDL1*, *IDL2* and *IDL3* in transgenic *Arabidopsis thaliana* have been performed. In the *IDL1::GUS* transgenic lines, GUS activity was detected in the two outermost cell layers of the columella root cap and in the epidermal tissues of the root differentiation zone. Based on the root expression pattern of *IDL1*, roots of transgenic *Arabidopsis* both downregulating and overexpressing *IDL1* were investigated. While downregulation of *IDL1* resulted in longer roots, our preliminary results showed that overexpression of *IDL1* resulted in shorter roots. The *IDL2* promoter directed GUS expression in lateral root caps, shoot meristems, floral organ abscission zones (AZs), and bases of the pedicels. *IDL3::GUS* activity was observed in roots, buds, floral AZs, and at the bases of the pedicels. Since *IDA* is involved in the cell separation process that induces the floral organs to be shed, it was interesting to find that the GUS expression of the three *IDL* genes in many cases was associated with AZs and other zones of cell separation. Overexpression of *IDL1*, *IDL2* and *IDL3* resulted in similar phenotypes featured by early senescence of rosette and cauline leaves, premature floral organ abscission, and shedding of organs that are normally not shed in *Arabidopsis*; pedicels and cauline leaves. SALK lines containing T-DNA insertions upstream of *IDL2* and *IDL3* have been investigated, and RNAi lines were generated for *IDL1* and *IDL3*. Additional analyses will be needed to further understand the biological functions of the *IDL* genes.

TABLE OF CONTENTS

1 INTRODUCTION

1.1 *Arabidopsis* as a model organism

Arabidopsis thaliana is a dicotyledonous plant from the mustard family (*Brassicaceae*). It is used as a model plant system for plant development, genetics and physiology. *Arabidopsis* has several advantages as a model organism, including short generation time, small size, and a large number of offspring. Since the plant is self-pollinating homozygous transgenic lines can be generated quickly. Compared to other higher plant species, the *Arabidopsis* genome is very small. The 125 Mb genome is organized into five chromosomes and contains about 25 500 genes. Sequencing of the *Arabidopsis* genome was completed at the end of year 2000 by the Arabidopsis Genome Initiative (The Arabidopsis Genome Initiative, 2000). This was the first plant genome to be completely sequenced, and access to the genome sequence provides a better foundation for functional studies of *Arabidopsis* genes, and facilitates the discovery and analysis of new genes and gene families.

1.2 Generation of transgenic plants

The ability to transfer DNA into higher plants and thereby alter their phenotypes is central in plant molecular biology. Different methods for transformation of plants are available; these include the use of *Agrobacterium tumefaciens*, microprojectile bombardment, electroporation, microinjection and delivery by virus. The most powerful method today for transforming dicotyledonous plants is the *Agrobacterium tumefaciens* method. This method is based on the natural transforming system between the gram-negative soil bacterium *Agrobacterium tumefaciens* and dicotyledonous plants.

1.2.1 The *Agrobacterium tumefaciens* method

In nature, *Agrobacterium tumefaciens* causes crown gall tumors on infected plant tissue. During the course of infection, *Agrobacterium* transfers a defined fragment of its DNA (transfer DNA or T-DNA) into the genome of dicotyledonous plants. The infectious agents

are plasmids called tumor-inducing (Ti) plasmids. The T-DNA element is a specific DNA fragment located on the Ti plasmid and delimited by two 25-bp (base pair) direct repeats, termed left (LB) and right (RB) T-DNA borders. These repeats are the only sequences on the T-DNA that are necessary for the T-DNA-transfer (Tinland et al., 1994; Zupan et al., 2000). Therefore any DNA fragment that has been introduced between the border sequences will be transferred to the plant genome. The other important region on the Ti plasmid is the virulence (vir) region which encodes the proteins that mediate the T-DNA transfer. Plant phenolic compound, secreted by the wounded plant cells, induce transcription of the virulence genes (Tinland et al., 1994; Tzfira et al., 2000; Zupan et al., 2000). The virulence proteins VirD1 and VirD2 act together in the processing of the single-stranded T-DNA from the Ti plasmid. During this process the VirD2 protein becomes covalently bound to the 5' end of the single-stranded T-DNA. Together with several Vir proteins this single-stranded nucleoprotein complex is exported into the host cell cytoplasm through a channel formed by *Agrobacterium* VirD4 and VirB proteins (Tzfira and Citovsky, 2002). VirE2 is a single-stranded DNA binding protein that probably coats T-DNA-strands (Gelvin, 2003). Both VirE2 and VirD2 have nuclear-localizing activities and they are likely to cooperate with cellular factors to mediate the nuclear import of the T-complex and integration into the host genome (Tzfira and Citovsky, 2002). The T-DNA integrates into the genome by illegitimate recombination (Gheysen et al., 1991; Mayerhofer et al., 1991; Zupan et al., 2000) via a little known mechanism. Probably microsimilarities are involved in the integration of both the RB and the LB and these similarities need only to occur over a stretch of 3 to 5 bp and can be between any T-DNA and genomic sequence (Brunaud et al., 2002). This allows T-DNA to integrate at any locus in the genome. Host proteins involved in DNA repair are suggested to play a role in the T-DNA integration. One or more T-DNAs can integrate into the nuclear genome either at one locus or at several independent loci (Koncz et al., 1989).

1.2.2 T-DNA as vectors for transforming plants

The Ti plasmid is modified in order to make transgenic plants. In a binary vector system the T-DNA region is on one plasmid and the vir region on a separate plasmid. DNA fragments to be transferred into the *Arabidopsis* genome are placed between the LB and RB of the T-DNA, in addition to a marker for selection. The T-DNA plasmid can easily be modified in *E. coli* and is then transformed into an *Agrobacterium* strain containing a helper plasmid with the vir

functions. This property has enabled the engineering of plants expressing exogenous or modified genes. One of the major contributions of *Agrobacterium* research to plant research has been the use of T-DNA as a mutagen. To date, it has not been possible to target T-DNA to any particular locus in the genome. Using T-DNA with a known sequence makes it possible to identify the integration site. More and more T-DNA insertion sites have been sequenced and thousand of transgenic lines carrying random T-DNA insertions throughout the genome have been deposited in public stock centers.

1.3 The GUS reporter gene system

The *β-glucuronidase* (*GUS*) gene is one of the most frequently used reporter genes in genetically modified plants. This gene is used to study and monitor gene expression, especially the tissue specificity of promoter sequences. The *GUS* gene was isolated from *Escherichia coli* and the encoded enzyme catalyses the hydrolysis of a wide variety of glucuronides (Jefferson, 1989). The main advantage of *GUS* is the absence of *GUS* activity in many organisms other than vertebrates. This makes it possible to visualize small quantities of GUS activity in the absence of any background signal (Jefferson, 1989). In fusion to a promoter, the promoter will regulate expression of the *GUS* gene, and the *GUS* gene will adopt the expression pattern of the gene originally regulated by the promoter. The GUS protein will split the histochemical substrate 5-bromo-4-chloro-3-indolyl β-D-glucuronide (X-Gluc) into a blue substance. Hence the tissue will stain blue and the gene activity of the gene of interest is visualized.

1.4 RNA-induced gene silencing

RNA-induced gene silencing is a method used to investigate the role of a gene by preventing gene function and observe what effect (if any) this has on the organism's phenotype. RNA induced gene silencing is named post-transcriptional gene silencing (PTGS) in plants, quelling in fungi and RNA interference (RNAi) in animals (Baulcombe, 2004; Meister and Tuschl, 2004). In plants RNA silencing has a natural role in virus defense, endogenous gene regulation, and DNA methylation and suppression of transcription (Baulcombe, 2004). The RNA silencing mechanism involves the cleavage of double stranded RNA (dsRNA) or hairpin RNA (hpRNA) by an RNase III-like protein, called Dicer, into small interfering RNA

(siRNA) of 21-26 nucleotides. These siRNAs will then guide an RNA-induced silencing complex (RISC) to destroy mRNAs that are complementary to the single-stranded siRNA (Waterhouse and Helliwell, 2003; Baulcombe, 2005; Wang and Metzlaff, 2005).

RNA-induced silencing has many advantages compared to mutagenesis based on T-DNA insertions. Inducible RNA silencing vectors can be used (Guo et al., 2003) and RNA silencing can be used to investigate duplicated genes that have redundant functions (Helliwell et al., 2002; Helliwell and Waterhouse, 2003). As of today, the mutagenesis strategies that exist for plants create random mutations; so to have a high probability a T-DNA insertion in any given gene, a large collection of mutant lines are necessary (Krysan et al., 1999). To date, T-DNA insertions in every *Arabidopsis* gene is still not available (Alonso et al., 2003).

1.5 The *Arabidopsis* root - structure and function

The *Arabidopsis* root system consists of the embryonically derived (primary) root and secondary (lateral) roots emerging from the primary root. The lateral roots are formed postembryonically and the lateral root primordium (LRP) proliferates from non-meristematic tissue in the primary root (Malamy and Benfey, 1997). The organization of primary and lateral roots is similar and they have the same organization of tissue layers. However, unlike the primary root, lateral roots have much variability in number of cell files in each layer (Dolan et al., 1993). The root is composed of four concentric cell layers: epidermis, cortex, endodermis and stele. Each layer is made of vertical cell files that can be traced to initial cells (stem cells) in the root meristem (Ueda et al., 2005) (figure 1.1 A). The root cap, at the tip of the root, protects the meristem and consists of (12) columella cells surrounded by lateral root cap cells (Dolan et al., 1993; Sablowski, 2004). The root cap cells are regularly shed as the root grows through the soil (see section 1.7.2). There are four sets of initials in the *Arabidopsis* root: one that forms the epidermis and the lateral root cap, one that forms the columella root cap, one that produces the cortex and epidermis, and one that produces the cells of the stele. The meristematic initial cells surround quiescent center (QC) cells, which promote the continuous cell division of the initial cells (Dolan et al., 1993).

The *Arabidopsis* root has three distinct zones (figure 1.1 B). Cells in the meristematic zone are overlaid by the root cap and undergo division. Proximal to the meristematic zone is the

elongation zone, where longitudinal elongation occurs. The next zone is the differentiation zone, in which elongated cells mature into fully differentiated cells. In this zone some epidermal cells will mature into root hairs and some will become hairless cells (Dolan et al., 1993).

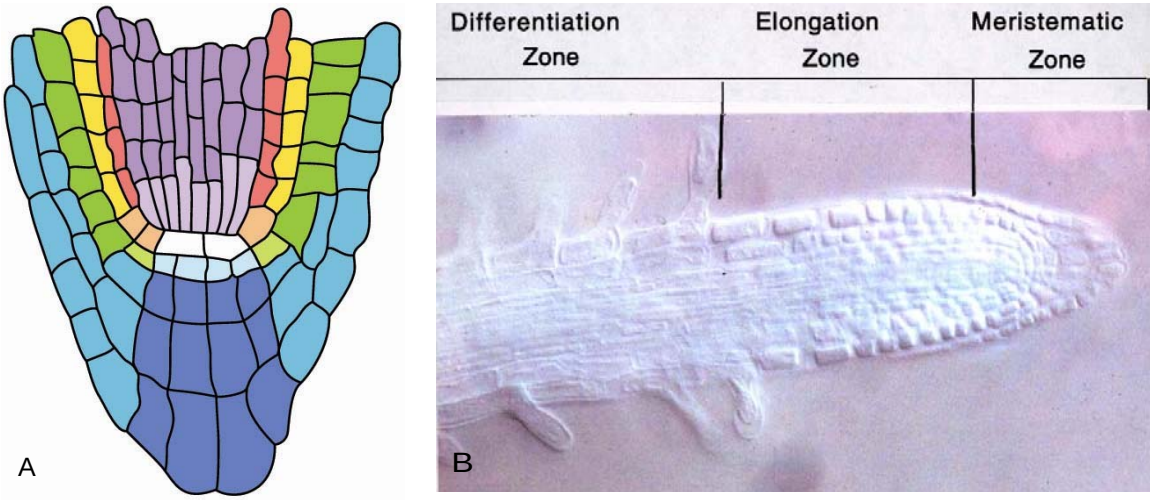

Figure 1.1 The *Arabidopsis* root. (A) The root tip. Epidermis (green), cortex (yellow), endodermis (pink), stele (purple), and lateral (turquoise) and columella (blue) root caps surround the apex. Initial cells, at the base of each cell file, surround the QC (white). Cortex and endodermis share a common initial as do lateral root cap and endodermis. (B) The external morphology of the root (Scheres et al., 2002).

The roots are important to the plant for their roles in anchorage, absorption, storage and conduction. The root cap at the tip of the root controls many biological and physiological processes that are crucial for the survival of the plant. Darwin even suggested in his book *The Power of Movement of Plants* in 1880 that plants have their brains in the root cap. The root cap is involved in growth responses including gravitropism, hydrotropism and thigmotropism (Barlow, 2003). Gravitropism allows roots to respond to gravity and grow downward into the soil. Columella cells in the root cap produce starch granules (amyloplasts). Sedimentation of amyloplasts triggers a signal transduction pathway that leads to root curvature (Chen et al., 2002). Hydrotropism directs roots in relation to a gradient in moisture and begins in the root cap with the sensing of the moisture gradient. The perception of moisture gradient triggers amyloplast degradation in the columella cells, and a following chain of events reorient the root in direction of moisture gradient (Eapen et al., 2005). As the roots grow through the soil, the root cap cells are the first to encounter obstacles. Thigmotropism allows the root to re-orient its growth and navigate around the obstacle (Massa and Gilroy, 2003).

1.6 Peptide signaling in plants

A central question in biology is how cells in multi-cellular organisms communicate. Signaling between cells coordinate cellular responses required for differentiation, growth and development. For many years most intercellular communication in plants has been explained on the basis of signaling by the six non-peptide plant-hormones: auxin, cytokinin, ethylene, gibberellin, abscisic acid (Kende and Zeevaart, 1997) and brassinolides (Mandava, 1988). It has recently become clear that plant cell communication also makes use of small peptide signals and specific receptors. To date, only a few ligand-receptor pairs have been identified in plants.

1.6.1 Signaling peptides in plants

The small size of peptide molecules and their cDNAs (complementary DNA) might be the reason that so few functional peptides have been identified to date. Small cDNAs are often not represented in cDNA libraries and the opportunities for peptide gene tagging by insertional mutagenesis are correspondingly small. Now more and more small signaling polypeptides have been identified. Many of the putative ligands are thought to interact with a receptor to trigger a downstream signaling pathway, (e.g. MAPK pathway) (Shiu and Bleecker, 2001b).

The signaling peptides are often produced by proteolytic processing. The putative ligands CLV3 (CLAVATA3) (Fletcher et al., 1999), SCR (S-LOCUS CYSTEINE-RICH) (Schopfer et al., 1999), IDA (INFLORESCENCE DEFICIENT IN ABSCISSION) (Butenko et al., 2003) (see section 1.8.1), PSK (PHYTOSULFOKINE) (Yang et al., 2001), NCR (NODULE-SPECIFIC CYSTEINE RICH) (Mergaert et al., 2003) and RALF (RAPID ALKALINIZATION FACTOR) (Pearce et al., 2001) all have an N-terminal signal sequence. The signal sequence is thought to be proteolytically removed and to direct the proteins through the secretory pathway to the extracellular space. Other putative signaling peptides lack the signal sequence. Tomato systemin, which was the first signaling peptide to be described in plants, is an 18 residue peptide processed from a 200 residue precursor protein (Pearce et al., 1991; Ryan and Pearce, 1998). Tomato systemin has no N-terminal signal

sequence but is found to move through the phloem and is somehow transported to the extracellular space. Recently, the two gene families *DEVIL* (*DVL*) (Wen et al., 2004) and *ROT FOUR LIKE* (*RTFL*) (Narita et al., 2004) were identified. The *DVL* and *RTFL* genes encode small polypeptides that all lack a signal sequence. The overexpression phenotypes suggest that these polypeptides may have a role in plant development.

Database searches have revealed that many of these predicted peptides seem to be part of putative ligand families. A large family of *SCR-LIKE* (*SCRL*) genes has been identified in the *Arabidopsis* genome based on their similarities to the *Brassica SCR* gene (Vanoosthuyse et al., 2001). This family of 114 genes is predicted to encode small, cystein-rich, secreted ligands. There are at least 25 *CLE* genes (*CLAVATA3/ESR-related*) in the *Arabidopsis* genome that share a conserved C-terminal domain (CLE-motif) with *CLV3*, and three maize ESR (embryo surrounding region) proteins (Cock and McCormick, 2001). They all encode small, secreted peptides. Five *IDA-LIKE* (*IDL*) genes were identified based on their similarities to *IDA*, and these six genes are suggested to represent a family of putative ligands in plants (Butenko et al., 2003) (see section 1.8).

1.6.2 The receptor-like kinases (RLKs)

Receptor-like kinases belong to one of the largest gene families in the *Arabidopsis* genome, with 625 members that represent nearly 2.5% of the organism's protein-coding genes (Shiu and Bleecker, 2001a, 2001b, 2003). All known plant RLKs contain serine/threonine kinase consensus sequences (Becraft, 2002). They are defined by the presence of a signal sequence, a ligand-binding extracellular domain, a transmembrane region, and a cytoplasmic kinase domain (Walker, 1994; Torii, 2000). There are also a large number of cytoplasmic plant kinases, termed receptor-like cytoplasmic kinases (RLCKs), without an extracellular domain (Shiu and Bleecker, 2001b). The receptor-like kinases vary greatly in their extracellular domains. Some motifs are implicated in protein-protein interactions, other motifs are involved in binding to carbohydrate substrates, including plant and microbial cell-wall components, or glycoproteins or steroids (Shiu and Bleecker, 2001b). Of particular interest are the RLKs with an extracellular leucine rich repeat (LRR) domain. The *Arabidopsis* genome contains 235 LRR-RLK genes (Shiu and Bleecker, 2001b). LRR domains are known to be involved in protein-protein or protein-peptide interactions (Kobe and Deisenhofer, 1994), but there may

be exceptions. The LRR-RLK subfamily has been found to regulate various developmental processes and defense responses (Torii, 2000). The subfamily includes the *Arabidopsis* proteins ERECTA (which is involved in organ elongation) (Torii et al., 1996), HAESA (which has a role in floral organ abscission) (Jinn et al., 2000), CLAVATA1 (CLV1) (which controls meristem cell fate) (Clark et al., 1997) and FLS2 (flagellin-sensitive2) (which mediates defense response) (Gomez-Gomez and Boller, 2000).

1.6.3 Ligand-receptor pairs in plant peptide signaling

In plant peptide signaling there are only a few known ligand-receptor pairs. Systemin is produced in response to wounding and is recognized by SR160 (systemin receptor 160 k-Da) receptor-like kinase, which induces defense gene activation (Scheer and Ryan, 1999). SR160 is a typical LRR-RLK (Scheer and Ryan, 2002). SR160 has shown homology to BRI1 (BRASSINOSTEROID-INSENSITIVE 1), an *Arabidopsis* LRR-RLK, thought to be involved in the perception of brassinolides (Scheer and Ryan, 2002). Therefore the same LRR-RLK may be the receptor for both brassinosteroids and systemin (Montoya et al., 2002). PSK is a sulfated pentapeptide that interacts with an LRR-type receptor-like kinase PSKR (PSK receptor) and activates a set of genes responsible for cellular differentiation and redifferentiation (Matsubayashi et al., 2002; Matsubayashi, 2003). In *Brassica*, sporophytic self-incompatibility is based on the specific interaction between the SCR (produced by the pollen) and the SRK (S-locus-specific RLK expressed in the pistil) (Kachroo et al., 2001).

1.6.3.1 The clavata system

The *CLAVATA* (*CLV*) signaling pathway is known to play a major role in stem cell maintenance in plant meristems by regulating the balance between meristem cell proliferation and differentiation (Matsubayashi, 2003). The *CLV* signaling pathway negatively regulates the expression of WUSCHEL (WUS), a transcription factor which maintains stem cell identity (Schoof et al., 2000). The pathway comprises CLV3, thought to act as a signal peptide, and a receptor complex consisting of CLV1 and CLV2 (a receptor-like protein with leucine-rich repeats LRR-RLP), thought to interact with CLV3 (Boller, 2005). Genetic evidence indicates that the products of CLV1 and CLV3 function in close association (Fletcher et al., 1999). The biochemical evidence for the physical interaction between CLV3 and CLV1 (Trotochaud et al., 2000) has been retracted (Nishihama et al., 2003). Currently there is no biochemical evidence for the ligand-receptor interaction between CLV1 and

CLV3. It has even been suggested that CLV3 is unlikely to act through CLV1, since *clv1* null mutations have a much weaker phenotype than *clv3* null mutations (Dievart et al., 2003). The CLV1/CLV2 and CLV3 pathways both regulate WUS expression but their interplay remains unknown (Boller, 2005).

1.7 Cell separation processes in plants

Plant cells are joined together by an adhesive matrix composed primarily of pectin. Processes that lead to loss of adhesion between cells play a critical role throughout the life cycle of a plant (Roberts et al., 2000; Roberts et al., 2002). Cell separation may be part of the highly programmed development of a plant or a response to environmental stress (Taylor and Whitelaw, 2001). Abscission and pod dehiscence are programmed processes of cell separation (Patterson, 2001). Abscission is the process by which organs such as leaves, flowers, or fruit are shed during the life of a plant (Sexton and Roberts, 1982), whereas pod dehiscence is the separation of the two silique valves and results in the shedding of seeds (Meakin, 1990). Other cell separation processes facilitate radicles to appear from germinating seeds, roots to penetrate the soil and lateral roots to emerge, cotyledons and leaves to expand and gaseous exchange to take place, pollen to be released from anthers and fruit to soften (Roberts et al., 2002) (see figure 1.2). Common for all these processes is the degradation of the cell wall.

The dicot cell wall consists of rigid, inextensible cellulose microfibrils held together by interpenetrating coextensive networks of matrix glycans, pectins and structural glycoproteins (Brummell and Harpster, 2001). The middle lamella is rich in pectin and a part of the cell wall. The middle lamella is shared by the neighboring cells and cements them firmly together (http://micro.magnet.fsu.edu/cells/plants/cellwall.html). A key step in the reduction of the cell-to-cell adhesion is the breakdown and resolution of the middle lamella. Cell wall modifying enzymes such as cellulases (β-1,4-glucanases), pectinases, expansins, xyloglycan endotransglycosylase (XET) and polygalacturonases (PG) are associated with breakdown of the middle lamella and wall degradation in different cell separation processes in plants (Roberts et al., 2002). The hydrolytic enzymes, cellulases, have been correlated with processes that require breakdown of cell wall, including fruit ripening, anther dehiscence, vascular tissue differentiation and abscission (del Campillo et al., 2004). The cellulase Cel5 is involved in abscission of tomato flowers (del Campillo and Bennett, 1996). Interestingly, the

Arabidopsis homolog, *AtCel5*, was shown to be expressed exclusively in the root cap cells (del Campillo et al., 2004). This suggests that the highly similar cellulases are involved in different cell-cell separation processess, e.g. abscission of flowers in tomato, and sloughing (see section 1.7.2), in *Arabidopsis* roots.

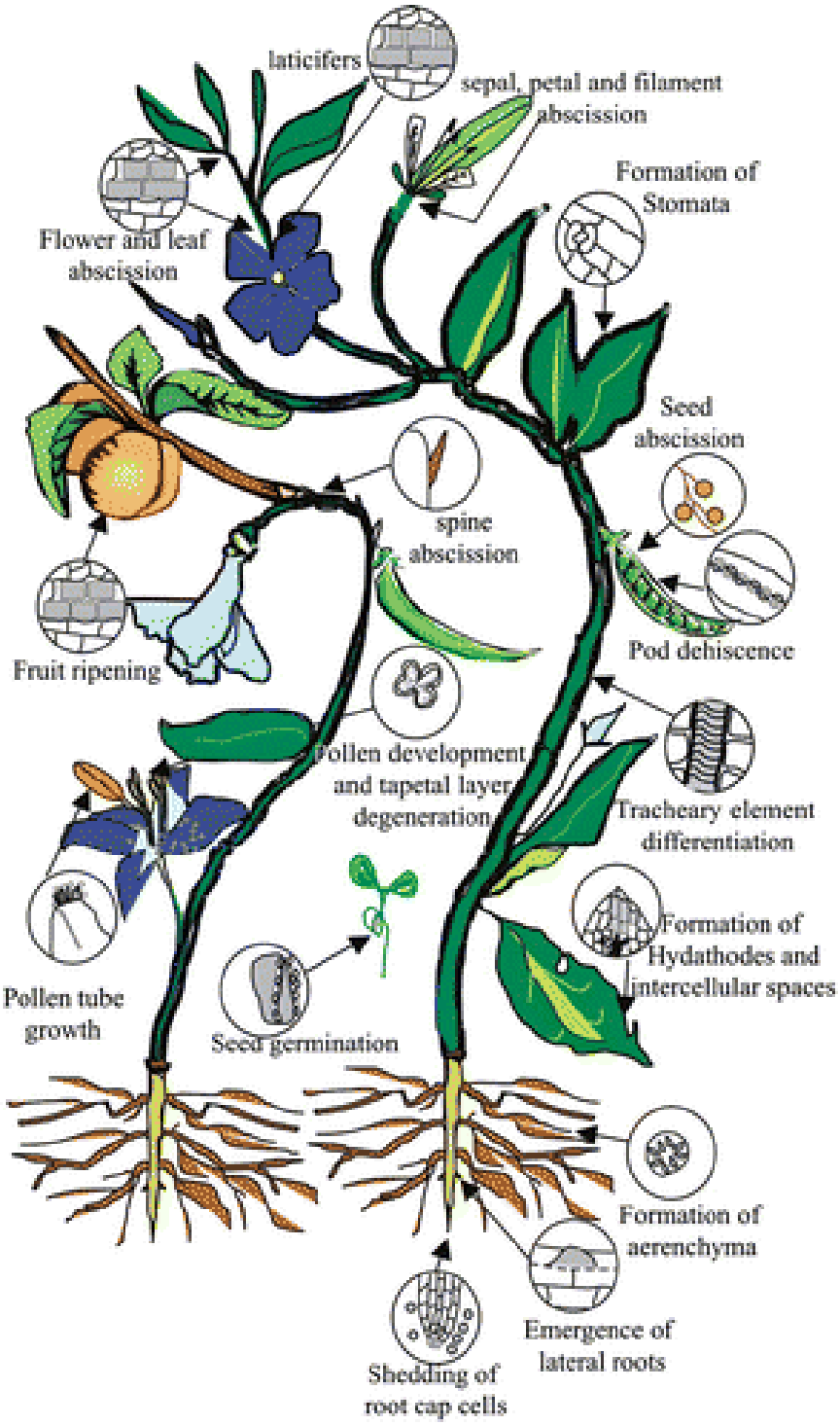

Figure 1.2 Sites of cell separation in plants. (Roberts et al., 2002)

1.7.1 Abscission

Abscission normally occurs at highly predictable positions (Taylor and Whitelaw, 2001), at sites comprising bands of cells that are positionally differentiated target cells (Osborne, 1989). These bands of cells, termed abscission zones (AZs), are often located in stems between the abscising organ and the body of the plant (Bleecker and Patterson, 1997; Patterson, 2001). The balance between the plant hormones ethylene and auxin has long been recognized to determine the timing of the abscission process where ethylene has been recognized as the inducing agent and auxin as the break (Taylor and Whitelaw, 2001). In response to the appropriate stimulus, the cells in the AZ enlarge and the middle lamella dissolves (Bleecker and Patterson, 1997). Shedding of the organ is followed by the continued enlargement of the cells and the differentiation of a protective layer (Bleecker and Patterson, 1997; Patterson, 2001).

Arabidopsis displays abscission of floral organs and seeds. Since this plant does not shed its leaves or fruits, the base of the petiole and the base of the pedicel are referred to as vestigial abscission zones. There are examples of *Arabidopsis* genes that are involved in true abscission processes and at the same time are expressed in vestigial AZs. Reduction in the level of the receptor-like kinase, HAESA, delays floral organ abscission (Jinn et al., 2000). Interestingly, *HAESA* is expressed in the floral organ AZs and at the base of pedicels and petioles. The expansin, *AtExp10*, is also expressed at the base of pedicels and petioles (Cho and Cosgrove, 2000), but not in any true AZs in *Arabidopsis*. However, abscission at the base of the pedicel was enhanced in plants over-expressing *AtExp10*, supporting the concept that expansins have a role in abscission (Cho and Cosgrove, 2000).

1.7.2 Sloughing

Sloughing is a programmed cell-cell separation process that takes place in the outer layers of the root cap and results in the shedding of living cells (del Campillo et al., 2004). The shedding of surface layers of root cap cells resembles abscission. As in abscission, modification of the cells in the outer surface results in expansion of the cells. This is followed by the breakdown of the cell walls and further expansion of the cells. The process is correlated with pectolytic enzyme and cellulase activity (Uheda, 1997). The cells that have

been shed degenerate and contribute to the mucilaginous material around the root tip (del Campillo et al., 2004). The continuous production and sloughing of root cap cells decreases frictional resistance to root penetration (Bengough and McKenzie, 1997; Iijima et al., 2003), and also function as a protection against pathogen attack (Vicre et al., 2005).

1.8 IDA and IDA-LIKE proteins – a group of putative ligands in plants

1.8.1 The *IDA* (*INFLORESCENCE DEFICIENT IN ABSCISSION*) gene

The *ida* mutant was identified from a collection of *Arabidopsis* T-DNA insertion lines (Butenko et al., 2003). In wild type *Arabidopsis*, floral organs are shed shortly after anthesis (Bleecker and Patterson, 1997). Even though a floral organ abscission zone develops in the *ida* mutant, floral organs remain attached indefinitely (figure 1.3) (Butenko et al., 2003). Since *ida* otherwise shows normal ethylene sensitivity, the deficiency is not influenced by ethylene. The *IDA* gene was identified by a complementation assay. This revealed that the *ida* phenotype was caused by a T-DNA insertion in the promoter of the gene *At1g68765*.

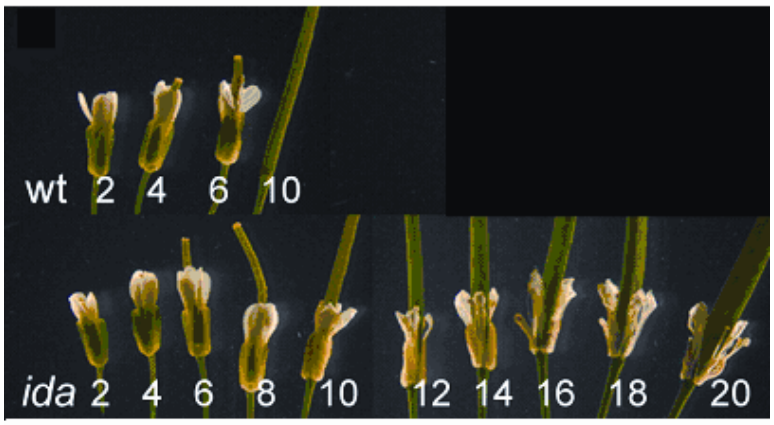

Figure 1.3 The *ida* mutant. The C24 wild type abscises its floral organs shortly after anthesis, whereas the *ida* mutant retains its floral organs indefinitely. Arabic numerals indicate flower positions on the inflorescence. Position 1 corresponds with the first flower with visible white petals. (Butenko et al., 2003)

The expression pattern of the *IDA* promoter has been investigated by the GUS assay (Butenko et al., 2003). *IDA::GUS* expression was restricted to the AZ at the base of all floral organs and the outgrowths of the nectaries. Prior to the abscission process (from position 1 to 4), expression was absent in flowers. During the course of abscission (from position 5 to 9), the specific AZ signal was at its strongest (see figure 1.4), expression was also seen through position 10. At later stages the GUS signal was more or less restricted to the outgrowths of the medial portion of the nectary. The GUS activity of the *IDA* promoter is consistent with an

involvement in floral organ abscission and the signal in the nectarines suggests that IDA also functions in the postabscission process.

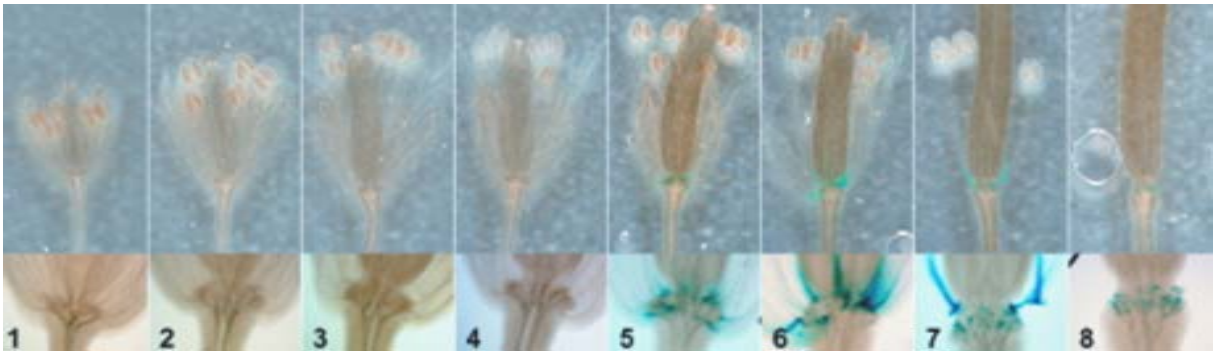

Figure 1.4 *IDA::GUS* expression. GUS activity was absent in flowers before the abscission process (position 1-4). At position 5 the AZ specific signal was detected and was maintained throughout the abscission process. Arabic numbers indicate flower position on the inflorescence. (Butenko et al., 2003)

The *IDA* gene encodes a small protein of 77 amino acids, with a high pI (isoelectric point) and an N-terminal hydrophobic region predicted to act as a signal peptide (Butenko et al., 2003). No other hydrophobic regions are found in IDA, indicating that it is a soluble protein. Subcellular localization of the IDA protein and the signal peptide, in an Onion Epidermis Transient Expression Assay, showed that both IDA-GFP (Green Fluorescent Protein) and the signal peptide-GFP fusion proteins were localized in the extracellular space. Its small size, high pI, and signal peptide are properties suggesting that IDA is a ligand. The IDA protein has a C-terminal that is distinct from the CLE motif of the CLE proteins and the Cys-rich pattern of the SCRL proteins; therefore IDA is not a member of these two classes of putative ligands. The IDA protein is predicted to be a ligand of an unknown receptor involved in the developmental control of floral abscission.

1.8.2 The *IDA-LIKE* (*IDL*) genes

The *IDL* genes were identified based on their similarities to *IDA*, and these genes are suggested to encode a new class of partners for plant receptors (Butenko et al., 2003). The C-terminal 20 amino acids of the IDA protein was used in tBLASTn (Basic Local Alignment Search Tool) searches against plant EST (Expressed Sequence Tag) collections and the *Arabidopsis* genome (figure 1.5A). *IDL* transcripts from eight different plant species, including one from *Arabidopsis* (*AtIDL1*), and four novel *IDL*-genes (*AtIDL2-AtIDL5*) in the *Arabidopsis* genome were identified. The *IDL* genes encode proteins of similar size and pI-

values (ranging from 11.02 to 12.62), and have predicted N-terminal signal sequences and a conserved C-terminal signature, termed PIP. RT-PCR showed that the *AtIDL* genes are expressed in diverse tissues (figure 1.5B), and thus have expression pattern distinct from that of *IDA*. The differential expression pattern suggests that the *IDL* genes may be important in diverse developmental processes in the plant.

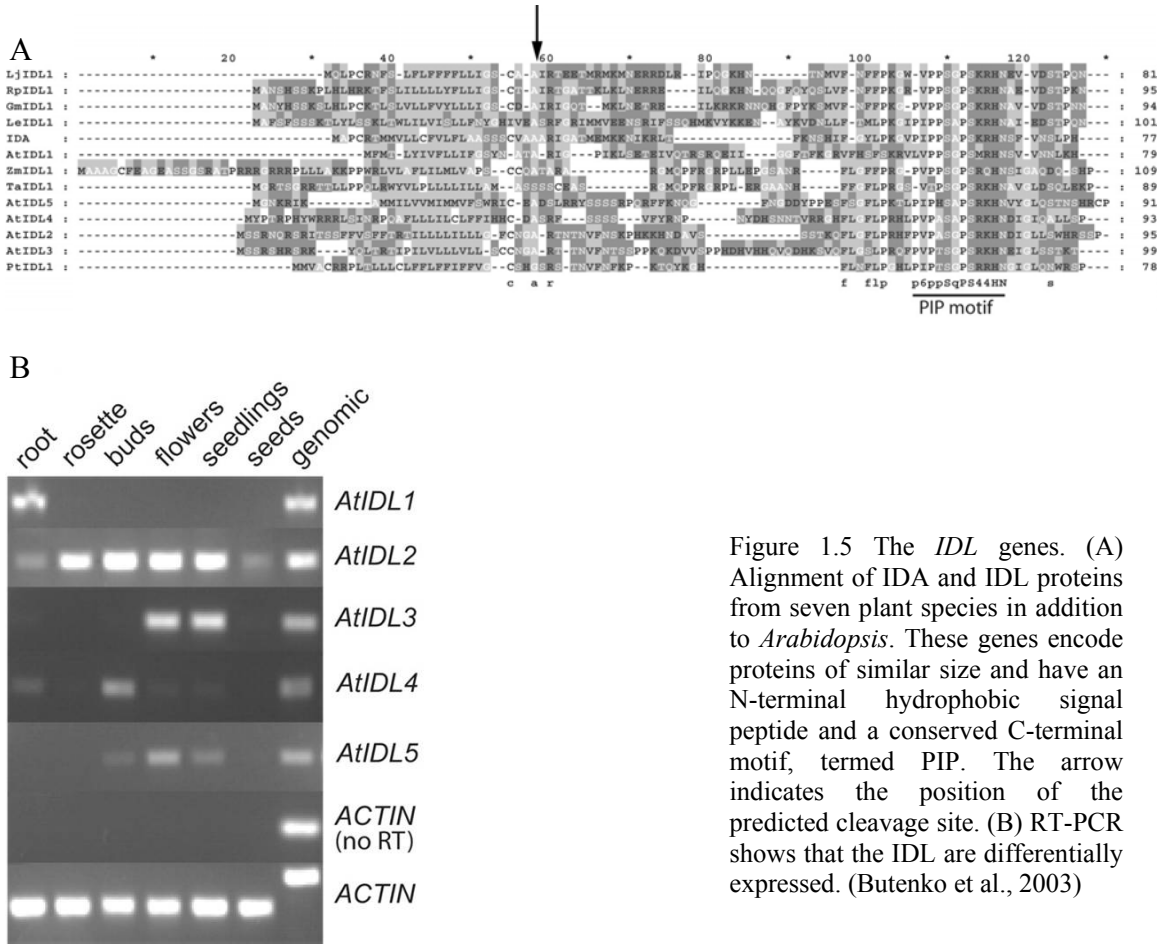

Figure 1.5 The *IDL* genes. (A) Alignment of IDA and IDL proteins from seven plant species in addition to *Arabidopsis*. These genes encode proteins of similar size and have an N-terminal hydrophobic signal peptide and a conserved C-terminal motif, termed PIP. The arrow indicates the position of the predicted cleavage site. (B) RT-PCR shows that the IDL are differentially expressed. (Butenko et al., 2003)

1.9 Aim of this study

This study is part of a larger project where the main goal is to characterize the five *IDL* genes. The aim of this study was to further investigate *IDL1* (*At3g25655*), *IDL2* (*At5g64667*) and *IDL3* (*At5g09805*) by performing expression studies and functional analyses. Promoter::*GUS* analyses were used to characterize the expression pattern of these genes. By subcellular localization we wanted to investigate the possibility of them being ligands. To further contribute to the understanding of the biological functions of the three *IDL* genes, SALK T-

DNA lines for *IDL2* and *IDL3* were investigated; in addition RNAi knock-down and overexpression lines were generated for all three genes.

2 MATERIALS AND METHODS

2.1 Plant studies

2.1.1 Surface sterilization and growth conditions

Seeds were surface sterilized using 70% ethanol and 20% chlorine in 0.1% Tween20 for 5 min, and then rinsed for 5 min in 0.001% Tween20. 0.1% agar was added to the seeds before plated on MS medium (Murashige and Skoog, 1962), supplemented with 2% sucrose (MS-2). For segregation analysis, selections of transformants, and genetically modified lines, either kanamycin (Km) (50mg/l) or hygromycin (Hyg) (20 mg/l), dependent on the construct used, was added to the medium. Plated seeds were cold treated at 4ºC for 18-36h and then transferred to growth chambers and cultivated at 22ºC, 8h dark and 16h light (100μE/$m^2 \cdot$ s). After two weeks the seedlings were transferred to soil and further cultivated under the same conditions.

For segregation analysis the medium were supplemented with kanamycin or hygromycin. T2 seedlings were scored for antibiotic resistance or sensitivity two weeks after germination. Seedlings that did not develop past the dicotylouse stage were considered to be antibiotic sensitive.

2.1.2 Root length measurements and gravistimulation

Seedlings were grown on MS medium supplemented with 1% sucrose (MS-1) and 7 g agar/L. The plates were placed vertically so that the roots would grow along the surface of the agar. Root length was measured after nine and ten days. Nine and ten day-old seedlings were gravistimulated by turning the agar plates (by 90º) so that the roots were horizontally positioned. Seedlings and a ruler held adjacent to the seedlings were digitally photographed. Root calculations were performed on the digital images using the NIH ImageJ software.

2.1.3 Chemical treatment

For induction of the IDL-GFP fusion proteins in the GFP transgenic plants, 10 µM dexamethasone (DEX) (Sigma) was added to the MS medium, and seedlings were grown in the medium for ten days before analysis in a magnifier and in a confocal microscope (Olympus FV1000, Scanning laser confocal microscope, Olympus, Hamburg, Germany).

2.1.4 Histochemical analysis

2.1.4.1 GUS analysis

Histochemical assay of β-glucoronidase (GUS) activity (Grini et al., 2002), was performed by prefixing plant material in 90% acetone, rinsed in staining buffer (50 mM $NaPO_4$, pH 7.2, 2 mM potassium-ferrocyanide, 2 mM potassium-ferricyanide, 0.1% Triton X-100) and incubated in staining buffer with 2mM X-Gluc substrate for 12-16 h at 37ºC. When the primary transformants (T1 or first transformant generation) were investigated for *GUS* expression, the stained plant material was rinsed three times in a 1:1 solution of 96% ethanol and 100% acetic acid to clear off the chlorophyll. The T2 (second transformant generation) and T3 (third transformant generation) generations were inspected in a Zeiss Axioplan2 imaging microscope equipped with differential interference contrast optics and a cooled Axiocam camera imaging system (Jena, Germany). Plant tissues were dehydrated in a graded ethanol series, 50 mM $NaPO_4$ solutions in ethanol (15%, 35%, 50%, 10 min each). To fix the plant tissues they were incubated 30 min on ice in a 10:7:2:1 solution of 96% EtOH (ethanol), dH2O, 100% acetic acid and 37% formaldehyde. The plant tissues were then rehydrated in the graded ethanol series. The tissues were kept in a 50 mM $NaPO_4$ solution until they were mounted on microscope slides in a clearing solution of 8:2:1 (w/v/v) chloral hydrate:dH_2O:glycerol (98%). The object glasses were incubated ON (over night) at 4ºC before investigation in the Zeiss Axioplan2 imaging microscope.

2.1.4.2 Lugol staining

Starch granules in the columella root cap were visualized with Lugol's solution (diluted iodine-potassium iodide solution, Merck) in 14 day-old GUS stained seedlings. Seedlings were stained for 45 min and rinsed with water before investigation in the Zeiss Axioplan2 imaging microscope.

2.1.5 Transformation of *Arabidopsis thaliana* by floral dipping

This method is based on the *Agrobacterium tumefaciens* ability to integrate T-DNA, from its pTi plasmid, randomly into the Arabidopsis genome, (Bechtold et al., 1993) modified by Clough and Bent (Clough and Bent, 1998).

2.1.5.1 Plant growth

Arabidopsis ecotype Col plants were grown to flowering stage. To obtain more floral buds, inflorescences were clipped; this encourages proliferation of many secondary bolts. Plants were dipped 4-6 days after clipping.

2.1.5.2 Culturing of *Agrobacterium tumefaciens* and transforming of plants

A T-DNA vector with the gene of interest was transformed into either the *Agrobacterium tumefaciens* strain C58 pGV2260 or GV3101 pMP90RK carrying a helper plasmid providing the vir functions. Bacteria were grown at 28ºC in YEB-medium, containing antibiotics, to the stationary phase (OD_{600} ~1.2). Cells were harvested by centrifugation for 10 min at room temperature at 5000 rpm and then resuspended in 5% sucrose solution to a final OD_{600} of 0.8. Before dipping, Silwet L-77 was added to a concentration of 0.02%. Above-ground parts of plant were dipped in the *Agrobacterium* solution for 2-3 min. Then the plants were placed in a tray with moist paper and covered with transparent plastic to maintain humidity. Plants were left in a low light location ON and returned to the growth chambers the next day. Plants were grown for a further 4-6 weeks when seeds were harvested 2-3 times.

2.2 Working with bacteria

2.2.1 Growth and storage of bacteria

For permanent storage of all cultures, 1ml culture containing 8% glycerol was made and stored at -80ºC.

2.2.1.1 *E. coli*

E. coli cultures were grown in LB-medium (10g/l Bacto tryptone, 5g/l Bacto yeast extract, 0.17M NaCl) at 37ºC with shaking. *E. coli* cells were plated onto LA-plates (LB-medium containing 15g agar per liter) to obtain single colonies.

● One Shot ® TOP 10 chemically competent (Invitrogen)

For cloning of PCR products the pCR® 2.1-TOPO® vector was used and transformed into TOP10 cells.

● Library efficiency® DH5α™ compentent cells (Invitrogen)

For the Gateway cloning DH5α cells were used. This strain does not contain the F`episome, which contains the *ccdA* gene, an antidote to the *ccdB* gene toxity, and will prevent negative selection with the *ccdB* gene.

2.2.1.2 *Agrobacterium tumefaciens*

The *Agrobacterium tumefaciens* strains C58 pGV2260 and GV3101 pMP90RK (compatible to the T-DNA vectors used) were used for transformation of wt (wild type) *Arabidopsis. Agrobacterium* cultures were grown in YEB-medium (5g/l Bacto beef extract, 1g/l Bacto yeast exstract, 1g/l Bacto peptone, 5g/l sucrose, pH 7.4, added 2ml 1M $MgSO_4$ per liter) at 28ºC with shaking. *Agrobacterium* was plated onto YEB-plates (YEB-medium containing 15g agar per liter) to obtain single colonies.

2.2.2 Transformation of bacteria

2.2.2.1 Transformation of *E. coli*

For both TOP10 and DH5α all transformations were done by heat shock, as described by the manufacturer (Invitrogen). After the heat shock SOC medium (2% bacto trypton, 0.5% bacto yeast extract, 100mM NaCl, 2.5M KCl, 10mM $MgCl_2$, 10mM $MgSO_4$, and 20% glucose) was added to the cells, and the cells were grown at 37°C for one hour with shaking. For selection of transformants, cells were spread on plates with the appropriate antibiotic, and incubated overnight.

2.2.2.2 Transformation of *Agrobacterium tumefaciens*

● Electrotransformation

Electrotransformation was used to introduce the RNAi constructs into *Agrobacterium.* Plasmid was added to competent *Agrobacterium* strain C58 pGV2260, and incubated on ice for 30-60 sec, then moved to a cold electroporation cuvette (Bio Rad) and shocked at 25µF, 200Ω and 2.4 kV. SOC medium was added and the cells were incubated one hour at 28ºC

with shaking. For selection of transformants the cells were spread on plates with appropriate antibiotic.

● Direct *Agrobacterium* transformation, freeze/thaw method

The overexpression and GFP constructs were transferred into *Agrobacterium* GV3101 pMK90RK by the freeze/thaw method. Cells were made competent by growing *Agrobacterium tumafaciens* at 28ºC in YEB-medium to an OD_{600} of 0.5-1.0. The culture was chilled on ice and centrifuged at 3000g for 5 min at 4ºC. The supernatant was discarded; the cells were resuspended in ice-cold 20 mM $CaCl_2$ and frozen in liquid nitrogen. For transformation 0.1-1µg of plasmid was added to the frozen cells which then were thawed by incubating in a 37ºC water bath for 5 min. 1 ml YEB medium was added to the cells and they were incubated at 28ºC for 2-3 h with gentle shaking. The cells were centrifuged for 30 s, resuspended in 100µl YEB-medium and spread on plates with appropriate antibiotic. To obtain single colonies the plates were incubated at 28ºC for 2 days.

2.3 Standard DNA techniques

2.3.1 Agarose gel electrophoresis

Separation of DNA fragments according to size was done by agarose gel electrophoresis (Sambrook and Russel, 2001). 1% agarose (SeaKem® LE agarose, Cambrex Biosciences) gels with 0.6µg/ml EtBr (ethidium bromide) were run in a 1xTAE buffer (40mM Tris-acetate, 1mM EDTA). An electric voltage of 5V/cm was applied. To determine the size of the DNA fragments GeneRuler™ 1kb DNA Ladder (Fermentas) was used.

2.3.2 Purification of DNA fragments

To purify DNA fragments from agarose gel, the fragments of interest were cut from the gel and isolated according to the QIAquick Gel extraction kit (QIAGEN). For purification of PCR DNA fragments, QIAquick PCR Purification kit (QIAGEN) was used.

2.3.3 Isolation of plasmids from *E. coli* cell cultures

The method is based on the fact that treatment of bacteria cultures with SDS (sodium dodecyl sulfate) and alkali leads to cell lysis and denaturation of proteins and genomic DNA while the plasmids are released in the supernatant.

2.3.3.1 Miniprep (Promega)
Isolation of plasmids from 3-6 ml culture was done with Wizard Plus SV Miniprep DNA purification system (Promega) according to the manual.

2.3.3.2 Midiprep (Promega)
Isolation of plasmids from 50 ml culture was done with Pure Yield ™ plasmid Midiprep system (Promega) and performed according to the manual.

2.3.4 Isolation of genomic DNA from *Arabidopsis*

2.3.4.1 Miniprep (Bio-Rad)
Isolation of small amounts of DNA was done using Aquapure genomic DNA isolation kit (Bio-Rad). DNA was extracted from N_2-frozen rosette leaves following the protocol from the manufacturer.

2.3.4.2 Maxiprep
For large quantities of DNA four to five rosette stage plants were frozen in liquid N_2 and homogenized prior to DNA extraction. DNA extraction was based on the protocol of Dellaporta *et al*. (1983) (Dellaporta et al., 1983), with some modifications. Absolute alcohol was used for the final DNA precipitation step instead of isopropanol. Isolated DNA was dissolved in 10mM Tris-HCl pH 8 and stored at 4°C.

2.3.5 Restriction of DNA with endonucleases

Restriction of DNA with restriction endonucleases was performed as recommended by the respective endonucleases manufacturer.

2.3.6 Quantification of DNA

Quantification of DNA samples was done with Hoefer® DyNAQuant 200 Fluorometer (Amersham pharmacia biotech) as described by the manufacturer.

2.3.7 Cloning of PCR products using the TOPO cloning system (Invitrogen)

The TOPO cloning system was used for cloning of the genomic regions flanking the left border of the T-DNA insertions in the lines SALK_022068 and SALK_065248 from the Salk institute Genomic analysis laboratory (http://signal.salk.edu/cgi-bin/tdnaexpress). Salk lines are T-DNA insertion lines where the genomic insertion site has been determined. The exact location of the T-DNA must, however, be confirmed by sequencing the genomic region flanking the left border of the T-DNA. The Salk lines SALK_022068 and SALK_065248 are predicted to contain T-DNA insertions upstream *IDL2* and *IDL3* coding regions, respectively. In order to clone the genomic region flanking the left border of the T-DNA in SALK_022068, the primers LBb1 and SALK_022068 RP (*IDL2* RP) (primer sequences are listed in appendix1) were used, while the primers LBb1 and SALK_065248 RP (*IDL3* RP) were used to clone the genomic region flanking the left border of the T-DNA in SALK_065248. The PCR products obtained were cloned into pCR® 2.1-TOPO®.

The plasmid vector pCR® 2.1-TOPO® is a linearized vector with single 3' thymidine (T) overhangs and covalently bound Topoisomerase I. The 3' T overhangs anneal to the 3' deoxyadenosine (A) ends of PCR products which were generated by the Taq polymerase. The 5' hydroxygroup of the PCR product attacks the energy-rich bond between the vector DNA and the Topoisomerase, the enzyme is released and the PCR product is ligated into the vector. The TOPO cloning was performed according to the manual.

2.3.8 Making constructs using the Gateway® Technology (Invitrogen)

The Gateway Technology is a cloning method based on the site specific recombination properties of the bacteriophage lambda. DNA segments that are flanked by recombination sites (att sites) are exchanged between vectors.

Two recombination reactions constitute the basis of the Gateway Technology. The BP reaction is a recombination reaction between an attB flanked PCR product or an attB expression clone and a donor vector (with an attP substrate). The BP reaction creates an attL-containing entry clone. The LR reaction is a recombination reaction between an entry clone and a destination vector (with an attR substrate) to create an attB-containing expression clone.

First a cointegrate molecule is generated which is then resolved to accomplish transfer of the cloned DNA segment into the entry or expression clone. The recombination reactions are mediated by conservative recombinases, no net synthesis or loss of DNA occurs during DNA segment transfer. In addition the recombination sites give high specificity, meaning that attB1 will recombine with attP1 but not with attP2, and this will provide control over reaction directionality.

The Gateway cloning system has two selection schemes. The entry clone and the destination vector contain different antibiotic resistance gene, this gives a positive selection of the entry or expression clone. Most Gateway vectors contain a Gateway cassette. The *ccdB* gene, which inhibits growth of *E. coli*, is part of these att-site flanked Gateway cassettes. After the BP or LR reactions the cassette is replaced by the gene of interest. This means that the presence of the *ccdB* gene allows negative selection of the donor and destination vector.

2.3.8.1 RNAi constructs

The RNAi constructs were made using the Gateway Technology. The attB flanked PCR products were amplified using the primers *IDL1* attB1, *IDL1* attB2, *IDL2* attB1, *IDL2* attB2, *IDL3* attB1 and *IDL3* attB2. The PCR products contain the coding sequences of *IDL1*, *IDL2* and *IDL3* without the stop codon. The PCR products were recombined into the donor vector pDONR™/zeo (Invitrogen). The BP reactions were performed according to the manual using half the volume recommended. DH5α-cells were transformed with the BP recombination mixes according to the manufactures instructions. Colonies were collected and entry clones from two ON cultures each gene were purified. The entry clones were confirmed by PCR using the primers *IDL1* attB1, *IDL1* attB2, *IDL2* attB1, *IDL2* attB2, *IDL3* attB1, *IDL3* attB2, M13 F and M13 R and by sequencing using the primers M13 F and M13 R.

In the LR reactions the entry clones were recombined with the destination vector pHELLSGATE 8 (Helliwell et al., 2002). As for the BP reactions half the volume recommended was used. DH5α cells were transformed with the LR reaction mixes according to the manual. Colonies were collected and expression clones were analyzed and confirmed with digestion analyses, using XbaI and XhoI, and by PCR using the primers p27 5', p27 3', HU, *IDL1* attB1, *IDL2* R and *IDL3* L. Correct clones for *IDL1* and *IDL3* were identified. After analyzing more than 90 clones in order to make an RNAi construct for *IDL2*, no correct clone was obtained.

2.3.8.2 GFP-constructs

GFP-constructs for both the transient onion expression assay and for stable GFP-expression *in planta* were made. pENTRY™/zeo containing the coding sequences of the *IDL1*, *IDL2* and *IDL3* genes were used. The sequences were amplified using the primers *IDL1* attB1, *IDL1* attB2, *IDL2* attB1, *IDL2* attB2, *IDL3* attB1 and *IDL3* attB2 (see section 2.3.8.1). For the onion-expression assay the destination vector pKEGAW-c.1-smGFP (Berg et al., 2003) was used, while the destination vector pTA7002 GAW-GFP (Thorstensen, 2005) was used for GFP-expression *in planta*. The expression clones were analyzed by PCR using the primers *IDL1* attB1, *IDL1* attB2, *IDL2* attB1, *IDL2* attB2, *IDL3* attB1 and *IDL3* attB2. By sequencing the clones using the primers within the vector sequence, 35SL and smGFPR, it was confirmed that the *IDL1*, *IDL2* and *IDL3* sequences were in the correct reading frame with the *GFP* gene sequence.

2.3.8.3 Overexpression constructs

The attB flanked PCR products were amplified using the primers *IDL1* attB1, *IDL1* stop-attB2, *IDL2* attB1, *IDL2* stop-attB2, *IDL3* attB1 and *IDL3* stop-attB2. The PCR products containing the coding sequences of the *IDL1*, *IDL2* and *IDL3* genes were recombined into the pDONR™/zeo. The entry clones were analyzed using the same primers that were used making the attB flanked PCR products.

The entry clones were recombined with the destination vector pK7WG2 (Karimi et al., 2005) which contains the constitutive promoter 35S. The expression clones were analyzed by PCR using the primers *IDL1* attB1, *IDL1* stop-attB2, *IDL2* attB1, *IDL2* stop-attB2, *IDL3* attB1 and *IDL3* stop-attB2 and by sequencing using the primer 35SL.

2.4 Polymerase chain reaction (PCR)

PCR was used for amplification of desired DNA fragments for cloning, screening for positive bacteria colonies, genotyping of T-DNA mutants, RT-PCR and RACE. Standard set up for one reaction was 1x reaction buffer, 200 µM dNTP (deoxyribonucleotide triphosphate), 0.2 µm primers, and 0.5-1 U DNA polymerase (DyNAzyme™ II DNA Polymerase (Finnzymes) or BD Advantage™ 2 Polymerase Mix (BD Bioscience Clonetech)). A negative control was always included.

Dynazyme is a thermostable polymerase for standard PCR such as screening. Advantage 2 Polymerase Mix includes a TaqDNA polymerase, a small amount of proofreading polymerase and TaqStart Antibody. This gives accurate and convenient amplification of DNA, and makes it suitable for cloning. Both polymerases generate a 3' A-overhang which facilitates ligation into a TOPO vector (see section 2.3.7)

All programs used were variations of the general program: 94ºC 5 min., 94ºC 20 sec., 52-68ºC 15-30 sec., 72ºC 3 min., 72ºC 7 min., and 4ºC ∞.

2.5 Reverse transcriptase PCR (RT-PCR)

RT–PCR was used to quantify the expression of *IDL1* in the RNAi transgenic lines and of *IDL3* in the SALK_065248 (Salk *IDL3*) lines and for RACE. RT-PCR can be used as a semi-quantitative method to investigate the expression level of a gene. First total RNA is isolated from a specific tissue, then first strand cDNA is synthesized using a reverse transcriptase enzyme, finally gene specific primers are used in a PCR reaction.

2.5.1 Isolation of total RNA (QIAGEN)

Total RNA was extracted from 100 mg N_2-frozen tissue using RNeasy Plant Mini Kit (QIAGEN). The procedure was performed according to the manual. The tissue was homogenized in liquid nitrogen and the lysed under denaturing conditions. The plant lysate was centrifuged through a QIAshredder™ homogenizer to remove insoluble material. Ethanol was added to provide selective binding of RNA to a silica-gel membrane, and then the sample

was applied to an RNeasy mini column where total RNA bound to the membrane. Removal of DNA from the sample was done as an on-column DNase digestion with the RNase-free DNase set (QIAGEN). The RNA was eluted in DEPC-water and stored at -80ºC.

2.5.2 Checking the RNA integrity

To check the RNA integrity isolated RNA was analyzed by agarose gel electrophoresis. The 28S and 18S rRNA (ribosomal RNA) bands should appear as strong bands and mRNA should appear as a smear.

2.5.3 Quantification of RNA

RNA was quantified on a Lambda 25 UV/Vis spectrophotometer (Perkin Elmer).

2.5.4 cDNA synthesis (Invitrogen)

First strand cDNA was synthesized from the isolated total RNA using the SuperScript™ III First Strand Synthesis System for RT-PCR (Invitrogen). Negative controls were used in which the reverse transcriptase was omitted. The reaction was performed as described in the manual.

2.5.5 RT-PCR reactions

For amplification in the PCR reaction DyNAzyme™ II DNA Polymerase (Finnzymes) was used and 2 µl of the first strand reaction was used as a template. *ACTIN 2-7* primers were used to control the quality and amount of first strand cDNA.

2.6 Rapid amplification of cDNA ends (RACE)

RACE was used to identify the 5' and 3' untranslated regions (UTRs) of *IDL2* and *IDL3*. The GeneRacer™ Kit from Invitrogen was used and the experiment was performed as described in

the instruction manual. An adapter sequence (RNA oligo) is added to the 5' end of mRNA to create a known priming site at the 5' end. An oligo dT primer is used as a 3' end primer. To obtain full-length 5' and 3' ends of cDNA, first strand cDNA is amplified using a gene specific primer and either a primer specific to the adapter sequence or an oligo dT primer. The PCR products are then cloned into a TOPO vector.

2.6.1 Ligating the RNA oligo to mRNA

To prepare the RNA, total RNA was extracted from 100 mg N_2-frozen seedlings using RNeasy Plant Mini Kit (QIAGEN) (see section 2.5.1). RNA concentration was quantified and the integrity was checked (see sections 2.5.2 and 2.5.3). To eliminate truncated mRNA or non-mRNA, the RNA was treated with calf intestinal phosphatase (CIP); this removes the 5' phosphates. Then the mRNA cap structure was removed treating the RNA with tobacco acid phosphatase (TAP) this leaves a 5' phosphate which is required for ligation of the RNA oligo. The GeneRacer™ RNA Oligo was ligated to the 5' end of the mRNA using T4 RNA ligase.

2.6.2 Reverse transcribing mRNA

The mRNA was reverse transcribed into cDNA using SuperScript™ III RT (Invitrogen).

2.6.3 Amplifying cDNA ends

The 5' and the 3' ends of *IDL2* and *IDL3* was amplified using Platinum® Taq DNA Polymerase High Fidelity and the primers *IDL2* RACE 5', *IDL2* RACE 3', *IDL3* RACE 5', *IDL3* RACE 3', GeneRacer™ 5' and GeneRacer™ 3'. The reactions were run according to the manufacturers' recommendation using hot start and touchdown PCR. The hot start PCR method minimizes mispriming and extension, and touchdown PCR increases specificity and reduces background amplification. The GeneRacer primers and the gene-specific primers are designed to have a high annealing temperature which allows only desired product to accumulate.

The cycling parameters were as following: 94°C 2 min, 94°C 30 sec and 72°C 1 min repeated 5 times, 94°C 30 sec and 70°C 1 min repeated 5 times, 94°C 30 sec, 66°C 30 sec and 68°C 1 min repeated 25 times, and finally 68°C 10 min.

After PCR the reactions were analyzed on an agarose gel.

2.6.4 Cloning and sequencing the PCR products

The PCR products of assumed correct size were purified from agarose gel (see section 2.3.2) and cloned into the pCR®4-TOPO® vector (see section 2.3.7) using TOPO TA Cloning® Kit for sequencing (Invitrogen). The products were sequenced in both directions using the primers M13 forward (F) and M13 reverse (R).

2.7 Subcellular localization of protein-GFP constructs

20mg gold (1.0 mikron, BioRad) was resuspended in 100% EtOH and pelleted. The gold was washed in dH_2O and resuspended in 50% glycerol, to a concentration of 20µg/µl for storage at 4°C.

For shooting the gold was added (in order), 1µg DNA, 25 µl 2.5M cold $CaCl_2$, and 10µl 100µM cold spermidine. After vortexing for 3 min, the gold/DNA was pelleted and washed twice, first in 70% EtOH, then in 100% EtOH. The gold/DNA was finally resuspended in 100% EtOH.

The gold was placed on macro-carrier, and shot at onion cells with a pressure of 1350psi.

2.8 Sequencing

Sequencing was performed with a MegaBACE™ 1000 instrument using a DYEnamic ET Dye Terminator Cycle Sequencing Kit (Amersham Biosciences) provided by the sequencing facility at the Department of Molecular Biosciences (IMBV).

2.9 Bioinformatics

To characterize the T-DNA flanking regions database searches were performed using the universal Basic local alignment search tool (BLAST) engine (Altschul et al., 1990) at the National Center for Biotechnology Information (NCBI http://www.ncbi.nlm.nih.gov/). For primerdesign Primer3 (http://frodo.wi.mit.edu/cgi-bin/primer3/primer3_www.cgi) was used. To find endonuclease restriction sites for various DNA sequences and for DNA analysis the Vector NTI v 9.0.0 (Informax) was used.

2.10 Statistics

2.10.1 Chi-square test

The chi-square test is based on a measure of the discrepancy existing between an observed and expected frequency as supplied by the statistic χ^2 (chi-square), given by the formula; $\chi^2 = \Sigma\ (O\text{-}E)^2 / E$, where O is the observed value and E is the expected value. Expected values are computed on the basis of our hypothesis. A 0.05% confidence and 1 degree of freedom was used in this test, and for $\chi^2 < 3.84$ the hypothesis holds with 95% accuracy and is not rejected.

2.10.2 Two-sample T-test

In the two-sample T-test the null hypothesis is defined in the form that there is no difference between the population means. The T-value is given by the formula $T = \left|\overline{Y}_1 - \overline{Y}_2\right| / \sqrt{(s_1^2 / n_1) + (s_2^2 / n_2)}$ where n_1 and n_2 are the number of samples in group 1 and 2, respectively, $\overline{Y}_1$ and $\overline{Y}_2$ are the sample means, and s_1^2 and s_2^2 are the sample variances (variance=σ^2 where σ is the standard deviation). In an unpaired T-test there are $n_1 + n_2 - 2$ degrees of freedom. A 0.05 significance value and 38 degree of freedom was used in the test and for $|T|>2.02$ we would reject the null hypothesis meaning that the population means are different with 95% accuracy.
(http://www.itl.nist.gov/div898/handbook/eda/section3/eda353.htm)

3 RESULTS

In this thesis the genes *AtIDL1*, *AtIDL2* and *AtIDL3* have been investigated. The expression pattern of the three genes has been examined by promoter::reporter gene analyses. In order to investigate the subcellular localization of the three IDL proteins, fusion proteins between the IDL proteins and the green fluorescent protein (GFP) for both the transient onion epidermis expression assay and for stable GFP expression *in planta* were made. Two SALK lines containing T-DNA insertions upstream of *IDL2* and *IDL3* were identified and investigated. Since no mutant phenotypes were observed among the Salk *IDL2* and Salk *IDL3* plants and no SALK line was available for *IDL1*, we generated RNAi lines for the three genes as an alternative method to study loss-of-gene function. Transgenic plants overexpressing *IDL1*, *IDL2* and *IDL3* were generated in order to investigate whether overexpression of the *IDL* genes would cause any mutant phenotype.

3.1 Analyses of promoter::reporter gene plants- the GUS assay

The expression pattern of *IDL1*, *IDL2* and *IDL3* had been crudely identified by RT-PCR (Butenko et al., 2003). *IDL1* was expressed in roots, *IDL2* in all organs but weaker in roots and seeds, and *IDL3* in flowers and seedlings. One method to investigate the temporal and spatial expression pattern of a gene in more detail is to use the β-glucuronidase (*GUS*; *uidA*) reporter gene system. The promoter region of the gene of interest is cloned in front of the *GUS* gene and will regulate the GUS expression. The GUS protein will be expressed according to the expression pattern of the given gene. The promoter::reporter gene constructs for the three *IDL* genes were made by Melinka A. Butenko and transformed into wt *Arabidopsis* (unpublished results). The promoter fragments, which included 1555, 1864 and 1908 bp upstream of the ATG of *IDL1*, *IDL2* and *IDL3* respectively, were cloned in front of the *GUS* gene in the vector pPZP211G-GAWI (figure 3.1).

Figure 3.1 The GUS constructs. The promoter regions of *IDL1*, *IDL2* and *IDL3* were cloned in front of the β-glucoronidase (*GUS*) gene in the vector pPZP211G-GAWI. The promoter fragments included 1555, 1864 and 1908 bp upstream of the ATG of *IDL1*, *IDL2* and *IDL3* respectively. t-Nos: Nos terminator, *nptII*: neomycin phosphotransferase, RB: right border, LB: left border. The figure is not to scale.

3.1.1 Investigation of the GUS expression in primary transformants

Primary transformants harboring the promoter::reporter gene constructs for the three *IDL* genes were investigated for GUS expression. Nine, ten and eight independent lines were examined for the *IDL1::GUS*, *IDL2::GUS* and *IDL3::GUS* transgenic plants, respectively. Tissues from above ground organs were incubated in X-gluc mixture at 37˚C over night (see materials and methods, section 2.1.4.1). As expected from the RT-PCR results, *IDL1::GUS* expression was just observed in aerial tissues in a couple of the primary transformants investigated. Therefore the T2 generation was examined for GUS expression in the roots. Eight lines carrying the *IDL2::GUS* construct expressed GUS, whereas five lines containing the *IDL3::GUS* construct showed GUS expression.

3.1.2 Segregation analysis

To gain information on the number of T-DNA loci in the GUS transgenic lines, the *nptII* segregation pattern in the T2 generations was examined by growing seedlings on Km-containing plates. The ratio of the segregation of kanamycin resistant (Km^r) to kanamycin sensitive (Km^s) seedlings indicates into how many independently loci the T-DNAs are integrated into in the plant genome. Segregation analysis was performed on seven transgenic lines for the *IDL1*-promoter::GUS construct, and on five transgenic lines for the *IDL2*-promoter::GUS and *IDL3*-promoter::GUS constructs (see table 3.1). After two weeks the segregation of Km^r and Km^s seedlings were scored and the number of T-DNA insertions predicted. A line containing one independent locus of the T-DNA insertion is expected to give a 3:1:Km^r:Km^s segregation ratio in the T2 generation. One with two independent loci is expected to segregate progeny in a 15:1:Km^r:Km^s ratio, whereas a line containing three independent loci is expected to segregate in a 63:1:Km^r:Km^s ratio. To establish if there was evidence that the T-DNA segregated as one, two or three Mendelian loci, the hypotheses were tested with the chi-square test of significance (materials and methods, section 2.10.1) (3:1:Km^r:Km^s, 15:1:Km^r:Km^s and 63:1:Km^r:Km^s). Expected values were computed on the basis of

our hypotheses. For a $\chi^2 < 3.84$ a hypothesis holds with 95% accuracy. The results are shown in table 3.1. For *IDL1::GUS*, six lines containing one T-DNA locus were identified. Among the *IDL2::GUS* transgenic lines three lines containing one locus were identified while two lines probably contained either two or three T-DNA loci. For *IDL3::GUS* there were identified three lines containing one T-DNA locus, one line containing two and one line containing three loci.

Table 3.1 Observed number of Km^r and Km^s T2 seedlings in the GUS lines for *IDL1*, *IDL2* and *IDL3*. The number of expected Km^r and Km^s plants for each hypothesis (3:1, 15:1 and 63:1) for each independent line was computed. Then the χ^2-values for Km^r and Km^s plants for each hypothesis were computed (data not shown) and thereafter these χ^2-values were summed up to give the total χ^2-value for each hypothesis. The segregation patterns 3:1, 15:1 and 63:1 corresponds to one, two and three independently integrated T-DNA loci, respectively. The hypotheses were tested with the chi-square test of significance in which total χ^2-value should be less than the critical value of 3.84. The χ^2-values written in bold mean that the hypothesis holds with 95% accuracy.

GUS Line	Obs Km^r/Km^s	Exp # Km^r/Km^s 3:1	Exp # Km^r/Km^s 15:1	Exp # Km^r/Km^s 63:1	χ^2 3:1	χ^2 15:1	χ^2 63:1
IDL1							
IDL1-5	20 / 7	20.3 / 6.8	25.3 / 1.7	26.6 / 0.4	**0.0**	17.84	104.2
IDL1-10	32 / 27	44.3 / 14.8	55.3 / 3.7	58.1 / 0.9	13.6	157.21	749.4
IDL1-11	25 / 9	25.5 / 8.5	31.9 / 2.1	33.5 / 0.5	**0.0**	23.73	137.1
IDL1-13	86 / 23	81.8 / 27.3	102.2 / 6.8	107.3 / 1.7	**0.9**	41.03	270.5
IDL1-15	116 / 43	119.3 / 39.8	149.1 / 9.9	156.5 / 2.5	**0.4**	117.33	671.2
IDL1-17	48 / 12	45.0 / 15.0	56.3 / 3.8	59.1 / 0.9	**0.8**	19.36	132.6
IDL1-44	68 / 27	71.3 / 23.8	89.1 / 5.9	93.5 / 1.5	**0.6**	69.70	445.6
IDL2							
IDL2-9	49 / 0	36.8 / 12.3	45.9 / 3.1	48.2 / 0.8	16.3	**3.27**	**0.8**
IDL2-17	47 / 21	51.0 / 17.0	63.8 / 4.3	66.9 / 2.1	**1.3**	70.42	380.1
IDL2-29	98 / 35	99.8 / 33.3	124.7 / 8.3	130.9 / 2.1	**0.1**	91.39	529.8
IDL2-30	69 / 33	76.5 / 25.5	95.6 / 6.4	100.4 / 1.6	**2.9**	118.61	628.7
IDL2-51	289 / 10	224.3 / 74.8	280.3 / 18.7	294.3 / 4.7	74.80	4.31	6.2
IDL3							
IDL3-3	88 / 23	90.8 / 30.3	113.4 / 7.6	119.1 / 1.9	**1.80**	37.22	243.8
IDL3-10	257 / 79	252.0 / 84.0	315.0 / 21.0	330.8 / 5.2	**0.4**	170.87	1052.5
IDL3-12	220 / 6	169.5 / 56.5	211.9 / 14.1	222.5 / 3.5	60.2	4.99	**1.8**
IDL3-18	150 / 0	112.5 / 37.5	140.6 / 9.4	147.7 / 2.3	50.0	10.0	**2.4**
IDL3-20	326 / 108	325.5 / 108.5	406.9 / 27.1	427.2 / 6.8	**0.0**	257.21	1534.8

3.1.3 *IDL1::GUS* expression

Since RT-PCR showed expression of *IDL1* in roots of 14 day-old seedlings, the T2 generation was examined for GUS expression in roots. Six lines which contained one locus of the

reporter-gene construct and one line (*IDL1-10*) with an unknown number of T-DNA loci were included in the study. All seven lines showed GUS expression in the root tips and the root differentiation zone. In addition to the root expression, four lines showed either a weak or a strong GUS expression in the shoot meristem and in the rosette leaves (results not shown). To determine if *IDL1::GUS* was expressed in aerial tissues of mature flowering plants, the seven lines expressing GUS in roots were examined for GUS staining in above ground organs. For five lines no GUS expression was detected at all, however expression was seen in the stem tissues and at some of the bases of the pedicels in two of the lines (results not shown).

Since the RT-PCR data showed *IDL1* root expression, and the *IDL1::GUS* expression in the roots was similar for all plants examined, we chose to concentrate the further investigation of the *IDL1* expression on the root and root cap. Two lines with one T-DNA locus that showed no expression in aerial tissues of mature plants were investigated further in the T2 and T3 generations. In addition three day-old seedlings were examined in line *IDL1-10* (unknown loci of T-DNA insertions).

3.1.3.1 The root cap expression of *IDL1*

The *IDL1::GUS* root tip expression was detected in both the primary and the lateral roots (figures 3.2, 3.3 and 3.4). The expression was specific to the two outermost cell layers of the columella root cap. The root cap columella cells contain amyloplasts which can be visualized with 1% Lugol solution. To confirm that *IDL1* was expressed in the columella cells, 14 day-old GUS stained seedlings were treated with Lugol solution (see materials and methods, section 2.1.4.2). The results showed that the GUS staining was localized to the same cells as the starch granules and also that there was a columella cell layer above the GUS stained cells (figure 3.2 D).

Root cap cells are continuously shed from the root tip as the root grows through the soil. It was interesting to note that *IDL1::GUS* expression was not only seen in cells that were still attached to the root, but also in cells that had been shed (figure 3.2 C).

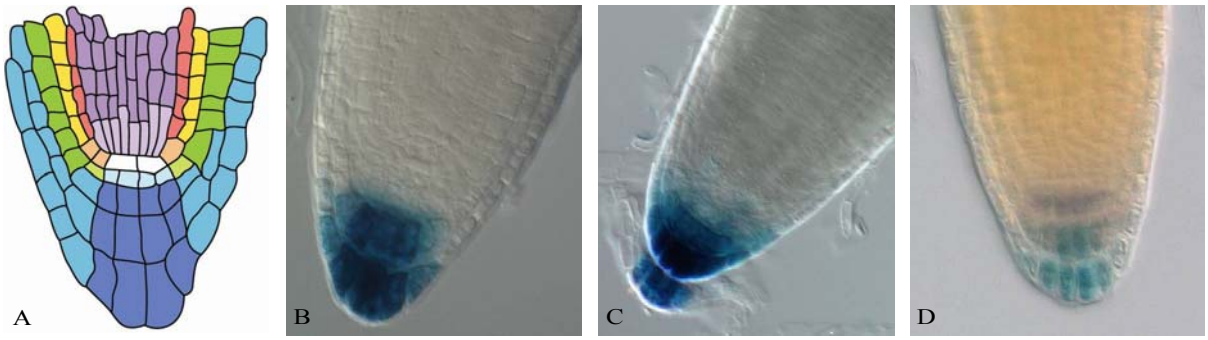

Figure 3.2 (A) The *Arabidopsis* root tip: Columella root cap (blue), lateral root cap (turquoise), epidermis (green), cortex (yellow), endodermis (pink), stele (purple), the corresponding initial cells are in lighter color at the base of each cell file. Initial cells surround the QC (quiescent center) (white). (B, C and D) GUS stained roots of 14 day-old seedlings. (B and C) *IDL1::GUS* expression in the two outermost columella cell layers (B-T3 generation). (C) GUS staining in columella cells that are still attached and in cells that have been shed from the root tip (T2). (D) Purple colored starch visualized in the columella cells (T3).

3.1.3.2 The onset of the *IDL1* root expression

To determine the onset of the *IDL1* expression, GUS staining was performed daily on seedlings grown on agar plates. No expression was detected during the initial emergence of the primary root (figure 3.3 A), but 36 hours post-germination a weak *IDL1::GUS* expression was detected in the primary root tip (figure 3.3 B). Similarly, no *IDL1* expression was detected at the emergence of lateral roots, but later in development expression was observed in the lateral root tips (figure 3.4). In both primary and secondary roots the expression was initially localized to the center of the outermost layer of the root tip (figures 3.3 B and 3.4 B). GUS activity was also observed in root-tips of six week-old plants grown in soil (data not shown).

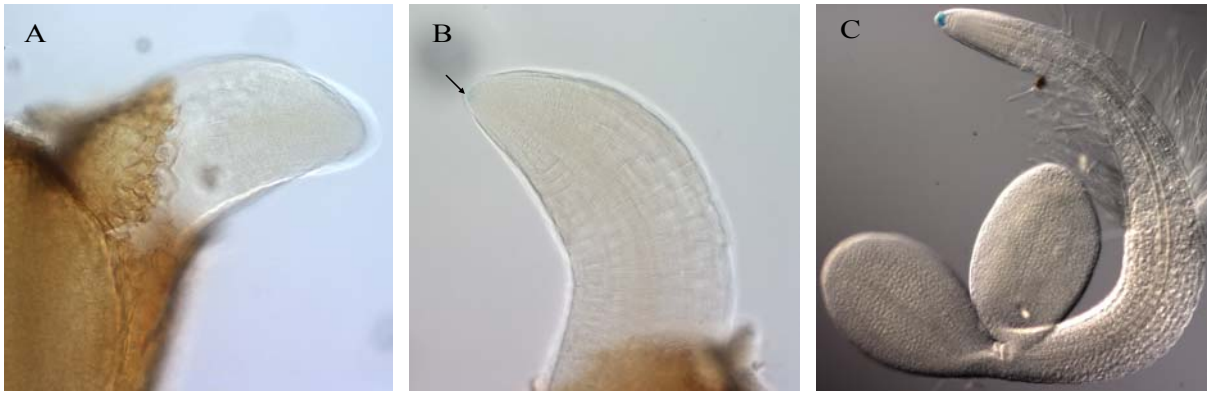

Figure 3.3 The onset of *IDL1* expression. (A) At 24 hours post-germination no *IDL1::GUS* expression was detected (T3). (B) The *IDL1* expression began in the primary root tip around 36 hours post-germination (T3). (C) Three day-old seedling (line *IDL1-10* T2).

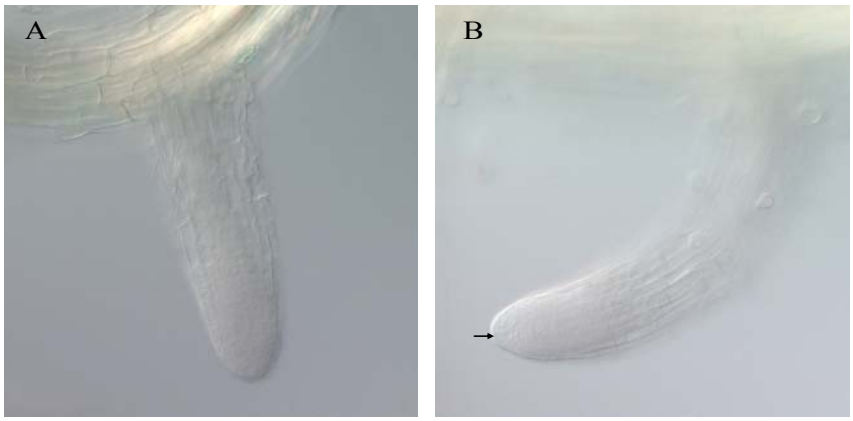

Figure 3.4 The onset of *IDL1* in lateral roots (T3). (A) Secondary root before *IDL1* expression starts. (B) Secondary root just starting to express GUS.

3.1.3.3 *IDL1* was expressed in the root differentiation zone

In addition to being expressed in the root cap, *IDL1::GUS* activity was also seen in the differentiation zone (figure 3.5). The expression was seen in the epidermal tissue in the root differentiation zone.

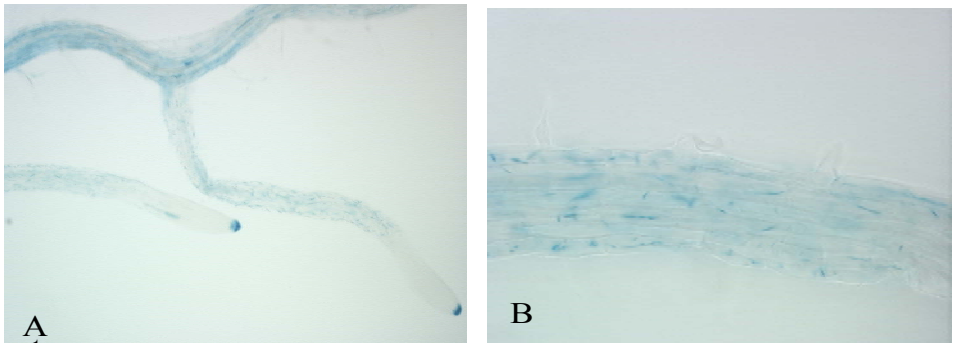

Figure 3.5 (A and B) GUS expression in the differentiation zone (T3).

3.1.4 *IDL2::GUS* expression

For the *IDL2::GUS* transgenic plants, five independent lines were investigated for GUS activity in the T2 generation. These lines contained both one and two loci of the *IDL2::GUS* construct, but no significant variation was found between the lines. In the aerial parts of mature flowering plants, GUS expression was detected in the floral organ abscission zones, at the base of the pedicels, and in the top-most region of the stem. Two lines containing one locus were GUS stained as 14 day-old seedlings, the GUS expression was observed in the rosette leaves, the shoot meristem, the root cap, and the vascular tissue of the root. T2 and T3 plants from these two lines were used in further investigation of the *IDL2::GUS* expression.

In-depth analyses were performed on the root cap expression, the meristem expression, and the abscission zone expression.

3.1.4.1 The *IDL2* root cap expression was limited to the lateral roots

To determine the onset of *IDL2* expression in the root cap, seedlings were examined daily for GUS staining. No *IDL2::GUS* expression was detected in the primary root during seedling development (figure 3.6 A). In seven day-old seedlings expression was observed in the lateral root caps (figure 3.6 B), and still no expression was detected in the primary root (figure 3.6 C). When both 10 and 14 day-old seedlings were investigated, it was confirmed that *IDL2* expression was limited to the lateral root tips. GUS activity was also observed in root tips of 6 week-old plants grown in soil (data not shown).

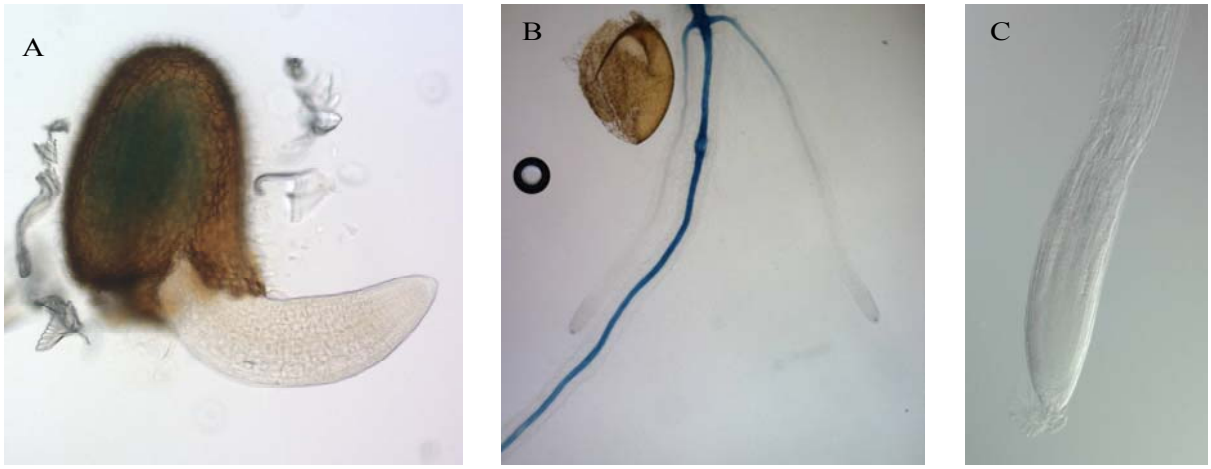

Figure 3.6 The *IDL2* root cap expression was limited to the secondary roots (T3). (A) GUS expression in the early embryo, 24 hours postgermination. (B) Seven day-old seedling expressing GUS in the root caps of lateral roots, (C) but not in the primary root. (B) Expression was also detected in the root vascular tissue.

3.1.4.2 The *IDL2* root cap expression was specific to the columella cells

The *IDL2::GUS* expression was observed in the root tip. In contrast to the columella initial cells, the columella root cap cells contain starch. To determine whether *IDL2* was expressed in the columella cells or the in the initials, 14 day-old GUS stained seedlings were treated with Lugol solution. Starch granules were seen in the GUS stained cells; this demonstrated that *IDL2* was localized to the columella cells (figure 3.7 C). In contrast to *IDL1* (figure 3.7 A), *IDL2* was not expressed in the outermost columella cell layer, but in the two cell layers above (figure 3.7 B).

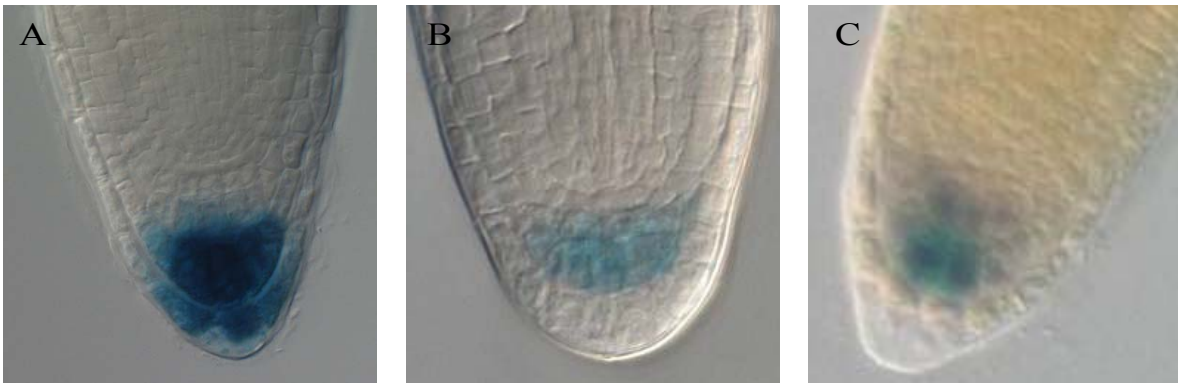

Figure 3.7 *IDL2* expression in the columella cells in 14 day-old seedlings (T3). (A) The *IDL1* expression is in contrast to *IDL2* detected in the outermost columella cell layer in addition to the second columella layer. (B) The *IDL2* expression is localized to the second columella cell layer. (C) Visualized starch demonstrates that *IDL2* is expressed in the columella cells.

3.1.4.3 The meristem expression of *IDL2*

When seedlings were examined for GUS staining, a strong *IDL2::GUS* activity was seen in the shoot apical meristem. The first expression was found as soon as the meristem was visible, approximately 48 hours post-germination (figure 3.8 A); however *IDL2::GUS* expression was also seen in the early embryo at 24 hours postgermination (figure 3.6 A). In addition to the meristem expression, GUS was seen in the cotyledons (figure 3.8). The *IDL2::GUS* signal persisted and increased in intensity during seedling development (see figure 3.8 A showing a two day-old seedling and figure 3.8 D showing a seven day-old seedling).

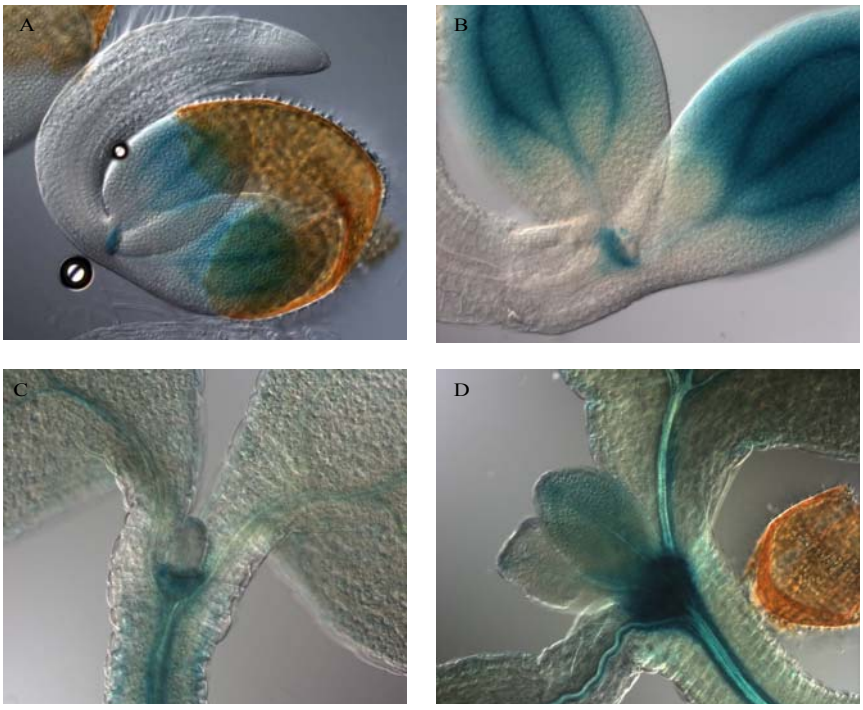

Figure 3.8 The *IDL2::GUS* meristem expression. (A) The first meristem expression was visible 48 hours post-germination, in addition GUS was seen in the cotyledons (T2). (B) Three day-old seedling expressing GUS in the meristem and the cotyledons (T2). (C) Five day-old seedling expssing GUS in the meristem and in the vascular strands of the cotyledons, the cotyledon petiols, and the hypocotyls (T3). (D) Seven day-old seedling showing a strong GUS activity in the meristem, in addition GUS was seen in the vascular strands of the cotyledons, the cotyledon petiols, and the hypocotyl and in the emerging rosette leaves (T3).

3.1.4.4 The abscission zone expression of *IDL2*

To investigate the abscission zone expression pattern of *IDL2* in more detail, flowers were numbered corresponding to their position on the inflorescence and stained for GUS activity (figure 3.9). Position 1 is the flower at anthesis, when carpels, anthers, and petals are of approximately similar lengths. *IDL2::GUS* activity was not seen in flowers at positions 1 and 2. At position 3 a weak *IDL2::GUS* expression was detected in the floral organ abscission zone. The weak signal persisted throughout position 8 and at position 9 the GUS activity increased in intensity. The strong signal was maintained throughout position 12, after which the activity decreased and persisted until position 18. In summary, the *IDL2::GUS* activity was at its strongest after the abscission process had taken place and all floral organs were abscised.

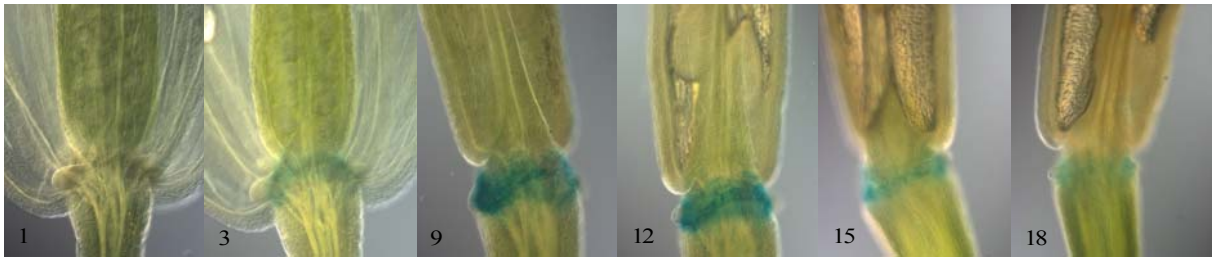

Figure 3.9 *IDL2::GUS* abscission zone activity. Developmental assay showing stage-specific abscission zone expression from position 1 to 18. Arabic numerals indicate flower positions on the inflorescence. (T3)

3.1.5 *IDL3::GUS* expression

IDL3::GUS transgenic plants were examined for GUS expression in the T2 generation. Four independent lines which contained either one or more loci of the *IDL3::GUS* construct were investigated. In the aerial parts of mature plants *IDL3::GUS* activity was detected at the base of the pedicels in all four lines (figure 3.10 F). GUS expression was also seen in the abscission zones in three of the lines (figure 3.10 E) and in the buds in two of the lines (figures 3.10 D). When 14 day-old seedlings were GUS stained, GUS activity was observed in the rosette leaves (data not shown), at the border sites in the lateral roots and in some of the root tips (figure 3.10 C). The root tip expression looked similar to the *IDL2* root cap expression, and was presumably specific to the columella cells. The first *IDL3::GUS* expression was detected in two day-old seedlings in the vascular tissue of the cotyledons (figure 3 .10A). In three day-old seedlings the expression spread to the vascular tissue of the hypocotyl and throughout the cotyledons (figure 3.10 B).

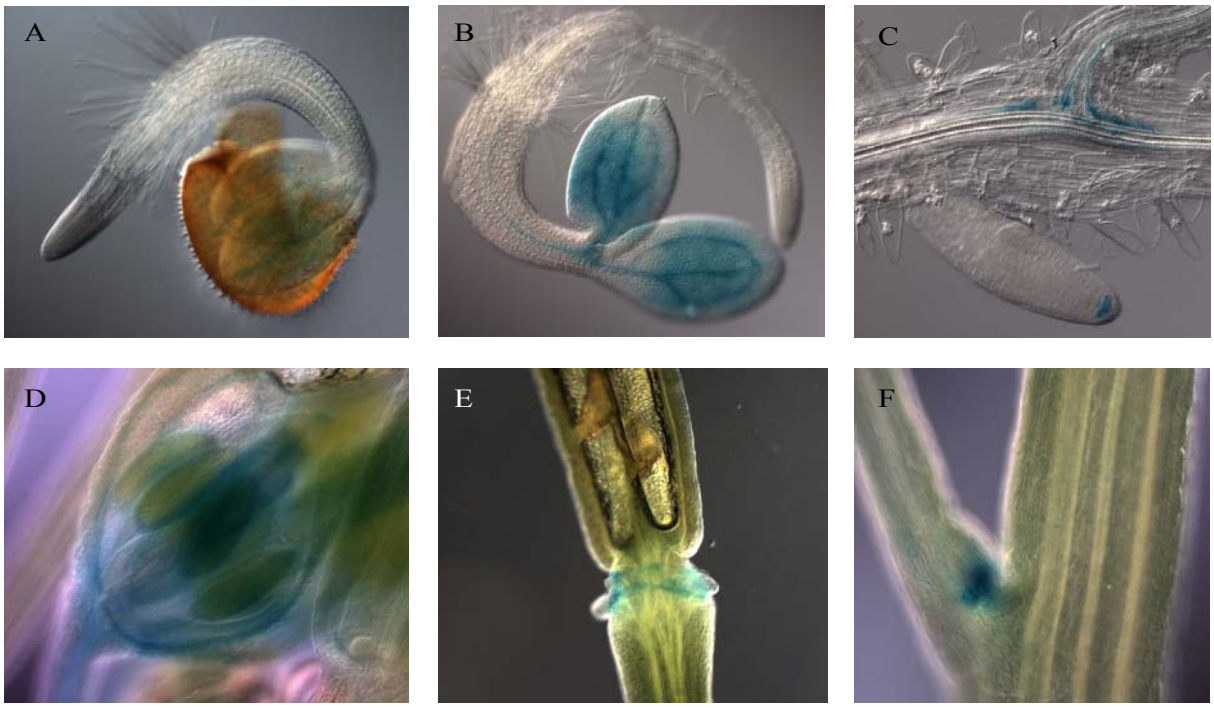

Figure 3.10 *IDL3::GUS* expression (T2). (A) GUS expression in two day-old seedlings was detected in the vascular tissue of the cotyledons. (B) GUS expression in three day-old seedlings was seen in the vascular tissue of the cotyledons and the hypocotyl and throughout the cotyledons. (C) In 14 day-old seedlings GUS expression was detected in the root tips and in the border lines of the lateral roots. In mature flowering plants GUS expression was seen in the buds (D), the abscission zones (E) and at the base of the pedicels (F).

The results of the *IDL3::GUS* expression are preliminary, they have not been investigated in much detail, and variance has been found between the transgenic lines.

3.2 The subcellular localization assay

The *IDA-LIKE* genes are putative ligands, they encode proteins that have predicted N-terminal signal sequences (Butenko et al., 2003). This suggests that the proteins are secreted from the cell, and are localized in the extracelluar space. To investigate the subcellular localization of the IDL1, IDL2 and IDL3 proteins, translational fusions between the coding sequences of the three *IDL* genes and the green fluorescent protein (GFP) were made using the Gateway system. GFP-constructs were used both in the onion epidermis transient expression assay and in GFP-expression *in planta*.

3.2.1 The onion epidermis cell bombardment

The entry clones containing the *IDL1*, *IDL2* and *IDL3* cds (coding sequence) were recombined with the destination vector pKEGAW-c.1-smGFP (see materials and methods,

section 2.3.8.2). Onion epidermis cells were bombarded with these constructs, pAVA 393 (von Arnim et al., 1998), which contains only the GFP sequence was used as a control. The assay was repeated five times, only two times did the positive control give results and the expression was just seen in one or two cells. The control gave, as expected, GFP expression in the whole cell (data not shown). Neither of the IDL::GFP constructs gave results. The reason for the lack of expression could be due to problems during the coating of gold with DNA, which leads to particle agglomeration. High humidity conditions during the drying of the DNA coated gold particles can also lead to particle aggregation. The quality of the onion cells is also a critical point.

3.2.2 GFP expression *in planta*

Since no results were obtained in the onion epidermis transient expression assay, constructs for GFP-expression *in planta* were made. GFP-expression *in planta* gives a more reliable result since the protein fusions are expressed under natural conditions. The entry clones containing the *IDL1*, *IDL2* and *IDL3* cds were recombined with the destination vector pTA7002 GAW-GFP (see materials and methods, section 2.3.8.2) which contains an inducible transcription system (figure 3.11).

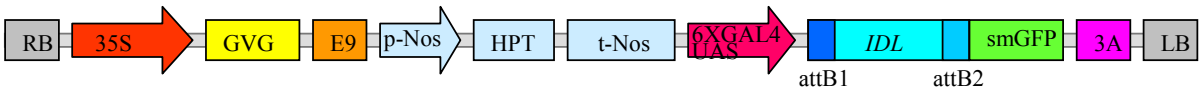

Figure 3.11 The GFP-constructs. The pTA7002 GAW-GFP contains the glucocorticoid receptor domain, VP16 transactivation domain, and the GAL4 DNA binding domain (GVG) driven by the 35S promoter. *IDL1*, *IDL2* and *IDL3* (*IDL*) were inserted downstream the cis-elements (6XGAL4 UAS) and fused to the *green fluorescent protein* (smGFP) gene. E9: pea rbcs-E9 terminator, p-Nos: Nos promoter, *HPT*: *hygromycin phopsphotransferase*, 3A: pea rbcs-3A terminator, RB: right border, LB: left border. The figure is not in scale.

The *GVG* gene consists of the hormone binding domain from the glucocorticoid receptor, the VP16 transactivation domain, and the GAL4 DNA binding domain. *GVG* is driven constitutively by a 35S promoter. The vector sequence contains six GAL4 UASs (upstream activating sequences) where GVG binds. When dexamethasone (a glucocorticoid) is added, it binds to GVG and activates transcription of the sequences downstream of the UAS. The three *IDL* genes were inserted downstream of 6XGAL4 UAS and fused to the *GFP* gene sequence. In the presence of dexamethasone, the expression of the IDL-GFP fusion protein is induced.

Agrobacterium was transformed with the expression clones. Correct colonies were confirmed by PCR and transformed into wt Col *Arabidopsis*. Primary transformants were selected on agar medium containing hygromycin and 30 transformants for each construct were transferred to soil to obtain their seeds. Three independent lines from each of the constructs were randomly chosen for GFP analysis in the T2 generation. To induce the IDL-GFP fusion expression, seeds were sown on agar medium containing dexamethasone and hygromycin. Plates without antibiotics and chemicals, as well as plates containing hygromycin and dexamethasone separately were used as control plates. Wild type *Arabidopsis* was used as a negative control. After ten days the transgenic plants were investigated for GFP expression in the roots using a fluorescent magnifier. For the plants containing the IDL1-GFP and IDL2-GFP fusion constructs no GFP expression was observed, about 100 siblings from each line were examined. For the IDL3-GFP construct, roots expressing GFP were observed. These plants were examined further using fluorescence confocal microscopy. IDL3-GFP was localized to the periphery of the cell (figures 3.12 A, B and C), and the expression pattern was common for all the induced siblings in the three independent lines investigated. By segregation analysis it was determined that two lines contained one locus of the GFP construct and one line contained two loci (data not shown). The wild type control did show some autofluorescence distributed over the whole cell (figure 3.12 D), but the IDL3-GFP signal was stronger compared to the wild type autofluorescence. The controls gave expected results.

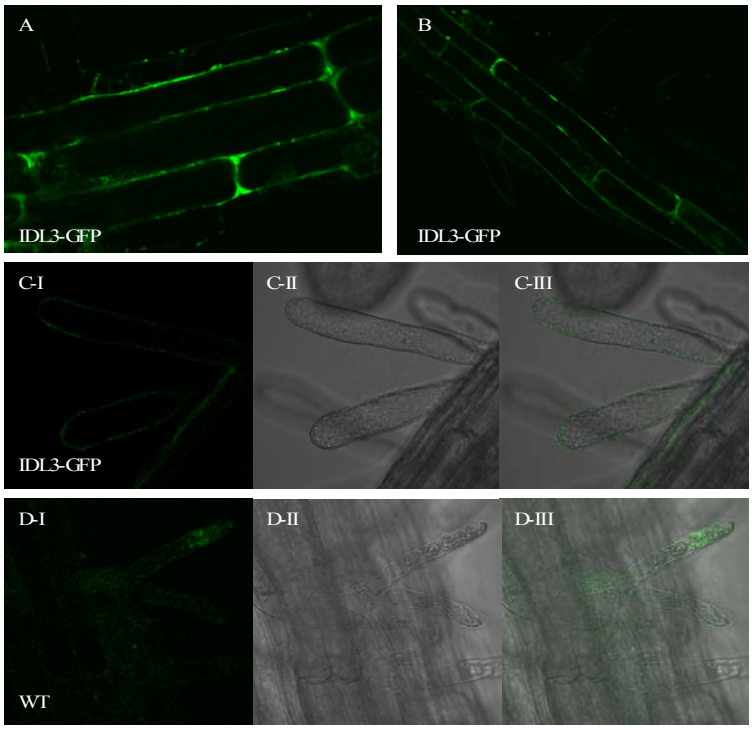

Figure 3.12 Subcellular localization. Root cells from *Arabidopsis* seedlings expressing IDL3-GFP fusion construct were investigated using fluorescence confocal microscopy. (A, B and C) IDL3-GFP was localized to the periphery of the cell. (C-II) Black/white section through a root hair cell. (C-III) An overlay between the GFP-expression and the black/white section demonstrated that IDL3-GFP was localized to the periphery of the cell and not to the cytoplasm. (D) In the wild-type negative control, autofluorescence was observed throughout the cell.

3.3 Identifying knock-out T-DNA lines

The Salk lines are T-DNA insertion lines generated by transformation of plants with *Agrobacterium tumefaciens* containing the vector pBIN-pROK2. The lines are distributed by The Arabidopsis Biological Resource Center (ARBC) and the Nottingham Arabidopsis Stock Center (NASC). The T-DNA insertion sites are identified by The Salk Institute Genome Analysis Laboratory (SIGnAL) (Alonso et al., 2003) and are available in the T-DNAExpress database (http://signal.edu/cgi-bin/tdnaexpress). The identifications of the insertion sites are high throughput operations and the exact location must be confirmed by sequencing the genomic region flanking the left border of the T-DNA.

To study loss-of-function mutations of the three *IDL* genes, the SIGNAL database was searched for lines with T-DNA insertions within *IDL1*, *IDL2* and *IDL3*. No Salk line with a T-DNA insertion closer than 1000 bp to the *IDL1* was identified. SALK_022068 and SALK_065248 are predicted to contain T-DNA insertions 252 and 60 bp upstream of the coding regions of *IDL2* and *IDL3,* respectively, and are from now on referred to as Salk *IDL2* and Salk *IDL3* (figure 3.13).

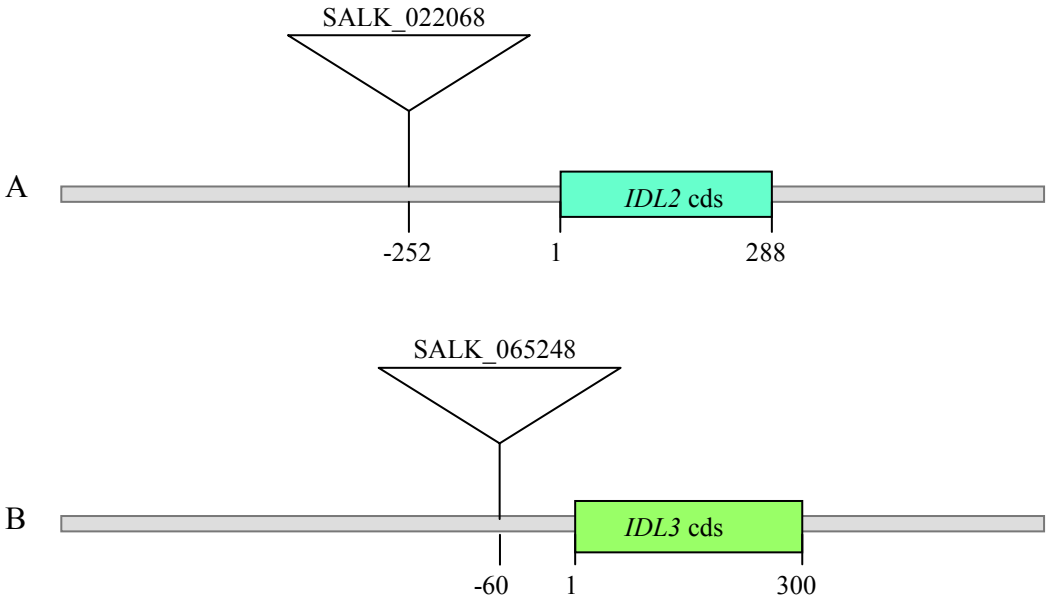

Figure 3.13 Salk *IDL2* and Salk *IDL3* T-DNA insertion lines. (A) Salk_022068 is predicted to have a T-DNA inserted 252 bp upstream of *IDL2* cds. (B) Salk_065248 is predicted to have a T-DNA inserted 60 bp upstream of *IDL3* cds. The figure is not to scale.

3.3.1 Genotyping

Since mutations due to T-DNA insertions are often recessive, it is necessary to identify plants that are homozygous for the T-DNA insertion by genotyping a small population of plants. Genomic DNA from T3 generation of Salk *IDL2* was isolated. The DNA was used to genotype the plants by two PCR reactions (figure 3.14). In the first reaction, the primers *IDL2* LP and *IDL2* RP, flanking the T-DNA insertion, amplified a PCR-product of about 1100 bp when no T-DNA was inserted. If a T-DNA was present, this fragment would be too long to give a PCR product with the extension time used (1 min.). The second reaction included a left border T-DNA primer, LBb1, and the primer flanking the left border of the T-DNA, *IDL2* RP, and amplified a PCR product of about 500 bp. If no T-DNA was inserted, no PCR product would be amplified (figures 3.14 and 3.15).

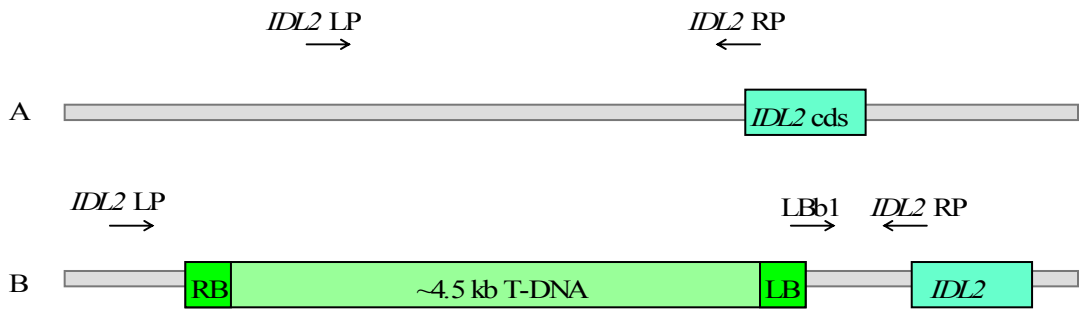

Figure 3.14 Genotyping of Salk *IDL2* T-DNA insertion lines. (A) If no T-DNA is inserted, the primers *IDL2* LP and *IDL2* RP will amplify a PCR product of approximately 1120 bp. (B) If there is a T-DNA inserted no PCR product will be amplified using the primers *IDL2* LP and *IDL2* RP. If there is a T-DNA inserted the T-DNA specific primer LBb1 and *IDL2* RP will give a PCR product of about 510 bp. The figure is not to scale.

Plants homozygous for the T-DNA insertion would give a PCR product in the second reaction, plants hemizygous for the T-DNA insertion would give one PCR product in each reaction, while plants with no T-DNA inserted would give a PCR product in the first reaction. Four homozygous plants were identified for Salk *IDL2*.

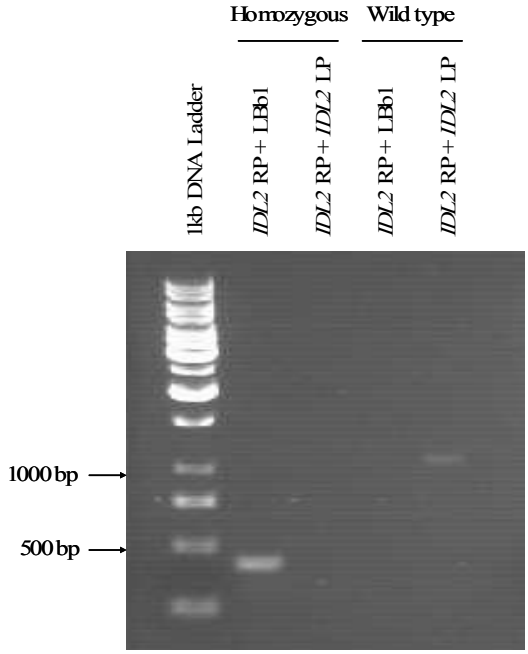

Figure 3.15 Genotyping of the Salk *IDL2* T-DNA insertion lines. A plant homozygous for the T-DNA insertion will give a PCR-product of about 500 bp using the primers *IDL2* RP and LBb1, but no PCR product will be amplified using the primers *IDL2* RP and *IDL2* LP. The *IDL2* RP–LBb1 band was smaller than expected due to a deletion in the T-DNA integration process (see 3.3.2). A wild type plant with no T-DNA inserted will give a PCR product of about 1100 bp using the primers *IDL2* RP and *IDL2* LP, and since no T-DNA is inserted, no product is obtained with *IDL2* RP and LBb1.

Salk *IDL3* had been genotyped by Ragnhild Nestestog, Norwegian Arabidopsis Research Center (NARC).

3.3.2 Genomic region flanking the left border of the T-DNA

The exact insertion point of the T-DNA may be located at a distance from the sequence provided in the database, due to overlapping reads of two or more sequences in these T-DNA lines. The first base provided is the first high quality base in the sequence trace and not necessarily the first base at the insertion site. The actual insertion site may be within 0-300 bp from what is predicated. Therefore the insertion site needs to be confirmed by sequencing the genomic region flanking the left border of the T-DNA.

The PCR products which were amplified when genotyping Salk *IDL2* and Salk *IDL3* were cloned into the pCR® 2.1-TOPO® vector. The products were sequenced in both directions using the primers M13 F and M13 R. The sequences obtained were aligned to the T-DNA sequence, the pCR® 2.1-TOPO® sequence and the *Arabidopsis* genome.

The T-DNA insertion in Salk *IDL2* was confirmed to be 252 bp upstream of the *IDL2* coding region. Sequencing of the flanking region revealed that almost 100 bp of the left border T-DNA had been deleted due to the T-DNA integration process. This explains why the PCR

product amplified with *IDL2* RP and LBb1 was about 100 bp shorter than expected (figure 3.15).

The T-DNA insertion in Salk *IDL3* was found to be 61 bp upstream of the *IDL3* coding region.

3.3.3 Rapid amplification of cDNA ends (RACE)

IDL1 had been annotated from a full-length cDNA and the 5' and 3' untranslated regions (UTRs) of *IDL1* were known. *IDL2* and *IDL3* had not been annotated and the UTRs for these genes were unknown. For the investigation of Salk T-DNA insertion lines it is often necessary to know the 5' and 3' untranslated regions of a gene. A T-DNA insertion in the 5'UTR might have a greater influence on the transcription level of the gene than an insertion in the promoter region. RACE was used to identify the 5' and 3' UTRs of *IDL2* and *IDL3* in order to decide whether the T-DNA insertions in Salk *IDL2* and Salk *IDL3* were located in the promoter regions or in the 5'UTRs. Total RNA was isolated from seedlings since RT-PCR (Butenko et al., 2003) and GUS-analyses have shown that both *IDL2* and *IDL3* are expressed in this tissue. The RACE products were ligated into pCR®4-TOPO® vector and then sequenced in both directions using the primers M13 F and M13 R. For *IDL2* 5'UTR no RACE product was obtained. The other sequences were aligned to the *Arabidopsis* genome. The 3' UTR for *IDL2* was 169 bp. For *IDL3* the 5' UTR was 54 bp and the 3' UTR 173 bp (figure 3.16).

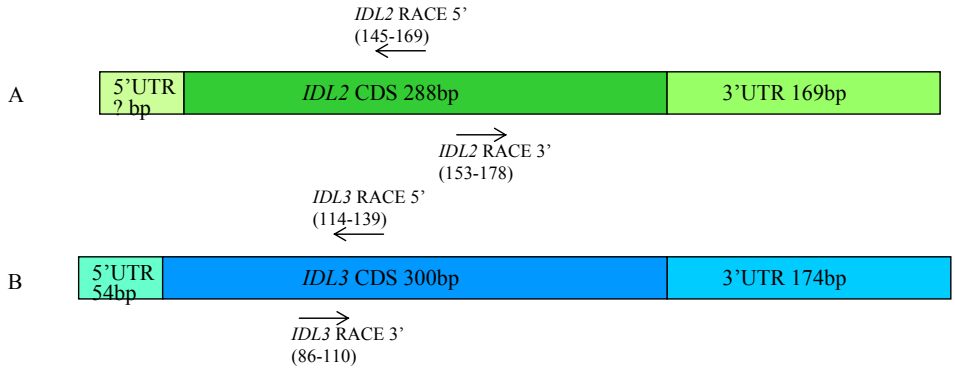

Figure 3.16 5' and 3' UTR for *IDL2* and *IDL3*. The positions of the primers with numbers in parentheses, relative to the start codon, are shown. (A) 3' UTR for *IDL2* is 169 bp. (B) 5' and 3' UTR for *IDL3* are 54 and 174 bp, respectively. The figure is not to scale.

Since the 5'UTRs of *IDA* and the *IDL* genes that are known range from 54 to 98 bp, it is reasonable to assume that the T-DNA insertion in Salk *IDL2*, which was located 252 bp upstream of *IDL2*, was in the promoter region. According to the RACE results the T-DNA insertion in Salk *IDL3*, which was 61 bp upstream of the *IDL3*, was just outside the 5' UTR.

3.3.3 Investigating the phenotype of the Salk lines *IDL2* and *IDL3*

Seeds from the homozygous Salk lines of *IDL2* and *IDL3* were grown and reconfirmed to be homozygous. The plants were inspected for abnormal phenotypes, but no mutant phenotypes were observed for either *IDL2* or *IDL3* under normal growth conditions.

3.3.4 Semi-quantification of the *IDL3* expression in the Salk *IDL3* plants

The T-DNA insertions in Salk *IDL2* and Salk *IDL3* were 252 and 61 bp upstream of the *IDL2* and *IDL3* start codons, respectively. None of the two Salk lines showed any mutant phenotypes under normal growth condition. Based on the fact that the T-DNA insertion in Salk *IDL3* was closer to the 5' UTR of *IDL3* than the T-DNA in Salk *IDL2* was to the 5'UTR of *IDL2*, we chose to further investigate Salk *IDL3*. To examine if the T-DNA insertion would affect the expression level of *IDL3* in Salk *IDL3* plants, semi-quantitative RT-PCR was performed. First strand cDNA was generated from total RNA of seedlings from two homozygous T-DNA lines (line 3 and 6) and Columbia wild type. Seedlings were chosen because RT-PCR (Butenko et al., 2003) and GUS have shown expression of *IDL3* in this tissue. PCR amplification of first strand cDNA using *ACTIN 2-7* primers was performed as a positive control and to assure that equal amounts of cDNA was being used. The PCR products obtained showed similar levels of amplification from both homozygous lines and from the wild type. The *ACTIN* primers span intron 2 of the *ACTIN* gene, giving larger PCR products genomic DNA than PCR products obtained form cDNA. Because there is no intron in *IDL3*, the PCR product generated from gene specific primers would be of the same size irrespectively if it was amplified from cDNA or DNA. To confirm that there was no DNA in the samples; control experiments were performed without reverse transcriptase using the *ACTIN* primers. The gene specific primers *IDL3* R and *IDL3* L were used to amplify the PCR product that quantified the *IDL3* expression level. The PCR was run for 27 cycles using 200 ng cDNA as template, and 30 cycles with both 100 ng and 200ng cDNA (results only shown

for 200ng). The results indicated that there were no differences in the expression level of *IDL3* in the Salk lines compared to wild type (figure 3.17).

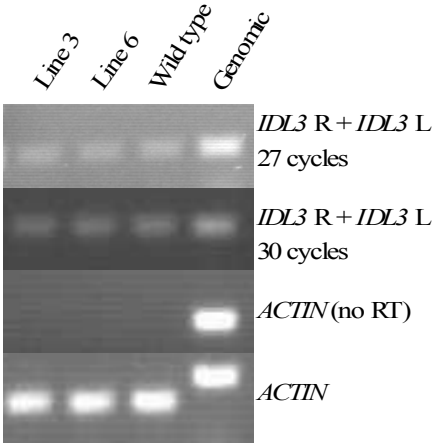

Figure 3.17 Semi-quantitative RT-PCR. The primers *IDL3* R and *IDL3* L amplified a fragment of 256 bp. The negative control using no RT and *ACTIN* primers yielded no PCR products except for the genomic control of 340 bp. The *ACTIN* control amplified PCR products of 255 bp at similar levels from the transgenic plants and the wild type control. Using the *ACTIN*-primers the PCR-product obtained from cDNA was smaller than the PCR-product obtained from genomic DNA.

3.4 RNA interference assay

Since no Salk insertion line was available for *IDL1* and the Salk lines for *IDL2* and *IDL3* did not show any phenotype, we wanted to use RNA interference as a method to make knock-down lines for all the three *IDL* genes and to investigate if this would show any mutant phenotypes.

3.4.1 The RNAi constructs

The RNAi constructs were made using the Gateway Cloning Technology (see materials and methods, section 2.3.8.1). The entry clones contained the coding sequences of *IDL1*, *IDL2* and *IDL3*. In the LR reaction the entry clones were recombined with the destination vector pHELLSGATE 8. The pHELLSGATE 8 vector has two destination sites separated by an intron. The orientation of the att-sites introduces the insertion of the cloned DNA fragments into an inverted repeat conformation. When the construct is expressed in plants, a hairpin RNA with the intron spliced out is produced. In the recombination reaction the intron either retains its forward orientation with respect to the promoter, or it is reversed with respect to the

direction of transcription. If the intron is reversed, the restriction sites flanking the intron are also reversed (figure 3.18). Restriction digest was used to investigate the orientation of the intron fragment, and both restriction digest and PCR were used to check for the presence of inserted sequences. Correct expression clones for *IDL1* and *IDL3* were identified (figures 3.19 A, B, C, E and F).

More than 90 clones were analyzed in order to make an RNAi construct for *IDL2*, many clones containing a reversed intron were obtained (figure 3.19 D), but no correct RNAi construct was identified.

Agrobacterium was transformed with the expression clones for *IDL1* and *IDL3*. Correct colonies were confirmed by PCR (figure 3.19 C and F) and used to transform wt *Arabidopsis*.

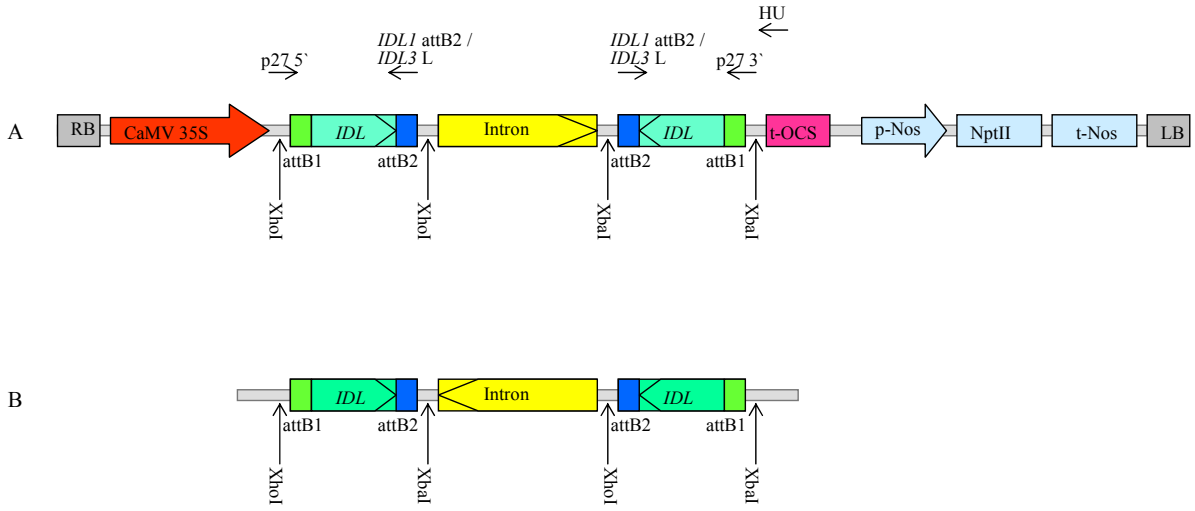

Figure 3.18 The RNAi constructs. (A) *IDL1* and *IDL3* were recombined into pHELLSGATE 8 using the LR-reaction. The self-complementary sequence is driven by the CaMV 35S promoter. The inserts are flanked by attB sites that are 25 bp in length. XhoI and XbaI restriction sites were used to digest recombined plasmids in order to check for the presence of the insert and the direction of the intron. Each enzyme will produce a product of approximately 400 bp. The primers p27 5`, p27 3`, HU and *IDL1*attB2 were used to check for the presence of *IDL1*, while the primers p27 5`, p27 3` and *IDL3* L were used to check for the presence of *IDL3*. t-OCS: OCS terminator, p-Nos: Nos promoter, *NptII*: *neomycin phosphotransferase* II, t-Nos: Nos terminator, RB: right border, LB: left border. (B) When the intron is reversed, the restriction sites flanking the intron are also reversed. The restriction enzymes will produce products of 1.3 kb (kilo base). The figure is not to scale.

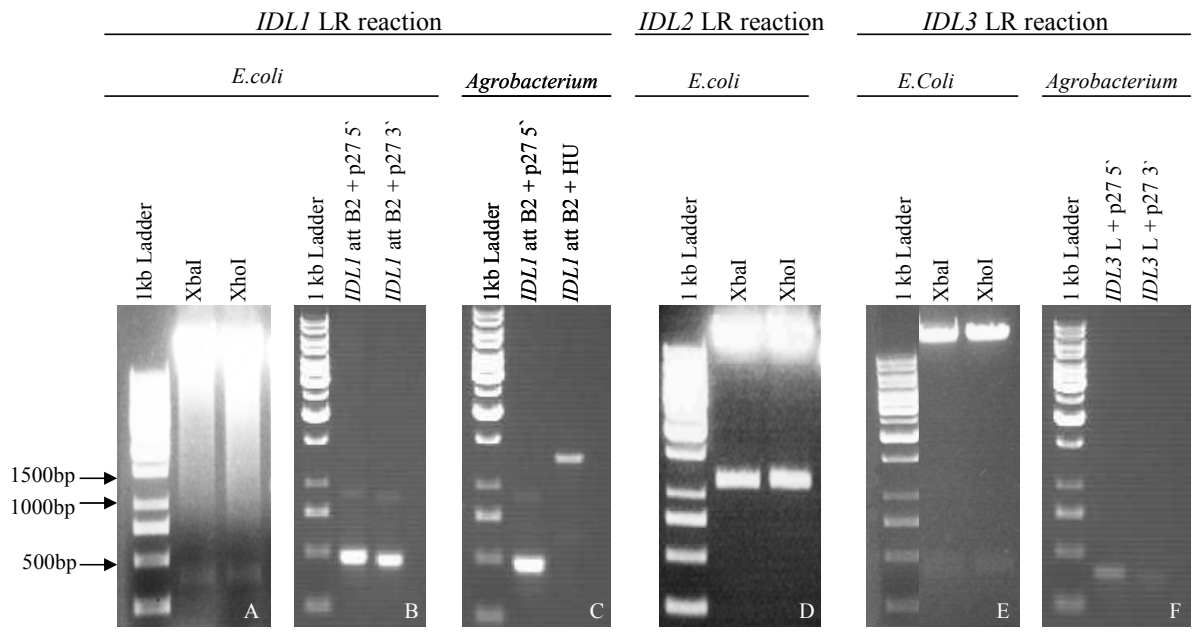

Figure 3.19 Making the RNAi constructs. (A, B and C) Correct expression clone for *IDL1* demonstrated with restriction digest and PCR. (A) Using the enzymes XbaI and XhoI, fragments of about 400 bp were produced, in both cases confirming the presence of the insert and the correct direction of the intron. (B) *IDL1* attB2 and p27 5`, and *IDL1* attB2 and p27 3` amplifies products of approximately 500 bp. (C) To confirm that the correct clone was present in *Agrobacterium* the primers *IDL1* attB2, p27 5` and HU were used. *IDL1* attB2 and HU amplified a product of 1.4 kb. (D) No correct expression clone for *IDL2* was identified. Using the enzymes XbaI and XhoI yielded fragments of about 1.3 kb, meaning that the intron is reversed. (E and F) Correct expression clone for *IDL3*. (E) Restiction digest using the enzymes XbaI and XhoI yielded fragments of about 400 bp. (F) Correct clone was confirmed in *Agrobacterium* using the primers *IDL3* L, p27 5` and p27 3`, which amplified PCR products of about 400 bp.

3.4.2 Investigation of the primary transformants

70 and 50 T1 plants harboring the RNAi constructs for *IDL1* and *IDL3* respectively were obtained. The plants were inspected for abnormal phenotypes, but no mutant phenotypes were observed among the transgenic plants under normal growth condition.

Since *IDL1* has shown an interesting expressing pattern in the roots, further investigation of the RNAi plants was concentrated on this gene.

3.4.3 Segregation analysis of T2 *IDL1*

In order to identify lines containing one independent integrated locus of the *IDL1* RNAi construct, segregation analysis was performed. T2 seedlings from 12 randomly chosen lines were scored for kanamycin resistance or sensitivity. The results are shown in table 3.2. Six

lines were identified as lines containing one locus due to the chi-square test of significance in which $\chi^2 < 3.84$ (see materials and methods, section 2.10.1).

Table 3.2 Observed (Obs) number of Km^r and Km^s T2 seedlings in the *IDL1* RNAi lines. The number of expected (Exp) Km^r and Km^s plants for each hypothesis (3:1, 15:1 and 63:1) for each independent line was computed. Then the χ^2-values for Km^r and Km^s plants for each hypothesis were computed (data not shown) and thereafter these χ^2-values were summed up to give the total χ^2-value for each hypothesis. The segregation patterns 3:1, 15:1 and 63:1 corresponds to one, two and three independent integrated T-DNA loci, respectively. The hypotheses were tested with the chi-square test of significance in which χ^2 should be less than the critical value of 3.84. The χ^2–values written in bold mean that the hypothesis holds with 95% accuracy.

***IDL1* RNAi line**	**Obs # Km^r/Km^s**	**Exp # Km^r/Km^s 3:1**	**Exp # Km^r/Km^s 15:1**	**Exp # Km^r/Km^s 63:1**	**χ^2 3:1**	**χ^2 15:1**	**χ^2 63:1**
1	157 / 33	142.5 / 47.5	178.1 / 11.9	187.0 / 3.0	5.9	40.1	303.8
2	119 / 1	90.0 / 30.0	112.5 / 7.5	118.1 / 1.9	37.4	6.0	**0.4**
7	107 / 7	85.5 / 28.5	106.9 / 7.1	112.2 / 1.8	21.6	**0.0**	15.5
8	136 / 0	102.0 / 34.0	127.5 / 8.5	133.9 / 2.1	45.3	9.1	**2.2**
36	79 / 26	78.8 / 26.3	98.4 / 6.6	103.4 / 1.6	**0.0**	61.4	367.4
38	110 / 1	83.3 / 27.8	104.1 / 6.9	109.3 / 1.7	34.4	5.4	**0.3**
41	66 / 29	71.3 / 23.8	89.1 / 5.9	93.5 / 1.5	**1.5**	95.6	518.1
44	80 / 38	88.5 / 29.5	110.6 / 7.4	116.2 / 1.8	**3.3**	135.6	720.3
45	76 / 17	69.8 / 23.3	87.2 / 5.8	91.5 / 1.5	**2.2**	23.0	169.0
52	108 / 31	104.3 / 34.8	130.3 / 8.7	136.8 / 2.2	**0.5**	61.1	388.7
54	86 / 25	83.3 / 27.8	104.1 / 6.9	109.3 / 1.7	**0.4**	50.2	317.0
79	116 / 7	92.3 / 30.8	115.3 / 7.7	121.1 / 1.9	24.5	**0.1**	13.6

3.4.4 Semi-quantitative RT-PCR showed reduced expression of *IDL1* in the *IDL1* RNAi transgenic plants

To investigate whether the expression of *IDL1* was reduced in the *IDL1* RNAi transgenic plants, RT-PCR was performed. Total RNA was isolated from roots from four lines containing one T-DNA locus (41, 44, 52 and 54) and from Columbia wild type, and first-strand cDNA was generated. Roots were the natural choice since RT-PCR (Butenko et al., 2003) and GUS showed expression of *IDL1* in this organ. To ensure that we detected the expression level of *IDL1 in planta* and not parts of the transcribed RNAi construct, the primers were placed in the 5` and 3` UTRs of *IDL1*, since this regions are not included in the construct. *ACTIN* primers were used to control the quality and amount of first strand cDNA and a negative control without RT was performed for all samples, as *IDL3*, *IDL1* contains no intron, see 3.2.4. 90 ng cDNA was used as template in the reactions. The RT-PCR was run a various number of cycles, ranging from 25 to 35, to see if it was possible to detect a

difference in the *IDL1* expression between the wild type and the transgenic plants. At 30 cycles, the *IDL1* expression in the transgenic RNAi plants was visibly weaker compared to the wild type (figure 3.20). When the number of cycles was reduced to 29, *IDL1* could no longer be detected in the transgenic plants, but a faint *IDL1*-band was detected in the wild type plants (figure 3.20). These results indicate that *IDL1* was down-regulated in the *IDL1* RNAi transgenic plants. In order to investigate the expression level in a more precisely manner, more quantitative methods, like northern or real time PCR, must be used.

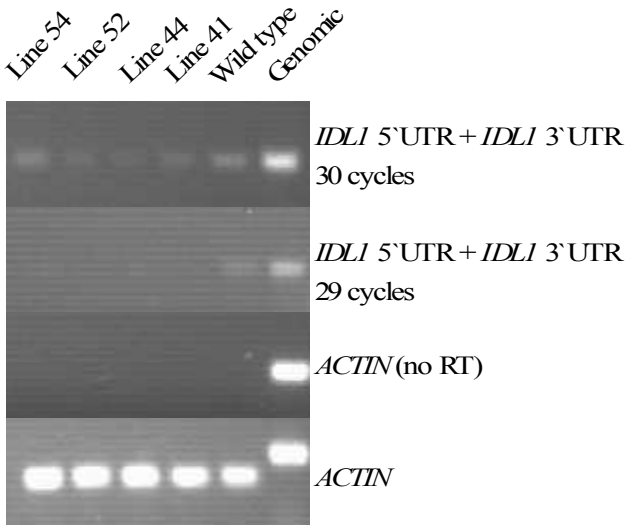

Figure 3.20 RT-PCR used to semi-quantify the *IDL1* expressionin the *IDL1* RNAi transgenic plants. The UTR primers amplified a fragment of 405 bp, here demonstrated with 30 and 29 cycles. The negative control using no RT yielded no PCR products except for the genomic control of 340 bp. The PCR was performed with 25 cycles for *ACTIN* and amplified a PCR product of 255 bp.

3.4.5 Segregation analysis of T3

The RNAi construct is genetically dominant; therefore phenotypes can be screened in T1 without the need to produce homozygous lines. As no mutant phenotype was observed in the T1 generation, homozygous lines were identified in order to do further phenotypic investigation. With a homozygous line it is not necessary to identify a 3:1 segregation pattern among the possible mutant phenotypes. In addition it is not necessary to use selection agar medium and therefore there is no possibility that the antibiotics will affect the root phenotype.

T2 seedlings from three lines containing one T-DNA locus (41, 52 and 54), exhibiting reduced expression of *IDL1*, were sown on selection agar medium and transferred to soil to obtain seeds. Since seedlings were initially grown on selection medium the lines were expected to give a 2:1:heterozygous:homozygous segregation pattern in the T3 generation. Seeds from 12 T3 siblings, from each of the three T2 lines, were sown on selection agar medium and the segregation of Km^r:Km^s was scored. A heterozygous line is expected to give

a 3:1 segregation of kanamycin resistance, while a homozygous line will segregate 1:0. In the T3 generation of each of the three T2 lines three homozygous lines were identified (results not shown). One homozygous sibling from each line was randomly chosen for further investigation.

3.4.6 Phenotypic investigation of roots

The *IDL1* RNAi transgenic plants did not show any apparent mutant phenotype under normal growth conditions, neither in aerial parts nor in roots. In order to reveal possible mutant phenotypes in the *IDL1* RNAi transgenic plants, the plants were investigated in a more systematic way. It was natural to examine the roots in more detail, since RT-PCR showed expression in roots and GUS showed expression in the root cap and the root differentiation zone.

3.4.6.1 Measurement of root length

In order to investigate if the knock down of *IDL1* mRNA would affect the root length in *Arabidopsis* plants, root length was measured in *IDL1* RNAi transgenic plants. Seedlings from three homozygous sublines (T3 generation) and wild-type were grown on vertical plates for nine and ten days, and the primary root length was scored. Approximately 20 seedlings from each line were measured. The roots of the RNAi plants seemed to be longer than those of the wild type. To establish if there was a significant difference between the mean values of the transgenic and the wild type plants, the two-sample T-test was used (see materials and methods, section 2.10.2). Each mean value of the transgenic plants was compared to the mean value of the wild type plants (table 3.3). The null hypothesis was defined to be that the mean values are equal. At a significance level of 0.05 and 38 (20+20−2) degrees of freedom the null hypothesis was rejected if the computed T-value was more than 2.02. The difference between the mean values of the transgenic and the wild-type plants was in all cases significant. Thus the roots of the three RNAi *IDL1* transgenic lines measured in this experiment were longer than those of the wild-type. Compared to the wild type the three transgenic lines had an average 13% longer root after nine days, and 9% after ten days.

Table 3.3 Primary root length of RNAi *IDL1* transgenic plants grown under light conditions. Two independent groups of seedlings have been measured, one group after 9 days and one after 10 days. For each line, ~ 20 seedlings were scored. Primary root length values are means ± SD (Standard deviation). Since all the T-values >2.02 the mean root lengths of the transgenic plants are significantly different compared to the wild-type by the two-sample t-test.

Seedling Type	Primary root length after 9 days (mm)	T-value 9 days compared to wild-type	Primary root length after 10 days (mm)	T-value 10 days compared to wild-type
Wild-type (Col-0)	39.62 ± 2.27		48.96 ± 4.45	
RNAi *IDL1*-41-13	45.40 ± 5.81	4.13	53.27 ± 4.80	2.53
RNAi *IDL1*-52-3	42.83 ± 4.07	3.06	53.98 ± 6.72	2.76
RNAi *IDL1*-54-13	46.18 ± 5.53	4.89	53.04 ± 5.28	2.08

3.4.6.2 Gravistimulation

IDL1 was expressed in the columella root cells. These cells are important in the gravitropism of plants. Therefore *IDL1* RNAi transgenic plants were gravistimulated in order to investigate if the downregulation of *IDL1* mRNA might affect the gravitropic response in *Arabidopsis* plants. Ten day-old seedlings from two homozygous sublines (T3 generation) were gravistimulated by rotating the agar plates by 90º, and the primary root curvature was measured 3, 8 and 24 hours after gravistimulation. The mean curvatures of each line are shown in table 3.4. The root curvature of the *IDL1* RNAi transgenic plants was compared to the wild-type curvature, but no significant difference (at a significance level of 0.05) was found by the two-sample T-test.

Table 3.4 Primary root curvature of RNAi *IDL1* transgenic plants. 10 day-old seedlings were gravistimulated by turning vertical agar plates by 90º so that the roots were horizontally positioned. Curvature was defined as the change in angle from the starting point. Root curvature was measured 3, 8 and 24 hours after gravistimulation. For each line, ~ 20 seedlings were scored. Root curvature values are means ± SD. Since all T-values <2.02, the root curvatures of the transgenic plants are not significantly different from the wild-type by the two-sample T-test.

Seedling Type	Root curvature 3 hours (º)	T-value 3 hours	Root curvature 8 hours (º)	T-value 8 hours	Root curvature 24 hours (º)	T-value 24 hours
Wild-type (Col-0)	47.6 ± 11.3		69.5 ± 7.8		86.1 ± 14.4	
RNAi *IDL1* 41-13	50.2 ± 12.1	0.61	64.2 ± 13.7	1.30	85.7 ± 6.1	0.11
RNAi *IDL1*-52-3	52.0 ± 7.5	1.37	69.4 ± 11.3	0.03	84.9 ± 10.5	0.30

3.4.6.3 Lugol staining pilot assay

The columella root cells contain starch granules, and displacement of the granules is the primary gravity-sensing mechanism in roots (Chen et al., 2002). In order to verify that *IDL1* is not involved in gravitropic responses, a small Lugol staining pilot experiment was performed. Ten day-old *IDL1* RNAi plants from three homozygous sublines were Lugol stained to visualize the starch granules. One plant in each line was examined. The *IDL1* RNAi roots were compared to the wild-type, but no differences in the starch content and organization was observed (data not shown).

3.5 Overexpression of the *IDL* genes

In order to know more about the biological functions of the three *IDL* genes, constructs over-expressing *IDL1*, *IDL2* and *IDL3* were made using the gateway system (see materials and methods, section 2.3.8.3). The coding sequences of the three genes were cloned behind the cauliflower mosaic virus (CaMV) 35S promoter in the vector pK7WG2 (figure 3.21). This promoter is supposed to be constitutively expressed in *Arabidopsis*, and should give a high expression of the genes in every tissue of the plant.

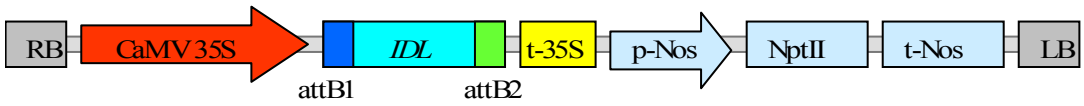

Figure 3.21 The overexpression constructs. Transcription of *IDL1*, *IDL2* or *IDL3* (*IDL*) is driven by the 35S promoter. The inserted *IDL* genes are flanked by attB sites that are 25 bp in length and followed by the 35S terminator (t-35S). p-Nos: Nos promoter, t-Nos: Nos terminator, *NptII*: *neomycin phosphotransferase* II, RB: right border, LB: left border. The figure is not to scale.

The overexpression constructs were transformed into wt *Arabidopsis*. 54 primary transformants were obtained for each construct.

3.5.1 Investigation of the 35S::*IDL1* primary transformants

The 35S::*IDL1* primary transformants were investigated for abnormal phenotypes. The transformants showed early senescence in the top-most region of the primary inflorescence (figures 3.22 A and B). Senescent 35S::*IDL1* plants showed reduced turgor pressure in the

top-most tissue of the stem. Later in development most of the 35S::*IDL1* plants also showed this phenotype in the secondary stems. In contrast, natural senescence in plants causes the whole plant to dry in and the plant will remain rigid.

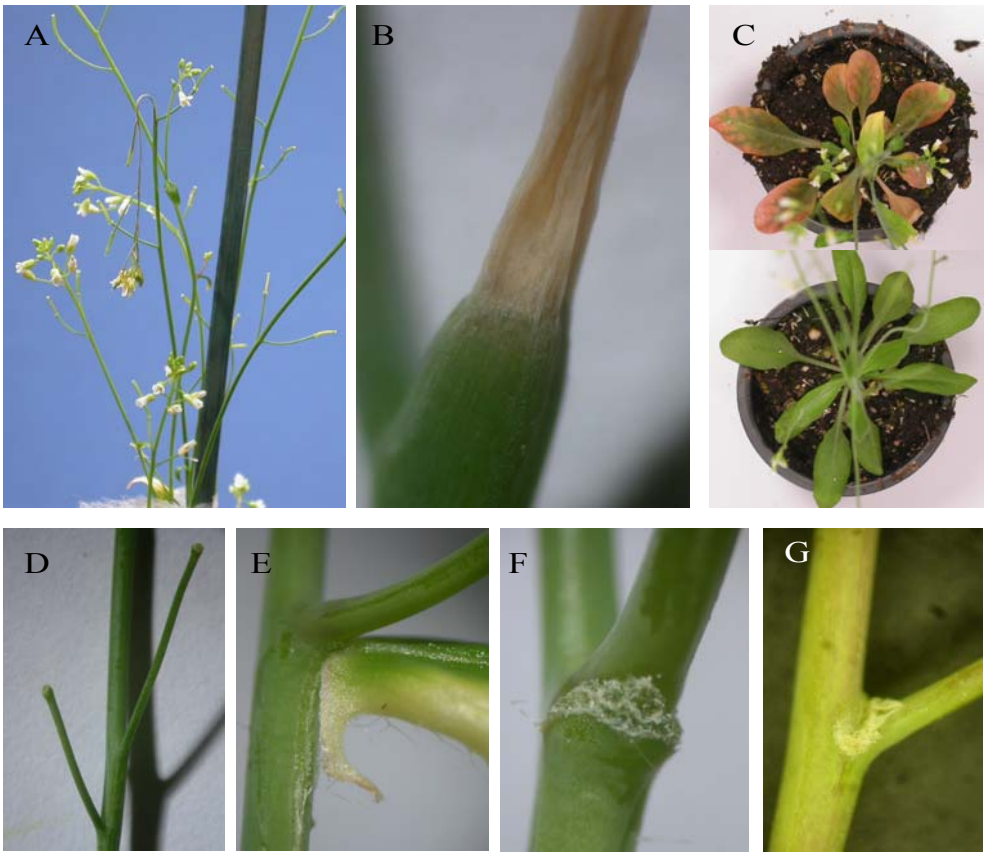

Figure 3.22 Phenotypes of 35S::*IDL1* plants (T1). (A and B) Five week-old 35S::*IDL1* plant demonstrates senescence in the top-most inflorescence tissue. (C) Five weeks old rosettes of 35S::*IDL1* plants (top) and wild-type (bottom). (D) Siliques have been shed. (E) Cauline leaf about to fall off. (F) Cauline leaf has abscised, leaving az-like cells covered with a white substance. (G) A white substance was also seen at the base of the pedicel.

The 35S::*IDL1* plants also exhibited early senescence in the rosette leaves (figure 3.22 C). The floral abscission process started earlier than in wild type (figure 3.23). The floral organs are abscised at position nine in wild type (Col) (see section 3.1.4.4); whereas the 35S::*IDL1* plants shed their floral organs at position seven. The cells in the floral abscission zones of the 35S transgenic plants seemed to be enlarged and a white substance was covering the cells (figure 3.23). In addition to premature abscission both siliques and cauline leaves were observed to fall off (figures 3.22 D, E and F). The cells at the base of the pedicel and the cauline leaves resembled the cells in the floral organ abscission zones (figures 3.22 F and G).

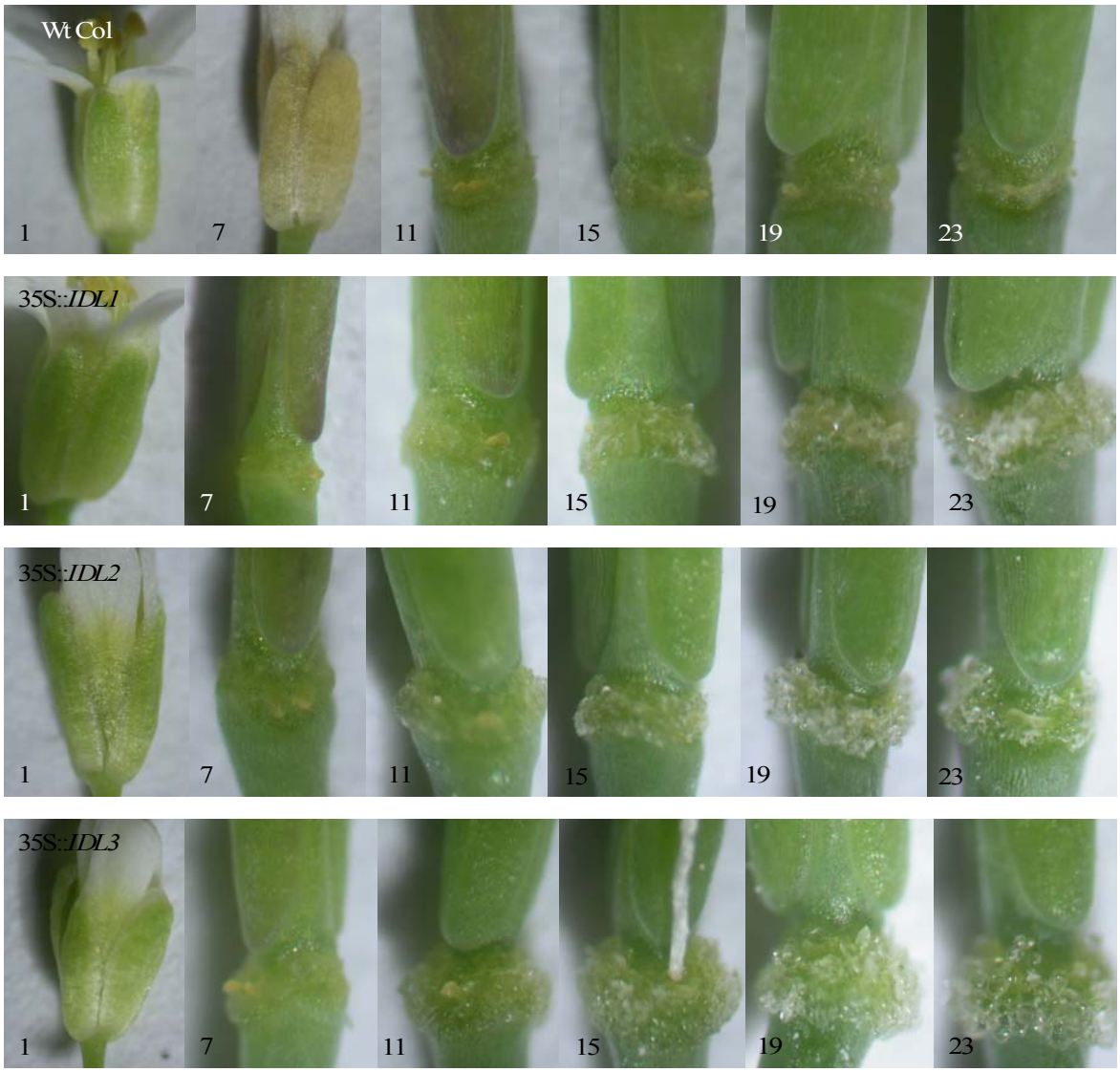

Figure 3.23. Abscission in 35S::*IDL1* (T1), 35S::*IDL2* (T2) and 35S::*IDL3* (T2) transgenic plants. At position 7, in the transgenic plants, all the floral organs have been shed, in contrast to wild-type which retains its floral organs to position 9. After abscission the AZ-cells started to enlarge and a white substance is visible. Note that the flowers in 35S::*IDL2* and 35S::*IDL3* plants did not open normally compared to the wild-type, see position 1. Arabic numerals indicate flower positions on the inflorescence.

3.5.1.1 Measurement of root length (pilot assay)

Since the RNAi *IDL1* plants displayed a longer root phenotype, we wanted to investigate whether the overexpression of *IDL1* would give the opposite effect. The experiment was performed as a pilot experiment since the number of integrated T-DNA loci and genotype still was unknown in these plants. The plants were grown on vertical MS-1 plates containing no antibiotics; therefore there might have been wild type plants among the transgenic plants. Root length was measured after nine days on T2 seedlings from three different lines and compared to wild type. The roots in the three transgenic lines, 6, 11 and 45, were 19, 43 and 13.5 % shorter that those of the wild type, respectively. The mean values of the transgenic

plants and the wild type are shown in table 3.5 The two-sample T-test demonstrated that the difference between the root lengths was significant (see section 3.4.6.1; and materials and methods, section 2.10.2). The results indicate that while the roots of RNAi *IDL1* plants were longer than those of the wild type, the 35S::*IDL1* plants displayed roots that were shorter than those of the wild type.

Table 3.5 Primary root length of 35S::*IDL1* transgenic plants grown under light conditions. Roots from three transgenic lines and wild type were measured after 9 days. For each line, ~ 20 seedlings were scored. Primary root length values are means ± SD. Since all the T-values >2.02 the mean root lengths of the transgenic plants are significantly different compared to the wild-type by the two-sample t-test.

Seedling Type	Primary root length (mm)	T-value compared to wild-type
Wild-type (Col-0)	37.38 ± 4.56	
35S::*IDL1-6*	30.05 ± 3.58	5.64
35S::*IDL1-11*	20.56 ± 9.35	6.95
35S::*IDL1-45*	32.23 ± 6.13	3.16

3.5.2 Investigation of 35S::*IDL2* transformants

The 35S::*IDL2* primary transformants were inspected for abnormal phenotypes. Compared to wild-type plants, 35S::*IDL2* plants were shorter and had fragile stems (figure 3.24 A). The rosette leaves of the short 35S::*IDL2* plants were smaller and rounder compared to those of wild-type plants (figure 3.24 D), and showed premature senescence (figure 3.24 C). Many of the 35S::*IDL2* plants had infertile flowers and the flowers did not open normally (figure 3.23, position 1). Like 35S::*IDL1* plants, 35S::*IDL2* plants exhibited early abscission (figure 3.23) and rounding of the cells in the abscission zone. Some of the plants also showed abnormal senescence in the top-most inflorescence tissue and shedding of cauline leaves and siliques (data not shown). Six independent lines were investigated in the T2 generation. The phenotypic feature that showed short, fragile plants was not observed. However, the other phenotypes observed in the primary transformants persisted in the T2 generation.

3.5.3 Investigation of 35S::*IDL3* transformants

The 35S::*IDL3* primary transformants were, like 35S::*IDL2* plants, smaller and had thin, fragile stems compared to the wild-type (figure 3.24 B). The rosette leaves were smaller and rounder and showed premature senescence (figures 3.24 C and D). Most of the 35S::*IDL3* primary transformants were infertile and like 35S::*IDL2* plants the flowers did not open properly (figure 3.23 position 1 compared to wt pos 1). Like 35S::*IDL1* and 35S::*IDL2*, the 35S::*IDL3* plants demonstrated early abscission of floral organs and rounding of the abscission zone cells (figure 3.23). Some of the plants also showed abnormal senescence in the top-most inflorescence tissue and shedding of cauline leaves and siliques (data not shown).

Six independent lines, five siblings of each line, were investigated in the T2 generation. The smallest 35S::*IDL3* plants were infertile in the T1 generation and without crossing these plants to wild type it was impossible to investigate these lines in the T2 generation. However, small 35S::*IDL3* plants were observed in one line and siblings within three lines exhibited fragile, thin stems. Premature abscission, early senescent rosette leaves, senescent top-most inflorescence tissue was also observed in the T2 generation.

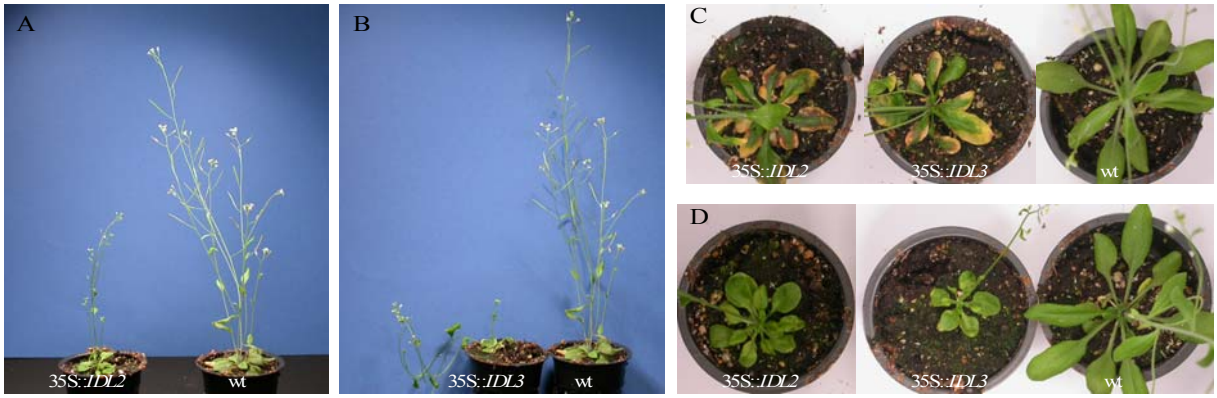

Figure 3.24 Phenotypes of 35S::*IDL2* and 35S::*IDL3* plants (five weeks old). (A and B) Wild-type, 35S::*IDL2* (T1), and 35S::*IDL3* plants (T2). (C and D) Comparison of 35S::*IDL2*, 35S::*IDL3* and wild-type. (C) Early senescence in rosette leaves (T2). (D) Smaller and rounder rosette leaves (T1).

3.5.4 Summary of the 35S::*IDL* results

In summary, the transgenic plants carrying over-expressing constructs for the three *IDL* genes showed many similar phenotypic features. However, it is necessary to confirm the

overexpression of the genes. The root length pilot assay indicated that the roots of the 35S::*IDL1* plants were shorter than those of the wild type. These results need to be confirmed. It would also be interesting to inspect the roots of the other 35S::*IDL* transgenic plants. In addition the aerial parts of the 35S::*IDL1* should be investigated in the T2 generation to see if the phenotypes persist. Future investigations would be easier working with a homozygous line containing one T-DNA locus.

4 DISCUSSION

The *IDL* genes were identified based on their similarities to the *IDA* gene, and together with *IDA* they form a family of putative ligands in plants (Butenko et al., 2003). The expression pattern of the *IDL* genes had been crudely identified by RT-PCR and suggested that they were involved in diverse developmental processes in plants. In this thesis *IDL1*, *IDL2* and *IDL3* were analyzed closer.

To get a better understanding of the functions of the three *IDL* genes, expressional and functional studies were performed. The expression patterns of *IDL1*, *IDL2* and *IDL3* were characterized by histochemical analysis of transgenic plants expressing fusions of their promoter sequences to the GUS reporter gene. Because *IDA* and the *IDL* genes encode putative ligands that are thought to be transported out of the cell to the extracellular space, we wanted to investigate the subcellular localization of *IDL1*, *IDL2* and *IDL3*. Constructs containing fusions between the three *IDL* genes and the green fluorescent protein (GFP) were made both for the onion epidermis transient expression assay and for stable GFP-expression *in planta*. Mutations can provide important knowledge about the biological function of a gene. Therefore Salk-lines containing T-DNA insertions in the promoter area of *IDL2* and *IDL3* were investigated. The *ida* mutant has a T-DNA in the promoter, reduced expression and a clearly visible phenotype (Butenko et al., 2003). However, the Salk *IDL2* and Salk *IDL3* did not show any abnormal phenotypes, and no Salk-line was available for *IDL1*. Therefore we wanted to generate RNAi lines for the three genes. RNAi-induced gene silencing is another valuable method to study loss-of-function mutations. In order to study gain-of-function of *IDL1*, *IDL2*, and *IDL3*, transgenic lines overexpressing these three genes were generated.

4.1 The expression pattern of *IDL1*

Consistent with the RT-PCR results (Butenko et al., 2003), *IDL1::GUS* was expressed in the roots. The root expression was seen in the root cap and in the root differentiation zone, and the expression pattern was common for all lines investigated. The columella root cap expression was specific to the two outermost cell layers; this was demonstrated by visualizing the starch in the columella cells with lugol's solution. The first expression in the primary root cap was detected approximately 36 hours post-germination, and expression in the lateral root caps was seen after the emergence of lateral roots; when the mature tissue pattern was formed (Laskowski et al., 1995). These results suggest that *IDL1* is not involved in the emergence of roots from seed or the initiation of lateral roots. The expression continued for at least six weeks, and indicates that *IDL1* plays a role in a developmental process taking place continuously during a plants life.

Root cap cells are continuously shed from the root tip as the root grows through the soil. *IDL1::GUS* expression was not only detected in the root cap cells that were still attached to the root, but also in cells that had already been shed (figure 4.1). This expression pattern is similar to the cellulase *AtCel5* which is suggested to be involved in sloughing, the process of root cap cell separation (del Campillo et al., 2004) (figure 4.1). Interestingly, GUS activity driven by the promoter of *IDA*, which is involved in abscission of floral organs, is seen in floral organ AZs and in floral organs that have been shed from the abscission zone (Butenko et al., 2003) (figure 4.1). Since *IDA* is involved in a process of cell-cell separation, these observations taken together may indicate that *IDL1* is involved in the shedding of root cap cells.

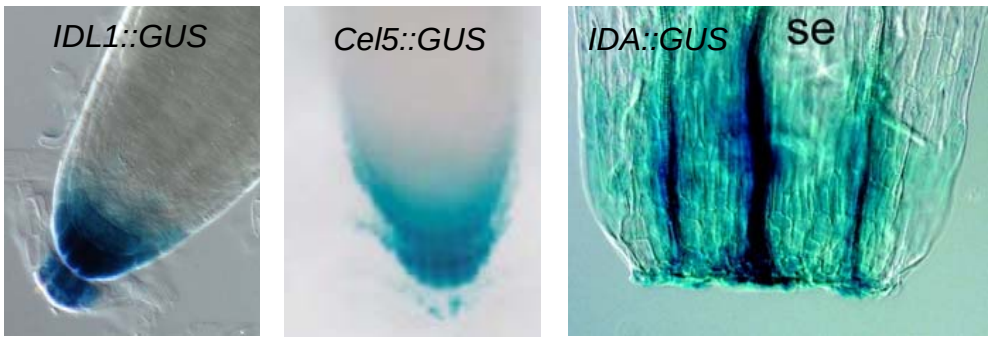

Figure 4.1 GUS expression in abscised organs/cells. *Cel5::GUS* (del Campillo et al., 2004), *IDA::GUS* (Butenko et al., 2003). See the text for details.

Arabidopsis root tips releases cell layers in an organized pattern that differs from the randomly dispersed release in other plant species studied to date. Therefore these cells are named border like cells (BLC) in *Arabidopsis*, in contrast to border cells (BC) in other species (Vicre et al., 2005). The root cap cells start to separate at the sides of the tip, while the cells at the central region of the tip separate last (del Campillo et al., 2004). BLC are spherical at the very tip of the root and become elongated during development as they move away from the tip (Vicre et al., 2005). *IDL1::GUS* expression in the detached cells was only seen in the spherical cells at the central region of the root tip and not in the elongated peripheral cells (figure 4.1). del Campillo *et al.* (2004) proposed that the peripheral cells experience more shearing forces than the central cells as the root meristem develops and the root expands and extends (del Campillo et al., 2004). This might explain why some genes involved in sloughing are only expressed in the central root cap cells.

In order to further investigate the possibility of *IDL1* being involved in sloughing, additional research on the *IDL1::GUS* transgenic plants should be done. Sloughing has been linked to the ability of the root to penetrate through the soil, therefore the expression of a gene involved in this process will increase with the resistance in the growth medium (del Campillo et al., 2004). This could be investigated by increasing the percentage of agar concentration in the medium.

IDL1::GUS expression was also seen in the epidermal tissue of the root differentiation zone (results, figure 3.5). The root epidermis is composed of two cell types; hair cells and non-hair cells (Ueda et al., 2005). Root hairs increase the surface area of the root and are likely to assist in absorption of nutrients and water, and microbe interactions (Larkin et al., 2003; Ueda et al., 2005). In order to determine more precisely in which epidermal cells *IDL1* is expressed and whether *IDL1* is expressed in specific cells within the epidermal cell layers, one could make transverse sections through a GUS stained root.

4.2 Investigation of roots in *IDL1* RNAi and 35S::*IDL1* plants

As expected from the GUS results, the primary transformants carrying RNAi constructs for *IDL1*, did not show any abnormal phenotypes in the aerial parts of the plants. Before performing in depth analysis on roots of *IDL1* RNAi plants, we wanted to investigate the

functionality of the RNAi constructs. First, since transgene expression levels from lines containing one T-DNA locus are more stable (through generations) than from lines containing multiple T-DNA loci, and one-locus RNAi lines show little variability in target transcription reduction (Kerschen et al., 2004), lines containing one T-DNA locus were identified. Furthermore one-locus lines are easily taken to homozygosity (Wang et al., 2005b). Semi-quantitative RT-PCR was used to measure the transcription level of *IDL1* mRNA in four T2 transgenic lines compared to wild type. This demonstrated that the target mRNA in these RNAi plants was reduced (results, figure 3.20). Homozygous sublines, that in T2 generation showed reduced *IDL1* mRNA level, were identified and used in further investigation of possible root phenotypes. The reduced mRNA level was not demonstrated in the T3 generation; however, Stoutjesdijk *et al*. have found that gene silencing achieved with intron-spliced hairpin construct was stably inherited over five generations (Stoutjesdijk et al., 2002).

Root length was measured on nine and ten day-old *IDL1* RNAi transgenic plants grown under normal growth condition. Compared to the control plants, there was a significant increase of root length in the transgenic plants and the three transgenic lines had an average 13% longer root after nine days, and 9% after ten days. Although the increase in root length seemed to be reduced after ten days compared to nine days, this difference was not significant (at a significance level of 0.05, data not shown). To decide whether the phenotypic differences decrease with time, further analyses will be needed. Our promoter studies suggest that *IDL1* may have a role in sloughing, possibly by inducing central root cap cells to fall off. It has been shown that sloughing of root border cells in maize reduces the friction between root cap surface and surrounding soil particles (Bengough and McKenzie, 1997; Iijima et al., 2004). In consistence with this, removal of root cap in maize increased root penetration resistance (Iijima et al., 2003). Vicrè et al. demonstrated that *Arabidopsis* plants with reduced BLC production showed an inhibition of root elongation (Vicre et al., 2005). Therefore one might expect that if *IDL1* was involved in sloughing, a reduction of *IDL1* would, in contrast to our results, give a reduction of root growth. Assuming that *IDL1* does not function in the production of root cap cells, only in their shedding, root cap cells would be produced as normal in the RNAi transgenic plants, but their falling off would be prevented. As a consequence the unshedded root cap cells could contribute to an increased root length. However, the increased root length of the transgenic plants was approximately 5 mm, which means that many cell layers would be needed to give this increasing effect. Based on our results, another possibility is that *IDL1* functions as an inhibitor of root cap sloughing,

whereby reduced inhibition of sloughing would lead to increased root penetration. Root length was also measured on 9 day-old plants overexpressing *IDL1*. Consistent with the long roots in the RNAi plants, the roots in the 35S::*IDL1* were shorter compared to the wild type roots. In order to confirm our root length measurements they need to be repeated, in addition it would be interesting to perform the measurements on both younger and older plants and observe how the phenotype develops over time.

The root cap is involved in many biological and physiological processes including gravitropism, thigmotropism and hydrotropism (Barlow, 2003). Since *IDL1* is expressed in the root cap columella cells, we wanted to investigate the possibility of *IDL1* being involved in any of these processes. In order to investigate whether *IDL1* plays a role in gravity sensing, ten day-old *IDL1* RNAi seedlings were gravistimulated. However, these plants showed normal gravity response, indicating that *IDL1* is not involved in gravity perception. Gravity perception involves the sedimentation of amyloplasts within the columella cells (Chen et al., 2002). To confirm that *IDL1* was not involved in gravity sensing, *IDL1* RNAi roots were stained with lugol solution. Consistent with the gravistimulation experiment, the lugol staining indicated that the amount of starch in the columella cells was the same in the transgenic plants as for the wild type.

When a vertically growing *Arabidopsis* root encounters an obstacle, the root reorients to form a step-like structure with bends in the central and distal elongation zones (Massa and Gilroy, 2003). In order to investigate whether *IDL1* is involved in thigmotropism, it is possible to compare the response to touch stimulation of the *IDL1* RNAi transgenic plants to the wild type response. Massa and Gilroy proposed that touch stimulation reduces gravitropic responses in the root cap (Massa and Gilroy, 2003). Similarly, it has been suggested that also hydrotropic responses downregulate the response to gravity (Eapen et al., 2005). Whether *IDL1* has a role in hydrotropism still needs to be investigated.

4.3 The expression pattern of *IDL2*

IDL2::GUS expression was observed in many organs and life stages of the plant. In seedlings, expression was detected in rosette leaves, meristem and in roots. In mature flowering plants, expression was seen in abscission zones, pedicel AZs, and the in top-most regions of

inflorescence tissues. In-depth analyses were performed on the root expression and the expression in meristem and abscission zone. Two lines containing one T-DNA locus were used in these experiments and they showed the same expression pattern.

In roots *IDL2::GUS* expression was detected in the root cap cells, but unlike *IDL1*, which was expressed in primary and secondary roots; *IDL2* was limited to the lateral roots. The root cap expression was specific to the columella cells; not to the outermost layer, like *IDL1*, but to the two cell layers above (results, figure 3.7). This specificity was confirmed by lugol-staining. The root cap expression persisted for at least six weeks. Lateral roots contribute to the root system by providing anchorage and by increasing the root surface thereby facilitating extraction of nutrients from the soil (Casimiro et al., 2003). The root caps of primary and secondary roots contribute to plant adaptations to environments and protect the root meristem (Wang et al., 2005a). The main difference between primary and lateral roots is that they have distinct origins, while the development of the primary root meristem is initiated in the embryo; the lateral root meristems are formed post-embryonically and originate from the pericycle in the primary root (Laskowski et al., 1995; Malamy and Benfey, 1997). First a lateral root primordium (LRP) is developed and then a meristem capable of producing a lateral root is formed (Laskowski et al., 1995). However, *IDL2::GUS* was detected in lateral root tips at later developmental stages when the organization of the LRP resembles that of the primary root tip (Malamy and Benfey, 1997). Based on our promoter studies, *IDL2* is not involved in formation of lateral root. To our knowledge, genes expressed solely in lateral roots at this stage in development have not been previously reported. Our results suggest that lateral roots in some way may have a different function than the primary root, even after the lateral root primordium is formed and the meristem is activated. However, it will be necessary to confirm these results by investigating additional *IDL2::GUS* transgenic lines.

IDL2::GUS expression was detected in the shoot apical meristem (results, figure 3.8). The expression was observed as soon as the meristem was visible approximately 48 hours post-germination and the signal persisted and increased in intensity during seedling development. The expansin *AtExp10::GUS* has been detected at the base of the emerging first two true leaves (figure 4.2) (Cho and Cosgrove, 2000) and the expression pattern resembles the *IDL2::GUS* pattern. Expansins are cell-wall-loosening proteins that have roles including control of organ size, morphology, and abscission (Cho and Cosgrove, 2000). The GUS

expression pattern of *IDL2* in the meristem may indicate a role for this gene in cell-wall-loosening or cell separation in the meristem.

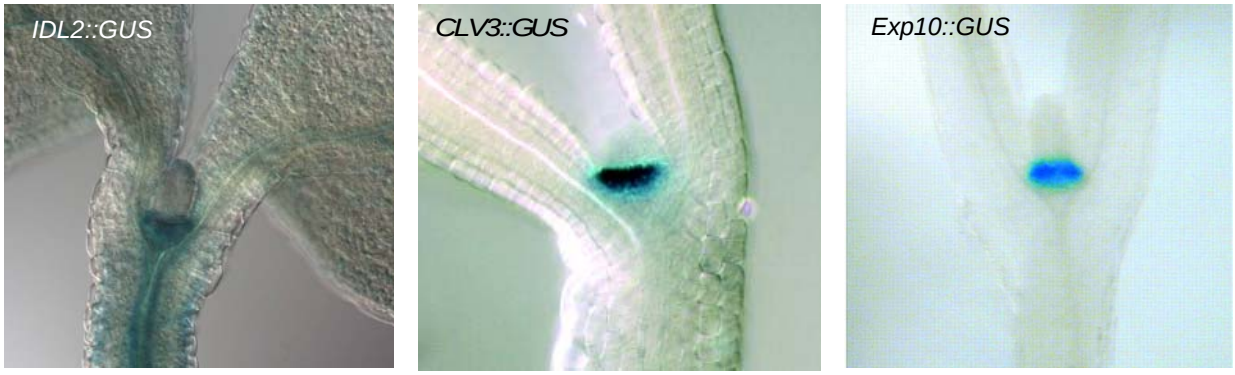

Figure 4.2 *CLV3::GUS* (Brand et al., 2002) *Exp10::GUS* (Cho and Cosgrove, 2000)

Another gene whose expression pattern resembles the *IDL2::GUS* activity in the meristem is *CLV3* (figure 4.2). *CLV3* is involved in stem cell maintenance in plant meristems (Fletcher et al., 1999). Interestingly, CLV3 is a putative ligand which has similar features to those of IDA and the IDA-LIKE proteins including a signal peptide, small size and high pI. In order to determine more precisely what part of the meristem in which *IDL2* is expressed, it would be possible to make longitudinal sections through a GUS stained plant. *In situ* hybridization could also be performed and it would be interesting to use a *CLV3*–probe to compare the expression patterns.

IDL2::GUS was observed in floral organ abscission zones (results, figure 3.9). Since *IDA* is expressed in AZs and involved in abscission, it was interesting to compare the expression pattern of *IDL2* in AZs to the *IDA::GUS* pattern. A weak *IDL2::GUS* signal was detected in floral AZs from flowers at position 3 through 8. From position 9 to 12 a strong signal was seen, after which the activity decreased and was maintained until position 18. In contrast to *IDA::GUS* expression (introduction, figure 1.4), which corresponds with the abscission process (Butenko et al., 2003), *IDL2::GUS* was at its strongest after the abscission process had taken place. These results suggest that if *IDL2* is involved in the abscission process, its major function is after the abscission of floral organs has taken place. However, these transgenic plants (*IDL2::GUS* and *IDA::GUS*) are of different ecotypes, and the experiments were not performed at the same time under exactly the same growth conditions. Therefore this GUS experiment should be repeated and should also include *IDA::GUS* plants.

4.4 The expression pattern of *IDL3*

Promoter GUS fusions of *IDL3* showed that *IDL3*, as *IDL2*, was localized in diverse plant tissues (results, figure 3.10). The first expression was detected in vascular tissues of the cotyledons. In two week-old seedlings, expression was also seen in rosette leaves, in root tips, and at border sites of lateral roots. In mature plants *IDL3::GUS* activity was observed at pedicel AZ, in floral organ abscission zones, and in buds. Interestingly, the emergence of lateral roots is associated with cell-cell separation (Roberts et al., 2000). Our result suggests that *IDL3* may be involved in the process that leads to loss of cell adhesion associated with the outgrowth of lateral roots. This possibility can be closer investigated by determining when the expression at the lateral root border sites begins. Expression in the floral organ abscission zone indicates that *IDL3* may have a role in the cell-cell separation process leading to the loss of floral organs. The base of the pedicel is not a true abscission zone in *Arabidopsis*; however, there are many plants that display flower or fruit abscission. The *IDL3::GUS*, activity in the base of the pedicel might be a vestige of an evolutionary lost abscission zone. However, the GUS results for *IDL3* are preliminary, and variance was found between the lines. Future GUS experiments should provide more secure knowledge about the *IDL3* function.

4.5 Subcellular localization of *IDL3*

The *IDL* genes show similarity to the *IDA* gene. They encode proteins with a predicted signal peptide, are of small size and have high pI-values, and have a common C-terminal motif. These are properties suggesting them to be ligands. In an Onion Epidermis Transient Expression Assay both IDA-GFP and IDA-signal peptide-GFP fusion proteins were localized in the extracellular space (Butenko et al., 2003). Onion epidermis cells were bombarded with constructs expressing fusion proteins of the three IDL proteins and GFP; however, no results were obtained. Instead, constructs for stable inducible GFP-expression *in planta* were generated. Our preliminary results indicated that the IDL3-GFP fusion protein was localized to the periphery and/or between root cells of transgenic *Arabidopsis* seedlings (results, figure 3.12). To decide whether the protein is exported out of the cell or is localized in the plasma membrane, it is necessary to induce plasmolysis. Osmosis is caused by treating cells with 0.8 M mannitol, and induces the plasma membrane to shrink. So far, the transgenic plants containing the IDL1-GFP and IDL2-GFP constructs have not showed induction of the fusion

proteins. Further analyses will be needed. It will also be possible to make fusions proteins between the signal peptide of the three IDL proteins and GFP. The signal peptide alone is predicted to direct whatever protein through the secretory pathway to the extracellular space. Another possibility is to make fusion proteins between GFP and the three IDL proteins with no signal peptide. Expected results would be that the proteins remain in the cytoplasm. Our preliminary results are in consistence with the hypothesis that the IDL proteins are localized to the apoplastic space, which is a necessary first step for them to be ligands.

4.6 Searching for loss-of-function mutants for *IDL2* and *IDL3*

We identified T-DNA insertion lines (Salk *IDL2* and Salk *IDL3*) harboring T-DNA insertions close to *IDL2* and *IDL3*. Sequencing the genomic regions flanking the left borders of the T-DNA insertions showed that the T-DNAs in Salk *IDL2* and Salk *IDL3* were localized 252 and 61 bp upstream of *IDL2* and *IDL3*, respectively. In order to determine whether these insertions were localized in the promoter or in the 5'UTRs, RACE was performed. RACE is a method to identify unknown cDNA ends and was used to identify the 3'UTR of *IDL2* and the 5' and 3'UTRs of *IDL3*. The 3' UTR for *IDL2* is 169 bp and the 5' and 3' UTRs of *IDL3* are 54 and 173 bp, respectively (results, figure 3.16). Since no RACE PCR product was obtained for *IDL2* 5'UTR, the 5'UTR of *IDL2* was not identified. The reason for this lack of RACE product is most likely RNA degradation (GeneRacer™ Kit, instruction manual, Invitrogen™). The RACE results indicate that the T-DNA insertion in Salk *IDL3* is in the *IDL3* promoter region. Although the 5'UTR of *IDL2* was not identified it is likely that also the T-DNA insertion in Salk *IDL2* is localized in the promoter (see results, section 3.3.3).

Since mutations due to T-DNA insertions often are recessive, the Salk plants were genotyped to identify lines homozygous for the insertion. Homozygous Salk *IDL2* and Salk *IDL3* plants were investigated for abnormal phenotypes; however, no mutant phenotype was identified under normal growth conditions. It has not been determined whether *IDL2* is knocked out in these plants and this needs to be analyzed in the future. It is likely that since the insertion is in the promoter area, this localization is not sufficient to knock out the transcription of *IDL2*. However, the *ida* mutant is caused by a T-DNA insertion in the *IDA* promoter (Butenko et al., 2003). Therefore, although no mutant phenotype was visible; it is possible that *IDL2* is knocked out in the Salk *IDL2* plants. Possibly, a mutant phenotype will be visible under stress

conditions (Bouche and Bouchez, 2001), nevertheless, strong GUS expression was observed under normal growth conditions. Another reason for no mutant phenotype may be redundancy between the *IDL* genes. In order to investigate the expression level of *IDL3* in the Salk *IDL3* plants, we used semi-quantitative RT-PCR. However, our results indicated that *IDL3* was neither knocked out nor reduced in the Salk *IDL3* plants (results, figure 3.17). Our RACE results and the sequencing of the genomic region flanking the left border of the T-DNA indicated that the T-DNA insertion in Salk *IDL3* was located 6 bp upstream of the transcription start point of *IDL3*. It is reasonable to assume that a T-DNA insertion just upstream of the transcription start of a gene would normally prevent or downregulate transcription. It has been suggested that transcription may start within the T-DNA and further transcribe the cds of the gene downstream of the insertion (Thorstensen, 2005). Therefore it is possible that transcription in the Salk *IDL3* plants started in the T-DNA resulting in a transcriptional fusion containing both parts of the T-DNA sequence and the *IDL3* sequence. This could give the opportunity for functional protein to be expressed and would explain why no mutant phenotype was observed. RT-PCR using a gene specific and a T-DNA specific primer could be used to investigate this possibility.

Since Salk *IDL2* and Salk *IDL3* plants showed no mutant phenotype, we wanted to generate RNAi knock-down lines for the two genes. For this purpose we used pHELLSGATE 8 which is a high-throughput vector for producing intron-spliced hairpin constructs (Helliwell et al., 2002). No correct RNAi construct, in which the intron retained its forward orientation, was identified for *IDL2*; only clones containing a reversed intron were obtained. Helliwell and Waterhouse found that the frequency of intron inversions most likely is dependent on the inserted sequence (Helliwell and Waterhouse, 2003). For future attempts to make an RNAi construct for *IDL2* one might use the pHELLSGATE 12 vector (Helliwell and Waterhouse, 2003) since this vector contains two introns in opposite direction. In contrast to *IDL2*, *IDL3* was successfully recombined into pHELLSGATE 8. The primary transformants were investigated for abnormal phenotypes; however, no mutant phenotype was identified. Earlier studies have reported that the effect of the RNAi construct vary for individual transformants; some display no phenotype while others exhibit extreme phenotypes (Wang et al., 2005b). Kerschen et al. proposed that the major variability between individual transformants is due to the presence of multiple copies of the RNAi construct (Kerschen et al., 2004). A possible explanation to why no mutant phenotype was observed among the *IDL3* RNAi plants may be the nature of the target gene (Wang et al., 2005b). It has been suggested that sequence

composition, spatial and temporal gene expression pattern and normal turnover rate of the targeted gene may affect the RNAi effectiveness (Kerschen et al., 2004). Perhaps the turnover rate of *IDL3* is so fast that the downregulation due to RNA interference is not sufficient to affect the *IDL3* function. Another reason that may affect the RNAi effectiveness is that the 35S promoter, which drives the RNAi construct, probably has a different activity in different tissues (Chuang and Meyerowitz, 2000). Furthermore, some tissues may partially resist RNAi and some phenotypes may be less sensitive to the level of gene activity (Chuang and Meyerowitz, 2000). For future analyses of the *IDL3* RNAi lines it will be necessary to identify lines containing one T-DNA locus and also investigate the functionality of the RNAi construct.

4.7 Overexpression of the *IDL* genes

Plants overexpressing the three *IDL* genes showed premature leaf senescence (results, figures 3.22 and 3.24). In addition, the majority of the 35S::*IDL1* plants and some of the 35S::*IDL2* and 35S::*IDL3* plants exhibited abnormal senescence in the top-most inflorescence tissues (results, figure 3.22), in which the tissues lost their turgor pressure and were degreened and desiccated. Leaf senescence is a programmed degeneration process (Lim et al., 2003) and is the final stage of development (Gan and Amasino, 1997; Hajouj et al., 2000). Senescence is regulated by many genes and is affected by endogenous developmental factors, such as age and hormones, and environmental factors, including stress, nutrient supply and pathogen attack (Lim et al., 2003). Overexpression of the *IDL* genes could be inducing senescence directly; however, another possibility is that they trigger the process indirectly, i.e. by affecting a stress response. In addition to premature senescence, plants overexpressing *IDL2* and *IDL3* had smaller and rounder rosette leaves and their stems were shorter and more fragile compared to the wild type. This phenotype may also be a consequence of stress responses due to the overexpression of the *IDL* genes.

Overexpression of the three *IDL* genes also led to premature floral organ abscission (results, figure 3.23). After the abscission process, the cells in the AZs became much more enlarged and rounded compared to the cells in the wild type AZs. A white substance was secreted and covered the cells and may be an overproduction of the protective layer that forms after the course of abscission. In some cases siliques and cauline leaves, which are normally not shed

in *Arabidopsis*, were abscised in plants overexpressing the *IDL* genes. The white substance was also seen in these abscission junctions, as well as at the base of the pedicels. Phenotypes similar to the above mentioned phenotypes were also observed in plants overexpressing *IDA* (Aalen et al., in press). The most likely explanation for the ectopic abscission is that the cells in these abscission junctions are already differentiated AZ cells whereby the IDL proteins induce the cell separation process. If this is the case the base of the pedicel and the base of the cauline leaves are vestigial AZ in *Arabidopsis*. In consistence with this, Cho and Cosgrove showed that overexpression of the expansin *AtExp10* enhanced breakage at the base of the pedicel (Cho and Cosgrove, 2000). The RLK, HAESA, which is involved in floral organ abscission, is expressed at the base of petioles and pedicels as well as in the floral organ AZs (Jinn et al., 2000). The authors suggested that the reason for no leaf and flower abscission in *Arabidopsis* is that not all the components necessary for AZ formation are present in these tissues (Jinn et al., 2000). The promoter activity of *IDL2* and *IDL3* at the base of the pedicels and the expression of *HAESA* and *AtExp10* at the base of pedicels and petioles may all be vestiges of evolutionary lost AZs.

Overexpression of the three *IDL* genes resulted in similar phenotypes, and suggests some degree of functional redundancy between the genes in this group of putative ligands. Normally, these genes are expressed in different parts of the plant; however, when they are constitutively expressed they might interact with each others putative receptors. Possibly, the IDL proteins interact with the putative *IDA* receptor and thereby induce premature abscission of floral organs. Further analyses will be needed in order to verify the actual overexpression of the three *IDL* genes in these transgenic plants. Supporting our data, it has been showed that *IDA* was overexpressed in the 35S::*IDA* transgenic plants (Bitte Stenvik, unpublished results). Wild type plants should also be transformed with the empty pK7WG2 vector to confirm that it is *IDA* and the *IDL* genes, and not the vector itself, that induces the phenotypes.

4.8 Conclusions and further work

Reverse genetic approaches have been undertaken in order to better understand the functions of *IDL1*, *IDL2* and *IDL3*. Our promoter analyses indicated that the three genes have diverse functions at different developmental stages during the *Arabidopsis* life cycle. Common for the three *IDL* genes is that they were all expressed at sites in which cell separation processes take

place; however, this cell separation zone specific expression pattern was not exceptional. Interestingly, overexpression of the *IDL* genes led to premature floral organ abscission and abscission of organs that are normally not shed in *Arabidopsis*. The overexpression phenotypes indicate a role in cell separation for the *IDL* genes, but also that these similar phenotypes may be a result of functional redundancy between the genes. The *IDL* genes are putative ligands and are thought to function through ligand-receptor interactions. Possibly, their ectopic expression gave interactions with one another's receptors. However, it still remains to verify whether the IDL proteins are localized to the apoplastic space, this will further indicate whether the proteins are ligands. If the *IDL* genes encode ligands, the next step would be to identify their putative receptors. The *Arabidopsis* genome encodes more than 600 RLKs (Shiu and Bleecker, 2003), and these receptors are of particularly interest in identifying interaction partners of signaling peptides.

To advance our understanding of the biological functions of the *IDL* genes, it will be necessary to continue the investigation of the knock-down lines. However, it would be advantageous to work with complete knock-out lines. Because of the small size of the *IDL* coding regions, T-DNA insertions causing loss-of-function mutations for these genes are likely to be rare. TILLING (Targeting Induced Local Lesions IN Genomes) is a new reverse genetic strategy to induce and identify point mutations as well as small insertions or deletions in any gene or specific region in the genome (McCallum et al., 2000; Slade and Knauf, 2005). This method could be used as an alternative to the T-DNA insertion strategy in order to identify knock-out lines for the *IDL* genes. Hopefully, knock-down lines will be available in the future and contribute to the knowledge of the biological functions of the *IDL* genes.

REFERENCES

Alonso, J.M., Stepanova, A.N., Leisse, T.J., Kim, C.J., Chen, H., Shinn, P., Stevenson, D.K., Zimmerman, J., Barajas, P., Cheuk, R., Gadrinab, C., Heller, C., Jeske, A., Koesema, E., Meyers, C.C., Parker, H., Prednis, L., Ansari, Y., Choy, N., Deen, H., Geralt, M., Hazari, N., Hom, E., Karnes, M., Mulholland, C., Ndubaku, R., Schmidt, I., Guzman, P., Aguilar-Henonin, L., Schmid, M., Weigel, D., Carter, D.E., Marchand, T., Risseeuw, E., Brogden, D., Zeko, A., Crosby, W.L., Berry, C.C., and Ecker, J.R. (2003). Genome-wide insertional mutagenesis of Arabidopsis thaliana. Science **301,** 653-657.

Altschul, S.F., Gish, W., Miller, W., Myers, E.W., and Lipman, D.J. (1990). Basic local alignment search tool. J Mol Biol **215,** 403-410.

Barlow, P.P.W. (2003). The root cap: cell dynamics, cell differentiation and cap function. Journal of plant growth regulation **21,** 261-286.

Baulcombe, D. (2004). RNA silencing in plants. Nature **431,** 356-363.

Baulcombe, D. (2005). RNA silencing. Trends Biochem Sci **30,** 290-293.

Bechtold, N., Ellis, J., and Pelletier, G. (1993). *I*n planta Agrobacterium mediated gene transfer by infiltration of adult Arabisopsis thaliana plants. C R Acad Sci III-Vie **316,** 1194-1199.

Becraft, P.W. (2002). Receptor kinase signaling in plant development. Annu Rev Cell Dev Biol **18,** 163-192.

Bengough, A., and McKenzie, B. (1997). Sloughing of root cap cells decreases the frictional resistance to maize (Zea mays L.) root growth. J Exp Bot **48,** 885-896.

Berg, A., Meza, T.J., Mahic, M., Thorstensen, T., Kristiansen, K., and Aalen, R.B. (2003). Ten members of the Arabidopsis gene family encoding methyl-CpG-binding domain proteins are transcriptionally active and at least one, AtMBD11, is crucial for normal development. Nucleic Acids Res **31,** 5291-5304.

Bleecker, A.B., and Patterson, S.E. (1997). Last exit: senescence, abscission, and meristem arrest in Arabidopsis. Plant Cell **9,** 1169-1179.

Boller, T. (2005). Peptide signalling in plant development and self/non-self perception. Curr Opin Cell Biol **17,** 116-122.

Bouche, N., and Bouchez, D. (2001). Arabidopsis gene knockout: phenotypes wanted. Curr Opin Plant Biol **4,** 111-117.

Brand, U., Grunewald, M., Hobe, M., and Simon, R. (2002). Regulation of CLV3 Expression by Two Homeobox Genes in Arabidopsis. Plant Physiol. **129,** 565-575.

Brummell, D.A., and Harpster, M.H. (2001). Cell wall metabolism in fruit softening and quality and its manipulation in transgenic plants. Plant Mol Biol **47,** 311-340.

Brunaud, V., Balzergue, S., Dubreucq, B., Aubourg, S., Samson, F., Chauvin, S., Bechtold, N., Cruaud, C., DeRose, R., Pelletier, G., Lepiniec, L., Caboche, M., and Lecharny, A. (2002). T-DNA integration into the Arabidopsis genome depends on sequences of pre-insertion sites. EMBO Rep **3,** 1152-1157.

Butenko, M.A., Patterson, S.E., Grini, P.E., Stenvik, G.E., Amundsen, S.S., Mandal, A., and Aalen, R.B. (2003). Inflorescence deficient in abscission controls floral organ abscission in Arabidopsis and identifies a novel family of putative ligands in plants. Plant Cell **15,** 2296-2307.

Casimiro, I., Beeckman, T., Graham, N., Bhalerao, R., Zhang, H., Casero, P., Sandberg, G., and Bennett, M.J. (2003). Dissecting Arabidopsis lateral root development. Trends Plant Sci **8,** 165-171.

Chen, R., Guan, C., Boonsirichai, K., and Masson, P.H. (2002). Complex physiological and molecular processes underlying root gravitropism. Plant Mol Biol **49,** 305-317.

Cho, H.T., and Cosgrove, D.J. (2000). Altered expression of expansin modulates leaf growth and pedicel abscission in Arabidopsis thaliana. Proc Natl Acad Sci U S A **97,** 9783-9788.

Chuang, C.F., and Meyerowitz, E.M. (2000). Specific and heritable genetic interference by double-stranded RNA in Arabidopsis thaliana. Proc Natl Acad Sci U S A **97,** 4985-4990.

Clark, S.E., Williams, R.W., and Meyerowitz, E.M. (1997). The CLAVATA1 gene encodes a putative receptor kinase that controls shoot and floral meristem size in Arabidopsis. Cell **89,** 575-585.

Clough, S.J., and Bent, A.F. (1998). Floral dip: a simplified method for Agrobacterium-mediated transformation of Arabidopsis thaliana. Plant J **16,** 735-743.

Cock, J.M., and McCormick, S. (2001). A large family of genes that share homology with CLAVATA3. Plant Physiol **126,** 939-942.

del Campillo, E., and Bennett, A.B. (1996). Pedicel breakstrength and cellulase gene expression during tomato flower abscission. Plant Physiol **111,** 813-820.

del Campillo, E., Abdel-Aziz, A., Crawford, D., and Patterson, S.E. (2004). Root cap specific expression of an endo-beta-1,4-D-glucanase (cellulase): a new marker to study root development in Arabidopsis. Plant Mol Biol **56,** 309-323.

Dellaporta, S., Wood, J., and Hicks, J. (1983). A plant DNA minipreparation: vertion II. Plant Mol Biol Rep **1,** 19-21.

Dievart, A., Dalal, M., Tax, F.E., Lacey, A.D., Huttly, A., Li, J., and Clark, S.E. (2003). CLAVATA1 dominant-negative alleles reveal functional overlap between multiple receptor kinases that regulate meristem and organ development. Plant Cell **15,** 1198-1211.

Dolan, L., Janmaat, K., Willemsen, V., Linstead, P., Poethig, S., Roberts, K., and Scheres, B. (1993). Cellular organisation of the Arabidopsis thaliana root. Development **119,** 71-84.

Eapen, D., Barroso, M.L., Ponce, G., Campos, M.E., and Cassab, G.I. (2005). Hydrotropism: root growth responses to water. Trends Plant Sci **10,** 44-50.

Fletcher, J.C., Brand, U., Running, M.P., Simon, R., and Meyerowitz, E.M. (1999). Signaling of cell fate decisions by CLAVATA3 in Arabidopsis shoot meristems. Science **283,** 1911-1914.

Gan, S., and Amasino, R.M. (1997). Making Sense of Senescence (Molecular Genetic Regulation and Manipulation of Leaf Senescence). Plant Physiol **113,** 313-319.

Gelvin, S.B. (2003). Improving plant genetic engineering by manipulating the host. Trends Biotechnol **21,** 95-98.

Gheysen, G., Villarroel, R., and Van Montagu, M. (1991). Illegitimate recombination in plants: a model for T-DNA integration. Genes Dev **5,** 287-297.

Gomez-Gomez, L., and Boller, T. (2000). FLS2: an LRR receptor-like kinase involved in the perception of the bacterial elicitor flagellin in Arabidopsis. Mol Cell **5,** 1003-1011.

Grini, P.E., Jurgens, G., and Hulskamp, M. (2002). Embryo and Endosperm Development Is Disrupted in the Female Gametophytic capulet Mutants of Arabidopsis. Genetics **162,** 1911-1925.

Guo, H.S., Fei, J.F., Xie, Q., and Chua, N.H. (2003). A chemical-regulated inducible RNAi system in plants. Plant J **34,** 383-392.

Hajouj, T., Michelis, R., and Gepstein, S. (2000). Cloning and characterization of a receptor-like protein kinase gene associated with senescence. Plant Physiol **124,** 1305-1314.

Helliwell, C., and Waterhouse, P. (2003). Constructs and methods for high-throughput gene silencing in plants. Methods **30,** 289-295.

Helliwell, C.A., Varsha Wesley, S., Wielopolska, A.J., and Waterhouse, P.M. (2002). High-throughput vectors for efficient gene silencing in plants. Funct Plant Biol **29,** 1217-1225.

Iijima, M., Higuchi, T., and Barlow, P.W. (2004). Contribution of root cap mucilage and presence of an intact root cap in maize (Zea mays) to the reduction of soil mechanical impedance. Ann Bot (Lond) **94,** 473-477.

Iijima, M., Higuchi, T., Barlow, P.W., and Bengough, A.G. (2003). Root cap removal increases root penetration resistance in maize (Zea mays L). J Exp Bot **54,** 2105-2109.

Jefferson, R.A. (1989). The GUS reporter gene system. Nature **342,** 837-838.

Jinn, T.L., Stone, J.M., and Walker, J.C. (2000). HAESA, an Arabidopsis leucine-rich repeat receptor kinase, controls floral organ abscission. Genes Dev **14,** 108-117.

Kachroo, A., Schopfer, C.R., Nasrallah, M.E., and Nasrallah, J.B. (2001). Allele-specific receptor-ligand interactions in Brassica self-incompatibility. Science **293,** 1824-1826.

Karimi, M., De Meyer, B., and Hilson, P. (2005). Modular cloning in plant cells. Trends Plant Sci **10,** 103-105.

Kende, H., and Zeevaart, J. (1997). The Five "Classical" Plant Hormones. Plant Cell **9,** 1197-1210.

Kerschen, A., Napoli, C.A., Jorgensen, R.A., and Muller, A.E. (2004). Effectiveness of RNA interference in transgenic plants. FEBS Lett **566,** 223-228.

Kobe, B., and Deisenhofer, J. (1994). The leucine-rich repeat: a versatile binding motif. Trends Biochem Sci **19,** 415-421.

Koncz, C., Martini, N., Mayerhofer, R., Koncz-Kalman, Z., Korber, H., Redei, G.P., and Schell, J. (1989). High-frequency T-DNA-mediated gene tagging in plants. Proc Natl Acad Sci U S A **86,** 8467-8471.

Krysan, P.J., Young, J.C., and Sussman, M.R. (1999). T-DNA as an insertional mutagen in Arabidopsis. Plant Cell **11,** 2283-2290.

Larkin, J.C., Brown, M.L., and Schiefelbein, J. (2003). How do cells know what they want to be when they grow up? Lessons from epidermal patterning in Arabidopsis. Annu Rev Plant Biol **54,** 403-430.

Laskowski, M.J., Williams, M.E., Nusbaum, H.C., and Sussex, I.M. (1995). Formation of lateral root meristems is a two-stage process. Development **121,** 3303-3310.

Lim, P.O., Woo, H.R., and Nam, H.G. (2003). Molecular genetics of leaf senescence in Arabidopsis. Trends Plant Sci **8,** 272-278.

Malamy, J.E., and Benfey, P.N. (1997). Organization and cell differentiation in lateral roots of Arabidopsis thaliana. Development **124,** 33-44.

Mandava, N.B. (1988). Plant growth promoting brassinosteroids. Annu Rev Plant Physiol Plant Mol Biol **39,** 23-52.

Massa, G.D., and Gilroy, S. (2003). Touch modulates gravity sensing to regulate the growth of primary roots of Arabidopsis thaliana. Plant J **33,** 435-445.

Matsubayashi, Y. (2003). Ligand-receptor pairs in plant peptide signaling. J Cell Sci **116,** 3863-3870.

Matsubayashi, Y., Ogawa, M., Morita, A., and Sakagami, Y. (2002). An LRR receptor kinase involved in perception of a peptide plant hormone, phytosulfokine. Science **296,** 1470-1472.

Mayerhofer, R., Koncz-Kalman, Z., Nawrath, C., Bakkeren, G., Crameri, A., Angelis, K., Redei, G.P., Schell, J., Hohn, B., and Koncz, C. (1991). T-DNA integration: a mode of illegitimate recombination in plants. Embo J **10,** 697-704.

McCallum, C.M., Comai, L., Greene, E.A., and Henikoff, S. (2000). Targeting Induced Local Lesions IN Genomes (TILLING) for Plant Functional Genomics. Plant Physiol. **123,** 439-442.

Meakin, P.P. (1990). Dehiscence of fruit in oilseed rape.1. Anatomy of pod dehiscence. J exp bot **41,** 995-1002.

Meister, G., and Tuschl, T. (2004). Mechanisms of gene silencing by double-stranded RNA. Nature **431,** 343-349.

Mergaert, P., Nikovics, K., Kelemen, Z., Maunoury, N., Vaubert, D., Kondorosi, A., and Kondorosi, E. (2003). A novel family in Medicago truncatula consisting of more than 300 nodule-specific genes coding for small, secreted polypeptides with conserved cysteine motifs. Plant Physiol **132,** 161-173.

Montoya, T., Nomura, T., Farrar, K., Kaneta, T., Yokota, T., and Bishop, G.J. (2002). Cloning the tomato curl3 gene highlights the putative dual role of the leucine-rich repeat receptor kinase tBRI1/SR160 in plant steroid hormone and peptide hormone signaling. Plant Cell **14,** 3163-3176.

Murashige, T., and Skoog, F. (1962). A revised Medium for Rapid Growth and Bio Assays with Tobacco Tissue Cultures. Physiol Plantarum **15,** 473-497.

Narita, N.N., Moore, S., Horiguchi, G., Kubo, M., Demura, T., Fukuda, H., Goodrich, J., and Tsukaya, H. (2004). Overexpression of a novel small peptide ROTUNDIFOLIA4 decreases cell proliferation and alters leaf shape in Arabidopsis thaliana. Plant J **38,** 699-713.

Nishihama, R., Jeong, S., DeYoung, B., and Clark, S.E. (2003). Retraction. Science **300,** 1370.

Osborne, D.J. (1989). Abscission. Crit. Rev. Plant Sci. **8,** 103-129.

Patterson, S.E. (2001). Cutting loose. Abscission and dehiscence in Arabidopsis. Plant Physiol **126,** 494-500.

Pearce, G., Strydom, D., Johnson, S., and Ryan, C.A. (1991). A polypeptide from tomato leaves induces wound-inducible inhibitor proteins. Science **253,** 895-898.

Pearce, G., Moura, D.S., Stratmann, J., and Ryan, C.A., Jr. (2001). RALF, a 5-kDa ubiquitous polypeptide in plants, arrests root growth and development. Proc Natl Acad Sci U S A **98,** 12843-12847.

Roberts, J.A., Elliott, K.A., and Gonzalez-Carranza, Z.H. (2002). Abscission, dehiscence, and other cell separation processes. Annu Rev Plant Biol **53,** 131-158.

Roberts, J.A., Whitelaw, C.A., Gonzalez-Carranza, Z.H., and McManus, M.T. (2000). Cell Separation Processes in Plants--Models, Mechanisms and Manipulation. Ann Bot **86,** 223-235.

Ryan, C.A., and Pearce, G. (1998). Systemin: a polypeptide signal for plant defensive genes. Annu Rev Cell Dev Biol **14,** 1-17.

Sablowski, R. (2004). Root development: the embryo within? Curr Biol **14,** R1054-1055.

Sambrook, J., and Russel, D.W. (2001). A laboratory manual. Molecular Cloning.

Scheer, J.M., and Ryan, C.A. (1999). A 160-kD systemin receptor on the surface of lycopersicon peruvianum suspension-cultured cells. Plant Cell **11,** 1525-1536.

Scheer, J.M., and Ryan, C.A., Jr. (2002). The systemin receptor SR160 from Lycopersicon peruvianum is a member of the LRR receptor kinase family. Proc Natl Acad Sci U S A **99,** 9585-9590.

Scheres, B., Benfey, P., and Dolan, L. (2002). Root Development. In The Arabidopsis Book, C.R. Somerville and E.M. Meyerowitz, eds (Rockville, MD: American Society of plant Biologists). doi/10.1199/tab.0101. http://www.aspb.org/publications/arabidopsis/.

Schoof, H., Lenhard, M., Haecker, A., Mayer, K.F., Jurgens, G., and Laux, T. (2000). The stem cell population of Arabidopsis shoot meristems in maintained by a regulatory loop between the CLAVATA and WUSCHEL genes. Cell **100,** 635-644.

Schopfer, C.R., Nasarallah, M.E., and Nasarallah, J.B. (1999). The male determinant of self-incompatibility in Brassica. Science **286,** 1697-1700.

Sexton, R., and Roberts, J.A. (1982). Cell biology of abscission. Annu Rev Plant Physio **33,** 133-162.

Shiu, S.H., and Bleecker, A.B. (2001a). Receptor-like kinases from Arabidopsis form a monophyletic gene family related to animal receptor kinases. Proc Natl Acad Sci U S A **98,** 10763-10768.

Shiu, S.H., and Bleecker, A.B. (2001b). Plant receptor-like kinase gene family: diversity, function, and signaling. Sci STKE **2001,** RE22.

Shiu, S.H., and Bleecker, A.B. (2003). Expansion of the receptor-like kinase/Pelle gene family and receptor-like proteins in Arabidopsis. Plant Physiol **132,** 530-543.

Slade, A.J., and Knauf, V.C. (2005). TILLING moves beyond functional genomics into crop improvement. Transgenic Res **14,** 109-115.

Stoutjesdijk, P.A., Singh, S.P., Liu, Q., Hurlstone, C.J., Waterhouse, P.A., and Green, A.G. (2002). hpRNA-mediated targeting of the Arabidopsis FAD2 gene gives highly efficient and stable silencing. Plant Physiol **129,** 1723-1731.

Taylor, J.E., and Whitelaw, C.A. (2001). Signals in abscission. New Phytol **151,** 323-339.

The Arabidopsis Genome Initiative. (2000). Analysis of the genome sequence of the flowering plant Arabidopsis thaliana. Nature **408,** 796-815.

Thorstensen, T. (2005). Identification and functional analysis of putative chromatin modifying histone lysine methyltransferases in *Arabidopsis thaliana*. In Faculty of Mathematics and Natural Sciences (Oslo: University of Oslo).

Tinland, B., Hohn, B., and Puchta, H. (1994). Agrobacterium tumefaciens transfers single-stranded transferred DNA (T-DNA) into the plant cell nucleus. Proc Natl Acad Sci U S A **91,** 8000-8004.

Torii, K.U. (2000). Receptor kinase activation and signal transduction in plants: an emerging picture. Curr Opin Plant Biol **3,** 361-367.

Torii, K.U., Mitsukawa, N., Oosumi, T., Matsuura, Y., Yokoyama, R., Whittier, R.F., and Komeda, Y. (1996). The Arabidopsis ERECTA gene encodes a putative receptor protein kinase with extracellular leucine-rich repeats. Plant Cell **8,** 735-746.

Trotochaud, A.E., Jeong, S., and Clark, S.E. (2000). CLAVATA3, a multimeric ligand for the CLAVATA1 receptor-kinase. Science **289,** 613-617.

Tzfira, T., and Citovsky, V. (2002). Partners-in-infection: host proteins involved in the transformation of plant cells by Agrobacterium. Trends Cell Biol **12,** 121-129.

Tzfira, T., Rhee, Y., Chen, M.H., Kunik, T., and Citovsky, V. (2000). Nucleic acid transport in plant-microbe interactions: the molecules that walk through the walls. Annu Rev Microbiol **54,** 187-219.

Ueda, M., Koshino-Kimura, Y., and Okada, K. (2005). Stepwise understanding of root development. Curr Opin Plant Biol **8,** 71-76.

Uheda, E.E. (1997). Morphological aspects of the shedding of surface layers from peanut roots. Can J bot **75,** 607-611.

Vanoosthuyse, V., Miege, C., Dumas, C., and Cock, J.M. (2001). Two large Arabidopsis thaliana gene families are homologous to the Brassica gene superfamily that encodes pollen coat proteins and the male component of the self-incompatibility response. Plant Mol Biol **46,** 17-34.

Vicre, M., Santaella, C., Blanchet, S., Gateau, A., and Driouich, A. (2005). Root border-like cells of Arabidopsis. Microscopical characterization and role in the interaction with rhizobacteria. Plant Physiol **138,** 998-1008.

von Arnim, A.G., Deng, X.W., and Stacey, M.G. (1998). Cloning vectors for the expression of green fluorescent protein fusion proteins in transgenic plants. Gene **221,** 35-43.

Walker, J.C. (1994). Structure and function of the receptor-like protein kinases of higher plants. Plant Mol Biol **26,** 1599-1609.

Wang, J.-W., Wang, L.-J., Mao, Y.-B., Cai, W.-J., Xue, H.-W., and Chen, X.-Y. (2005a). Control of Root Cap Formation by MicroRNA-Targeted Auxin Response Factors in Arabidopsis. Plant Cell **17,** 2204-2216.

Wang, M.B., and Metzlaff, M. (2005). RNA silencing and antiviral defense in plants. Curr Opin Plant Biol **8,** 216-222.

Wang, T., Iyer, L.M., Pancholy, R., Shi, X., and Hall, T.C. (2005b). Assessment of penetrance and expressivity of RNAi-mediated silencing of the Arabidopsis phytoene desaturase gene. New Phytol **167,** 751-760.

Waterhouse, P.M., and Helliwell, C.A. (2003). Exploring plant genomes by RNA-induced gene silencing. Nat Rev Genet **4,** 29-38.

Wen, J., Lease, K.A., and Walker, J.C. (2004). DVL, a novel class of small polypeptides: overexpression alters Arabidopsis development. Plant J **37,** 668-677.

Yang, H., Matsubayashi, Y., Nakamura, K., and Sakagami, Y. (2001). Diversity of Arabidopsis genes encoding precursors for phytosulfokine, a peptide growth factor. Plant Physiol **127,** 842-851.

Zupan, J., Muth, T.R., Draper, O., and Zambryski, P. (2000). The transfer of DNA from agrobacterium tumefaciens into plants: a feast of fundamental insights. Plant J **23,** 11-28.

Aalen, R.B., Butenko, M.A., Stenvik, G.E., Tandstad, N.M., and Patterson, S.E. (in press). Genetic control of floral abscission. In Floriculture, Ornamental and Plant Biotechnology: advances and topical issues, (1st ed.) Global Science Books Ltd., London

ABBREVIATIONS

35S	CaMV (Cauliflower mosaic virus) 35S promoter
Agrobacterium	*Agrobacterium tumefaciens*
Arabidopsis	*Arabidopsis thaliana*
AZ	abscission zone
BC	border cell
BLC	border like cell
bp	base pair
BLAST	Basic Local Alignment Search Tool
BRI1	BRASSINOSTEROID-INSENSITIVE 1
cDNA	complementary DNA
cds	coding sequence
CLE	*CLAVATA3/ESR-RELATED*
CLV	*CLAVATA*
Col	Columbia
DEX	dexamethasone
DNA	deoxyribonucleic acid
dNTP	deoxyribonucleotide triphosphate
dsRNA	double stranded RNA
DVL	*DEVIL*
E. coli	*Escherichia coli*
EST	Expressed Sequence Tag
EtBr	ethidium bromid
EtOH	ethanol
FLS2	Flagellin-sensitive2
GFP	Green Fluorescent Protein
GUS	*β-glucoronidase*
hpRNA	hairpin RNA
Hyg	hygromycin
IDA	*INFLORESCENCE DEFICIENT IN ABSCISSION*
IDL	*IDA-LIKE*
kb	kilo base
Km	kanamycin
Km^r	kanamycin resistant
Km^s	kanamycin sensitive
LB	T-DNA left border
LRP	lateral root primordium
LRR	leucine rich repeat
mRNA	messenger RNA
NCR	NODULE-SPECIFIC CYSTEINE RICH
nptII	*Neomycin phosphotransferase* gene
OD	optical density
ON	over night
PCR	Polymerase Chain Reaction
PG	polygalacturonase
pI	Isoelectric point

PSK	PHYTOSULFOKINE
PSKR	PSK receptor
pTi	tumor inducing plasmid
PTGS	post transcriptional gene silencing
QC	quiescent center
RALF	RAPID ALKALINIZATION FACTOR
RB	T-DNA right border
RACE	rapid amlification of cDNA ends
RISC	RNA-induced silencing complex
RLCK	receptor like cytoplasmatic kinase
RLK	receptor like kinase
RNA	ribonucleic acid
RNAi	RNA interference
rRNA	ribosomal RNA
RTFL	*ROT FOUR LIKE*
RT-PCR	reverse transcriptase PCR
SCR	S-LOCUS CYSTEINE-RICH
SCRL	*SCR-LIKE*
SD	standard deviation
SDS	sodium dodecyl sulfate
siRNA	small interfering RNA
SR160	systemin receptor 160 kDa
SRK	S-locus specific RLK
T1	first transformant generation
T2	second transformant generation
T3	third transformant generation
T-DNA	transfer DNA
Tm	melting temperature
UTR	untranslated region
vir	virulence
wt	wild type
WUS	WUSCHEL
X-Gluc	5-bromo-4-chloro-3-indolyl β-D-glucuronide

APPENDIX 1

Primer	Sequence	Tm (ºC)
IDL1 attB1	5'-GGGGACAAGTTTGTACAAAAAACGAGGCTTAATAGCTAAATTAGTGTCTCCTCCTC-3'	65
IDL1 attB2	5'-GGGGACCACTTTGTACAAGAAAGCTGGGTAGTGTTTGAGATTATTCACCACAG-3'	66
IDL1 stop attB2	5'-GGGGACCACTTTGTACAAGAAAGCTGGTTAGTGTTTGAGATTATTCACCACA-3'	64
IDL1 5'UTR	5'-CCGCCTTCTTAAAATCCAAAA-3'	43
IDL1 3'UTR	5'-TTGAAGCAAATCCTAAGAGSTTGA-3'	45
IDL2 attB1	5'-GGGGACAAGTTTGTACAAAAAACGAGGCTGCATGTCGTCTCGAAACCAAAGATC-3'	66
IDL2 attB2	5'-GGGGACCACTTTGTACAAGAAAGCTGGGTACGGAGAAGATCGATGCCAACTAAG-3'	68
IDL2 stop attB2	5'-GGGGACCACTTTGTACAAGAAAGCTGGTCACGGAGAAGATCGATGCCAACTAAG-3'	68
IDL2 R	5'-GGAGAAGATCGATGCCAAC-3'	46
IDL2 L	5'-CGTCTCGAAACCAAAGATCAAG-3'	48
IDL2 RP	5'-TCTTTGGTTTCGAGACGACATTG-3'	48
IDL2 LP	5'-TGTTAAACTTATCCACCAGAAAGA-3'	45
IDL2 RACE 5'	5'-AAACGGCGTCGTTGTGCTTCTTGTG-3'	54
IDL2 RACE 3'	5'-GCGCAACGACGCCGTTTCTTCTTCAA-3'	56
IDL3 attB1	5'-GGGGACAAGTTTGTACAAAAAACGAGGCTGCATGTCTTCTCGAAGCCACCG-3'	68
IDL3 attB2	5'-GGGGACCACTTTGTACAAGAAAGCTGGGTAAGTCTTAGTACTTAAACCGATTTCG-3'	66
IDL3 stop attB2	5'-GGGGACCACTTTGTACAAGAAAGCTGGTTAAGTCTTAGTACTACTTAAACCGATTTCG-3'	65
IDL3 R	5'-CTCGAAGCCACCGATCAAG-3'	48
IDL3 L	5'-TTTCTGGAAGGACCAGAAGTTG-3'	48
IDL3 RP	5'-TTGGAACCGGAAACTGACGTG-3'	49
IDL3 RACE 5'	5'-GTTTGGGTGGCGAGCTTGTGTTGAA-3'	54
IDL3 RACE 3'	5'-GCTGCAATGGAGCAAGAACCACGAA-3'	54
LBb1	5'-GCGTGGACCGCTTGCTGCAACT-3'	55
ACTIN2-7_antisense	5'-CCGCAAGATCAAGACGAAGGATAGC-3'	54
ACTIN2-7_sense	5'-CCCTGAGGAGCACCAGTTCTACTC-3'	56
M13 F	5'-GTAAAACGACGGCCAG-3'	41
M13 R	5'-CAGGAAACAGCTATGAC-3'	41
p27 5'	5'-GAGCTACACATGCTCAGG-3'	45
p27 3'	5'-GGGATGACGCACAATCC-3'	44
HU	5'-AAAGGGGGATGTGCTGCAAGGCG-3'	56
35 SL	5'-CAACCACGTCTTCAAAGCAA-3'	45
smGFP-R	5'-TGCCCATTAACATCACCATC-3'	45
GeneRacer™ 5'	5'-CGACTGGAGCACGAGGACACTGA-3'	56
GeneRacer™ 3'	5'-GCTGTCAACGATACGCTACGTAACG-3'	54